The role of YAP signaling in thermogenic adipose tissues

Dissertation
zur
Erlangung des Doktorgrades (Dr. rer. nat.)
der
Mathematisch-Naturwissenschaftlichen Fakultät
der
Rheinischen Friedrich-Wilhelms-Universität Bonn

vorgelegt von
Juhee Yang
aus
Jeju, Südkorea

Bonn, 2020

Angefertigt mit Genehmigung der Mathematisch-Naturwissenschaftlichen Fakultät der Rheinischen Friedrich-Wilhelms-Universität Bonn.

1. Gutachter: Prof. Dr. med. Alexander Pfeifer

2. Gutachterin: Prof. Dr. Christa E. Müller

Tag der Promotion: 08.12.2020

Erscheinungsjahr: 2021

Acknowledgement

First of all, I would like to express my sincere thanks to Prof. Dr. med. Alexander Pfeifer for the supervision, and providing me the opportunity to conduct my doctoral studies in his work group. I would also like to thank Prof. Dr. Christa E. Müller and Prof. Dr. J. Silvio Gutkind for their help and support during my study.

I extend my heartiest thanks to Jelena Zurkovic, Birte Niemann, Dr. Laia Reverte Salisa, Dr. Staffan Hildebrand, Laura Prünte, and Karsten Motzler for being such wonderful colleagues and friends. I would like to specially thank Dr. Katarina Klepac for teaching and helping me to initiate my PhD project. I would like to express my special thanks to Elena Weidner, Hannah Lamby, and Patricia Zehner for their help. I would also like to thank Dr. Elisabeth Mies-Klomfass and all the members of AG Pfeifer, past and present, for the kind assistance.

마지막으로, 항상 저를 응원하고 지지해주시는 우리 엄마 김미정 여사님, 아빠 양태석 선생님, 수임언니,손현수 형부, 양창현, 소은이 지호, 그리고 모든 친구들 고맙고 사랑합니다.

Abbreviations

°C	Degree Celsius
8-Br cGMP	8-Bromoguanosine 3′,5′-cyclic monophosphate
ABP	L-Ascorbate, d-Biotin, Panthothenate
AC	Adenylyl Cyclase
AdipoQ	Adiponectin gene (*Mus musculus*)
AP2	Adipocyte protein 2 (same as fatty acid-binding protein)
ATP	Adenosintriphosphate
BAT	Brown adipose tissue
BMI	Body-mass index
bp	Base pair
BSA	Bovine serum albumin
C/EBP	CCAAT/enhancer-binding protein
Ca^{2+}	Calcium ion
$CaCl_2$	Calcium chloride
cAMP	Cyclic adenosine monophosphate
CCL2	Chemokine (C-C motif) ligand 2
cDNA	Complementary DeoxyriboNucleic Acid
cGMP	Cyclic guanosine monophosphate
CMV promotor	Cytomegalovirus promotor
Cidea	Cell death-inducing DFFA-like effector a
Cyr61	Cysteine-rich angiogenic inducer 61
DAG	Diacylglycerol
DMEM	Dulbecco's modified Eagle's medium
DMSO	Dimethyl sulfoxide
DNA	DeoxyriboNucleic Acid
DREADD	Designer receptor exclusively activated by designer drugs
Dq	$G\alpha_q$-coupled designer receptor DREADD
ECL	Enhanced Chemiluminescence
EDTA	Ethylenediaminetetraacetic acid
Ednra	Endothelin receptor type A
EE	Energy expenditure
Elovl3	Elongation of very long chain fatty acids protein 3 (*Mus musculus*)
ET	Endothelin
F4/80	EGF-like module-containing mucin-like hormone receptor-like 1
FBS	Fetal bovine serum
FFA	Free fatty acid
FR	FR900359, a selective $G\alpha_{q/11}$ inhibitor
GAPDH	Glyceraldehyde 3-phosphate dehydrogenase
GEF	Guanine nucleotide exchange factor
GM	Growth medium
GDP	Guanosine diphosphate
GPCRs	G protein-coupled receptors
G Protein	Guanine nucleotide-binding proteins
GTP	Guanosintriphosphate
H&E	Haemotoxylin and Eosin

HEPES	Hydroxyethyl piperazineethanesulfonic acid
HPRT	Hypoxanthin-Phosphoribosyl-Transferase
HSL	Hormon sensitive lipase
IBMX	Isobutylmethylxanthin
IL-6	Interleukin 6
IL-10	Interleukin 10
IM	Induction medium
i.p.	Intraperitoneal injection
IP_3	Inositol 1,4,5-trisphosphate
kDA	Kilo Dalton
M/mM/µM	Molar/millimolar/micromolar
mRNA	Messenger RNA
MSCs	Mesenchymale stem cells
Myf5	Myogenic-regulatory factor 5
NaCl	Sodium chloride
NaF	Sodium fluoride
NE	Norepinephrin
PAGE	Polyacrylamide gel electrophoresis
PBS	phosphate-buffered saline
PCR	Polymerase chain reaction
PDE	Phosphodiesterase
PET/CT	Positron-Emissions-Tomographie/Computertomographie
PFA	Paraformaldehyde
PGC-1α	Peroxisome proliferator-activated receptor γ-coactivator 1
PIP_2	Phosphatidylinositol 4,5-bisphosphate
PKA	Proteinkinase A
PKG	Proteinkinase G
PPAR	Peroxisome proliferator activated receptor
PRDM16	pRD1-BF-RIZ1 homologous domain containing protein 16
P/S	Penicillin/Streptomycin
qRT-PCR	Quantitative real time polymerase chain reaction
RGS	Regulators of G protein signaling
RIPA	Radioimmunoprecipitation assay buffer
RNA	RiboNucleic Acid
ROCK	Rho-associated protein kinase
SDS	Sodium dodecyl sulfate
SDS-PAGE	Sodium dodecyl sulfate polyacrylamide gel electrophoresis
s.e.m.	Standard error of the mean
shRNA	Short hairpin RNA
SV40	Simian Virus 40
SVF	Stromal vascular fraction
T3	Triiodothyronine
TNFa	Tumour Necrosis Factor alpha
UCP1	uncoupling protein1
WATg	White adipose tissue gonadal
WATi	White adipose tissue inguinal
Y27632	Y27632 dihydrochloride

Contents

1. Introduction

1.1 Obesity and Adipose tissues

1.1.1 Obesity

Obesity is a metabolic disease that presents excessive fat accumulation in the body. The major cause of obesity is energy imbalance in which energy intake exceeds energy expenditure. Obesity is simply measured by body mass index (BMI) as a person's weight in kilograms divided by the square of his height (kg/m^2) and the individual who has a BMI over 30 kg/m^2 is considered an obese person. Across the world, obesity is considered as a public health problem. World Health Organization (WHO) has reported that the rate of obese people has remarkably increased since 1975. In 2016, it was estimated that about 13% of adult population in the world are obese. The global prevalence of obesity has almost tripled between 1975 and 2016 (Rodgers, Tschöp et Wilding 2012). This is more than an aesthetic problem, obese people can develop a variety of health complications such as cardiovascular diseases, type 2 diabetes (T2D), and musculoskeletal disorders. Therefore, a proper therapy is needed to prevent this global health problem.

1.1.2 Obesity therapies

Even though diverse trials to prevent obesity have implemented up to present, the effective therapies are limited. To date, bariatric surgery is the most effective treatment of obesity. The surgical intervention leads to malabsorption of nutrients in stomach or intestine, thereby reducing weight gain and improving insulin-resistance metabolic syndrome (Rodgers, Tschöp et Wilding 2012; Kral et Näslund 2007). However, this method is finite because of surgical risks and costs. In past years, a variety of therapeutic agents for combating obesity have been developed, which reduce body weight by controlling food intake or regulating energy homeostasis (Cooke et Bloom 2006; Kang et Park 2012; Sargent et Moore 2009). For example, Sibutramine has been widely used for long-term weight management, which was used as an appetite suppressant until 2010, however, it was withdrawn from the market because of risk of heart attack (Kang et Park 2012). Now, Orlistat is the only approved drug for long-term use and it acts as a lipase inhibitor, thereby preventing the absorption of fat (Kang et Park 2012). As most of anti-obesity drugs have shown limited success or have been withdrawn from the market due to unexpected side effects (Kang et Park 2012; Rodgers, Tschöp et Wilding 2012), new therapeutic agents are urgently needed.

1.1.3 Adipose tissues

Since the adipose tissue is a major metabolic organ and obesity is defined as excessive fat accumulation, this organ has become a key target to combat obesity. Mammals have two distinct types of adipose tissues: brown and white fat. Brown adipose tissue (BAT) plays a role in dissipating energy through non-shivering thermogenesis, on the other hand, white adipose

tissues (WAT) stores excess energy in form of triglycerides (Cannon et Nedergaard 2004; Harms et Seale 2013; Kajimura et Saito 2014; Pfeifer et Hoffmann 2015). Aside from classical BAT, inducible brown-like adipose tissues named beige fat is exhibited in WAT.

1.1.3.1 Brown adipose tissue (BAT)

In mammals, BAT is located in the interscapular region and it functions to maintain body temperature in newborn or infants (Cannon et Nedergaard 2004; Bartelt et Heeren 2014; Harms et Seale 2013; Kajimura et Saito 2014) . In the past, it was thought that only human infants have active BAT. However, several studies showed that metabolically active BAT exists in the lower neck area of adult humans. Besides, it has been shown that the activity of BAT is reduced in human subjects who are obese, and there is a negative correlation between BAT activity and body weight (van Marken Lichtenbelt Wouter D. et al.; Saito et al. 2009; Nedergaard, Bengtsson et Cannon 2007; Virtanen Kirsi A. et al.). Brown adipocytes (BAs) have distinct morphological characteristics compared to white adipocytes (WAs) (Cannon et Nedergaard 2004; Kajimura et Saito 2014; Bartelt et Heeren 2014; Pfeifer et Hoffmann 2015). BAs have numerous small lipid droplets, large numbers of mitochondria, giving them the appearance of brown color (Figure 1). In BAT mitochondria, uncoupling protein 1 (UCP1), a BAT-specific marker, is highly expressed in the inner mitochondria membrane. This protein mediates uncoupling process for generating heat called thermogenesis. UCP1 disrupts the proton gradient of the respiratory chain, thereby inhibiting mitochondrial ATP synthesis ("uncoupling reaction"), to produce heat as a by-product. Cold stimulation or β-adrenergic agonists are well known physiological activators of BAT thermogenic capacity. Norepinephrine (NE) released from sympathetic nerves activates the β-adrenergic receptor signaling pathway, especially via β3 receptors in BAT. β receptors activate adenylyl cyclase (AC), followed by increasing the production of intracellular cyclic adenosine monophosphate (cAMP). Subsequently, cAMP activates protein kinase A (PKA), stimulating lipolysis, which leads to mobilization of free fatty acids (FFAs) from triacylglycerol. The released FFAs are used as a substrate for activating thermogenesis by UCP1.

1.1.3.2 White adipose tissue (WAT)

White adipose tissue is distributed widely through the body, mostly located in intraabdominal and subcutaneous region in mammals (Gesta, Tseng et Kahn 2007). The classical role of WAT is to store energy in the form of triglycerides. Under deprivation of energy, white adipocytes (WAs) can release fatty acids and glycerol from triglycerides and the released fatty acids and glycerol are delivered to other organs. Another role of adipose organ is producing bioactive factors including hormones, growth factors, cytokines that is crucial for body metabolism. Among them, leptin is one of the most important hormones released from white adipocytes, which plays a role in regulation of satiety and energy balance (Amitani et al. 2013; Coelho, Oliveira et Fernandes 2013; Trayhurn et Beattie 2001). In contrast to brown adipocytes, WAs have a single, unilocular lipid droplet, low mitochondria density, and do not express UCP1 (Figure 1) (Pfeifer et Hoffmann 2015; Bartelt et Heeren 2014; Cannon et Nedergaard 2004). Because of the role of WAT in energy storage, it contributes to development of obesity.

1.1.3.3 Beige/Brite adipocytes

UCP1-positive adipocytes reside in WAT and these adipocytes are called beige or brite (= brown-in-white) adipocytes (hereafter referred to as beige adipocytes). The beige adipocytes are induced in response to diverse stimuli such as cold, β-adrenergic agonists, cGMP, and natriuretic peptides (NPs), a process referred to as “browning” (Cannon et Nedergaard 2004; Bartelt et Heeren 2014; Kajimura et Saito 2014; Pfeifer et Hoffmann 2015). Beige adipocytes display multilocular lipid droplets and a higher number of mitochondria in white fat depots (Figure 1). Similar to brown adipocytes, they express UCP1 and brown fat-specific genes including Cidea, Pgc1a, Elovl3, and Dio2, thus, these cells dissipate energy.

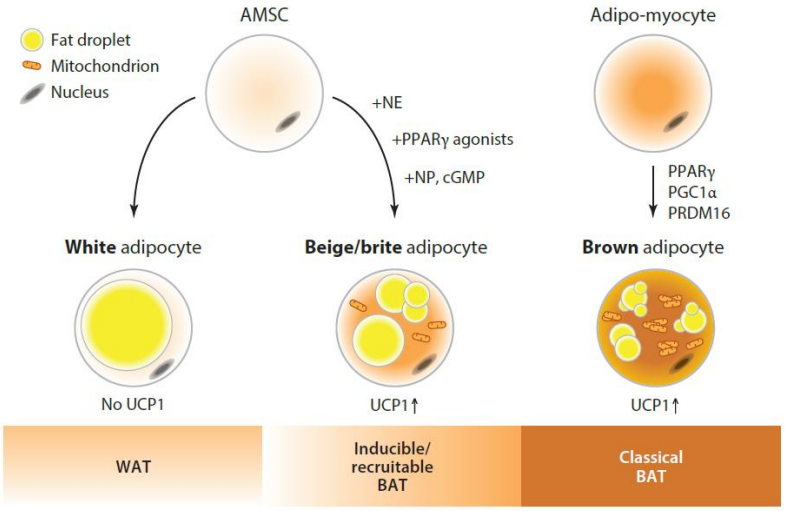

Figure 1. Types of adipocytes and characteristics (Adapted from: (Pfeifer et Hoffmann 2015)).

1.1.3.4 The origins of adipocytes

Mesenchymal stem cells (MSCs) are developed from the mesoderm that gives rise to fat bundles, the dermis, and muscle cells (Sanchez-Gurmaches et al. 2012; Seale et al. 2008; Harms et Seale 2013; Gesta, Tseng et Kahn 2007; Berry et al. 2013). Since MSCs are multipotent stem cells, they have a potential to differentiate to osteoblasts, chondrocytes, endothelial cells, adipocytes, myocytes and hematopoietic cells. Even though both white adipocytes and brown adipocytes are derived from MSCs, they differ in their progenitor cells. One distinct point is that brown precursors exhibit skeletal myogenic transcriptional expression by expressing the myogenic regulatory factor 5 (Myf5) (Sanchez-Gurmaches et al. 2012). Consistent with the origin and Myf5 expression, brown adipocytes and muscle cells are considered having similar characteristics. In contrast, a precursor of white adipocytes has no Myf5 expression and the lineage of beige adipocytes remains unclear. The current hypothesis of origin of beige cells includes; (1) whether beige adipocytes come from white adipocytes by transdifferentiation (2) whether the cells derive from a separate precursor.

1.1.3.5 Transcriptional regulation of adipocytes

Although brown and white adipocytes have differences in developmental origins and functions, they share similar transcriptional regulation for differentiation. Peroxisome Proliferator-Activated Receptor gamma (PPARg) and the CCAAT/enhancer binding proteins (C/EBPs) are key transcription factors for both brown and white adipocyte differentiation. C/EBPs cooperate with PPARg to stimulate transcriptional cascade for adipogenesis and lipolysis through upregulation of downstream genes such as UCP1 and fatty acid binding protein 4 (FABP4, also known as aP2). Even though this transcriptional regulation confers adipogenic differentiation in both brown and white adipocytes, BAs or beige adipocytes need to activate a specific transcriptional program to become thermogenic adipocytes. These transcriptional cues of brown or beige adipocytes include C/EBPβ, PRD1-BF-RIZ1 homologous domain containing protein-16 (PRDM16), PPAR-co-activator-1 alpha (PGC-1α). C/EBPβ is highly expressed in BAs than WAs (Kajimura et al. 2009) and it is essential for regulating the thermogenic program in BAs by cooperating with other transcriptional regulators (Kajimura et Saito 2014). C/EBPβ forms a transcriptional complex with PRDM16 and the C/EBPβ-PRDM16 complex serves as a molecular switch for brown cell fate decision (Kajimura et al. 2009). PRDM16 is dispensable for embryonic BAT development, whereas it is required for maintenance of postnatal BAT identity and function (Harms et al. 2014). PGC-1α is important for adaptive thermogenesis and it is responsible for regulating mitochondrial biogenesis. Ectopic expression of PGC-1α in WAs stimulates the expression of mitochondrial genes and thermogenic gene UCP1 (Seale, Kajimura et Spiegelman 2009; Kajimura, Seale et Spiegelman 2010).

1.2 G protein-coupled receptors

G protein-coupled receptors (GPCRs), also known as seven transmembrane receptors, represent the largest family of integral membrane proteins. Upon binding to diverse extracellular ligands such as hormones, neurotransmitters, chemokines and ions, GPCRs couple via heterotrimeric G proteins to regulate effector proteins for cellular functions (Wang et Wong 2009). More than 800 GPCR genes are identified in the human genome data (Vassilatis et al. 2003) and more than 30% of the Food and Drug Administration (FDA) approved drugs are designed to bind and target to GPCRs (Overington, Al-Lazikani et Hopkins 2006).

1.2.1 G protein activation/deactivation cycle

GPCRs remain mostly in inactivated state on the cell surface until binding to extracellular ligands. Upon ligand stimulation, GPCRs undergo a conformational rearrangement at the intracellular region, leading to G protein binding. A G protein is a heterotrimeric protein composed of the three subunits α, β, and γ. The Gα subunit binds guanine nucleotides and controls the extent of G-protein signaling. In an inactive state, Gα subunit is bound to guanosine diphosphate (GDP) and the complex is associated to the GPCR together with Gβγ (Figure 2). Upon ligand binding to the GPCR, the conversion of Gα-bound nucleotide from inactive GDP to active GTP (guanosine triphosphate) is triggered by guanine nucleotide exchange factors (GEFs). Afterwards, Gα-GTP and Gβγ dissociate from the receptor and both of them interact with downstream effector proteins to proceed a signal transduction. For deactivation, Gα hydrolyzes GTP to GDP, thereby inactivates the signal cascade. Additionally, GTPase-activating protein (GAP) such as Regulator of G protein Signaling (RGS) family accelerates this process. When GTP is hydrolyzed to GDP, Gα-GDP is alienated from its effectors and re-associates with βγ-subunits, thereby returning to the inactive state (Pierce, Premont et Lefkowitz 2002; Milligan et Kostenis 2006; Johnston et Siderovski 2007).

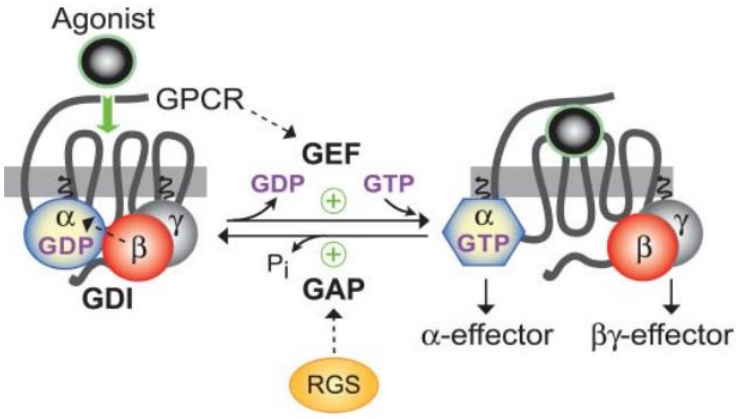

Figure 2. G protein activation/deactivation cycle (Adapted from: (Johnston et Siderovski 2007)). On binding of ligands (e.g. agonist), GPCRs facilitate G protein nucleotide exchange (GDP to GTP) to initiate a downstream signal. The signal is terminated on hydrolysis of GTP to GDP in the Gα subunit, which is accelerated by GTPase activating proteins (GAP) such as Regulator of G protein Signaling (RGS) proteins.

1.2.2 G protein-dependent signaling

Based on alpha subunit structure and function, G-proteins are divided into four families: $G\alpha_s$, $G\alpha_{i/o}$ ($G\alpha_i$), $G\alpha_{q/11}$ ($G\alpha_q$), and $G\alpha_{12/13}$. Each G protein subclass regulates specific downstream effectors and mediates distinct signal transduction (Figure 3) (Neves, Ram et Iyengar 2002; Pierce, Premont et Lefkowitz 2002; Wang et Wong 2009).

$G\alpha_s$ and $G\alpha_i$: Activation of $G\alpha_s$-GPCRs stimulates adenylyl cyclase (AC) to convert adenosine triphosphate (ATP) into cyclic adenosine monophosphate (cAMP). Enhanced cAMP works as a second messenger and leads to the activation of protein kinase A (PKA) that is an important enzyme for cell metabolism. In contrast to $G\alpha_s$, $G\alpha_i$-mediated signaling inhibits AC, thereby decreasing the cAMP concentration (Lefkowitz 2007; Pierce, Premont et Lefkowitz 2002).

$G\alpha_q$: The canonical $G\alpha_q$ signaling activates phospholipase C-β (PLCβ), which hydrolyzes plasma membrane phosphatidyl inositol lipids, releasing the second messenger inositol 1,4,5-trisphosphate (IP_3) and diacylglycerol (DAG). The released IP_3 promotes Ca^{2+} mobilization through IP_3 receptors in the membrane of the endoplasmic reticulum (ER), while DAG activates protein kinase C (PKC) (Sánchez-Fernández et al. 2014). Another important $G\alpha_q$ effector is the small GTPase protein RhoA. $G\alpha_q$ signaling activates RhoA and its downstream effector Rho-associated protein kinase (ROCK). The activated RhoA/ROCK functions as a molecular switch that mediates signal transduction to regulate diverse cellular processes (Etienne-Manneville et Hall 2002).

$G\alpha_{12/13}$: $G\alpha_{12/13}$-mediated signaling activates Rho-guanine nucleotide exchange factors (RhoGEFs; p115-RhoGEF, PDZ-RhoGEF, and LARG), which regulates RhoA activity. RhoA is a small GTPase protein that is associated with cytoskeleton regulation. Upon binding to GTP, RhoA can further activate various proteins such as Rho-kinase (ROCK) for cytoskeleton

regulation which develop contractile force generation (Rath et Olson 2012). GPCRs coupled to $G\alpha_{12/13}$ can often interact also with other subclasses, often $G\alpha_q$ (Worzfeld, Wettschureck et Offermanns 2008).

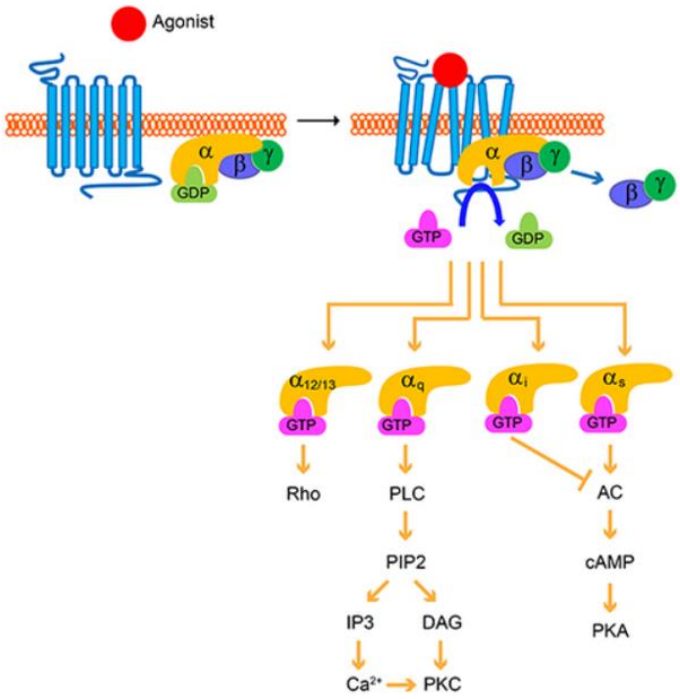

Figure 3. G protein-dependent signaling (Modified from: (Wang, Gareri et Rockman 2018)). $G\alpha_s$-mediated signaling stimulates adenylyl cyclase (AC) for cAMP production, whereas $G\alpha_i$-mediated signaling inhibits AC. $G\alpha_q$-coupled receptor signaling activates phospholipase C-β (PLCβ), increasing intracellular Ca^{2+} mobilization. $G\alpha_{12/13}$-mediated signaling activates Rho GTPases.

1.2.3 GPCRs in brown adipocytes

Although GPCR signaling is an indispensable regulator for biological processes in various tissues including adipose tissue (Wettschureck et Offermanns 2005), only few studies have identified the function of GPCRs in brown adipocytes. One of the most explored GPCRs in BAT is the $G\alpha_s$-coupled β3 adrenergic receptor. β3 adrenergic receptors are highly expressed in BAT and their activation stimulates lipolysis and thermogenesis. Upon activation of β3 adrenergic receptors by NE, ACs promote a production of cAMP, followed by activation of PKA. Thereby, PKA phosphorylates hormone sensitive lipase (HSL) leading to lipolysis. As a result of lipolysis, FFAs are released from lipid droplets and further induce UCP1 activation (Cannon et Nedergaard 2004). Adenosine A_{2A} receptor, a $G\alpha_s$-coupled receptor, was recently shown to increase BAT dependent thermogenesis (Gnad et al. 2014). Pharmacological or genetic inhibition of A_{2A} receptor in mice results in a decrease of BAT thermogenesis. In contrast, A_{2A} agonists or A_{2A} overexpression stimulate energy expenditure and protect against high-fat diet induced obesity.

Recently, gene profiling data of GPCRs in brown adipocytes demonstrated that 21% of GPCRs link to $G\alpha_q$ proteins, implicating a potential role of $G\alpha_q$-coupled GPCRs in BAT (Klepac et al. 2016). However, the role of $G\alpha_q$-signaling in brown adipocytes is poorly understood. One study by our group suggests a negative effect of $G\alpha_q$-coupled GPCRs on brown adipocytes by inhibiting brown adipocytes differentiation (Klepac et al. 2016). The inhibitory effect of $G\alpha_q$-GPCRs on brown adipogenesis acts through RhoA/ROCK signaling cascade. The constitutively active $G\alpha_q$ protein in BAT reduced UCP1 expression and energy expenditure *in vivo* (Klepac et al. 2016). Another study showed a possible positive effect of $G\alpha_q$ signaling, indicating that $G\alpha_q$-coupled GPR120 signaling promotes metabolic health and BAT activation (Schilperoort et al. 2018; Quesada-López et al. 2019). The agonist of GPR120, TUG-891 enhanced UCP1 activity, further increasing oxygen consumption in BAT (Schilperoort et al. 2018). These debate warrants further investigation to decipher the role of $G\alpha_q$-coupled GPCRs and related intracellular mechanisms in brown adipocytes.

1.3 Hippo pathway

The Hippo pathway has been a compelling regulator of cellular proliferation, differentiation, and tissue homeostasis (Hansen, Moroishi et Guan 2015; Ardestani, Lupse et Maedler 2018). Now that the effectors of Hippo pathway signaling contribute to many physiological processes in the cells and tissues, its dysregulation is engaged in diverse pathological diseases such as cancers and metabolic diseases (Ardestani, Lupse et Maedler 2018).

Hippo pathway signaling contains: (1) a serial of kinase cascade reactions by kinase proteins, STE20-like protein kinase 1/2 (MST1/2) and large tumor suppressor 1/2 (LATS1/2), and (2) transcriptional regulation by transcriptional co-activator yes-associated protein (YAP) and WW Domain Containing Transcription Regulator 1 (TAZ). The kinase modulators, MST1/2 and LATS1/2, work in combination with their adaptor proteins salvador family WW domain-containing protein 1(SAV1) and MOB kinase activator 1A/B (MOB1A/B), respectively. When Hippo pathway is on, MST1/2 initiates signaling cascade via phosphorylation of SAV1 and MOB1A/B, which further leads to recruitment and activation of LATS1/2 by phosphorylation. The activated LATS1/2 inhibits the transcription module by direct phosphorylation of YAP and TAZ leading to cytoplasmic retention and proteasomal degradation (Figure 4 left) (Ardestani, Lupse et Maedler 2018). Contrary, shutting down of Hippo signaling promotes dephosphorylation of YAP and TAZ. These transcriptional effectors are able to translocate into nucleus and interact with transcription factors such as TEAD family to induce target gene expression (Figure 4 right).

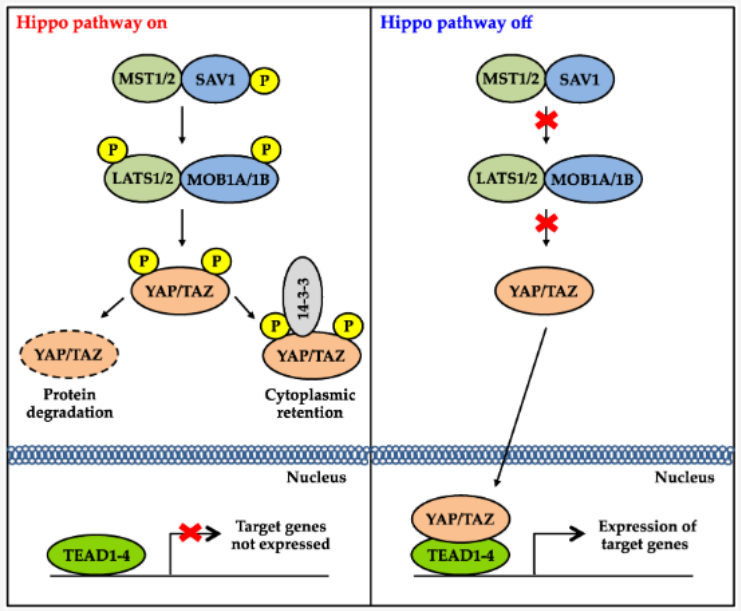

Figure 4. The overview of Hippo signaling pathway (Adapted from: (Juan et Hong 2016)). The activated Hippo signaling leads to phosphorylation of MST1/2, followed by phosphorylation of LATS1/2. Subsequently, the phosphorylated LATS1/2 inhibits YAP and TAZ by direct phosphorylation. Phosphorylated YAP and TAZ recruit 14-3-3 proteins that induce cytoplasmic retention or undergo proteasomal degradation. In contrast, YAP and TAZ are dephosphorylated when Hippo pathway is inactivated, thereby move to nucleus and induce a target gene expression.

1.3.1 Upstream regulators of the Hippo pathway: GPCRs

The Hippo pathway is regulated by a number of stimuli including cell-contact inhibition (Gumbiner et Kim 2014; Zhao et al. 2007), mechanical stress (Panciera et al. 2017), cytoskeletal arrangement (Zhao et al. 2012; Seo et Kim 2018), and GPCRs (Yu et al. 2012; Zhou et al. 2015). Extensively studied upstream regulators are members of GPCRs and Hippo downstream effectors are differently regulated by different G proteins (Zhou et al. 2015). $G\alpha_s$-PKA signaling has been shown to activate the Hippo pathway causing YAP/TAZ inhibition via increased phosphorylation in cancer cell lines (Yu et al. 2013; Iglesias-Bartolome et al. 2015; Yu et al. 2012). Whereas, $G\alpha_q$-coupled GPCRs are involved in YAP/TAZ activation (Feng et al. 2014; Yu et al. 2014; Annala et al. 2019). The activated $G\alpha_q$ signaling activates Rho GTPases resulting in LATS1/2 inhibition, thereby promoting YAP/TAZ activity via direct dephosphorylation. Serum-borne lysophosphatidic acid (LPA) or sphingosine 1-phosphophate (S1P) that act through $G\alpha_{12/13}$-GPCRs are shown to inhibit LATS1/2, thereby activating YAP/TAZ in HEK293A cells (Yu et al. 2012).

1.3.2 The link between $G\alpha_q$ signaling and YAP

So far, most of the YAP studies with respect to $G\alpha_q$ signaling have been conducted in cancer cells. Uveal melanoma (UM) is the most common case of human eye cancer harboring activating mutation in *GNAQ* and *GNA11* that encodes members of the $G\alpha_q$ subunits. The cancer-associated $G\alpha_{q/11}$ mutation in UM cells reveals YAP activation, but the activation of YAP is inhibited by knock down of $G\alpha_q$ (Yu et al. 2014). The underlying mechanism of YAP activation in $G\alpha_q$ mutant cells is independent from PLCβ activation, but requires Rho GTPase, whose activation is mediated by $G\alpha_q$-specific RhoGEF Trio (Feng et al. 2014). Most recently, FR900359, a selective $G\alpha_{q/11}$ inhibitor, has been identified as an inhibitor of $G\alpha_q$-driven YAP activation in UM cells harbouring constitutively active $G\alpha_{q/11}$ mutation (Annala et al. 2019). Endothelin 1 (ET1) is an endogenous hormone that can activate $G\alpha_q$ signalling. ET1 signals through $G\alpha_q$-coupled Endothelin receptor type A (Ednra) to activate RhoA/ROCK, leading to colon cell proliferation and tumorigenesis via the activation of YAP/TAZ (Wang et al. 2017). Thus, these findings suggest that the non-canonical $G\alpha_q$ signaling is involved in YAP activity via RhoGEF-mediated RhoA activation.

1.3.3 Hippo pathway signaling in adipocytes

Previously, the role of the Hippo pathway in adipocyte proliferation, differentiation and adipogenesis has been studied. LATS2, one of Hippo kinase effectors is identified as a positive regulator of adipocyte differentiation by inhibiting YAP/TAZ activity in cultured 3T3-L1 adipocytes (An et al. 2013). In contrast to LATS2, the inhibitory role of YAP/TAZ in adipocyte differentiation was determined in the white adipocyte cell line 3T3-L1 (Yu et al. 2012). This paper showed that knockdown of YAP/TAZ promotes adipocyte differentiation, whereas overexpression of YAP suppresses adipocyte differentiation. Mechanistically, TAZ, but not YAP, binds to and inhibits PPARg leading to reduced adipocyte differentiation in mesenchymal stem cells (MSCs) (Hong et al. 2005). *In vivo*, adipocyte-specific TAZ knockout in mice resulted in enhanced PPARg activity, improved glucose tolerance, and decreased adipose tissue inflammation (El Ouarrat et al. 2020). Similarly, YAP overexpression in mice caused

TAZ downregulation, PPARg activation, thereby leading to white adipocyte differentiation and expansion (Kamura et al. 2018). All these data identify the inhibitory role of TAZ in PPARg activity and adipocyte differentiation. Moreover, the role of YAP in cell fate decision of MSCs was examined, which promotes osteogenesis and suppresses adipogenesis (Chen et al. 2016; Pan et al. 2017; Pan et al. 2018). To date, only one finding proposed the role of YAP/TAZ in thermogenic adipocytes. This study showed that adrenergic stimulation induces cellular stiffness promoting cellular respiration and UCP1 in thermogenic adipocytes and this process is regulated by YAP/TAZ (Tharp et al. 2018). However, the independent role of YAP in thermogenic adipocytes is not studied yet.

1.4 Aim of thesis

$G\alpha_q$ signaling has been shown to inhibit brown adipocyte differentiation via RhoA/ROCK signaling cascade (Klepac et al. 2016). However, the downstream effectors of $G\alpha_q$/RhoA/ROCK are still unknown. Previous studies have demonstrated that $G\alpha_q$-mediated signaling can stimulate the transcriptional cofactor YAP through RhoA GTPase, leading to cancer cell proliferation and growth (Yu et al. 2012; Feng et al. 2014; Yu et al. 2014). Therefore, this thesis focused on YAP as a downstream effector of $G\alpha_q$-coupled receptor signaling in brown adipocytes. Moreover, since the role of YAP in brown adipocytes is not fully understood, this study assessed the effect of YAP on brown adipogenesis and function.

The major questions addressed in this thesis are:

1) Does $G\alpha_q$ signaling have a role in regulation of YAP activity in brown adipocytes?
2) Does YAP have a functional effect on brown adipocyte differentiation and/or thermog enesis?
3) Does YAP play a role in diet-induced obesity?

2. Materials and Methods

2.1 Materials

If not further specified, all common chemicals were purchased from: Carl Roth, Gibco-Invitrogen, Merck, Roche, Sigma-Aldrich, AppliChem, and VWR International. Specific chemicals have also been described in respective sections.

2.2 *in vivo* experiments

2.2.1 Mice

Breeding pairs of YAP-floxed mice (*YAP*$^{loxP/loxP}$, stock: Yap1$^{tm1.1Dupa}$/J) and adiponectin-Cre (*Apn-Cre*, stock: B6.FVB-Tg(Adipoq-cre)1Evdr/J) were purchased from Jackson laboratories, USA. YAP-floxed mice were crossed with *Apn-Cre* mice at 8 weeks of age and the offspring was separated by sex and marked with ear punch at the age of 3-4 weeks after birth. Genomic DNA isolated from ear snips were used for PCR analysis for genotyping and the primer list is indicated in the table below (Table 1). The PCR was processed according to the instructions from Jackson laboratories. YAP homozygous floxed mice with *Apn-Cre* (genotype: *YAP*$^{loxP/loxP}$;*Apn-Cre*, YKO) were used for loss of function experiments and the control groups were littermate animals without Cre expression (genotype: *YAP*$^{loxP/loxP}$, ctrl). Wild type C57Bl/6J mice were purchased from Charles River laboratories. All mice were maintained on a daily cycle of 12 h light (06:00–18:00 hours) and 12 h darkness (18:00–06:00 hours), and were allowed free access to standard chow and water. Mice were maintained and bred in the animal facility of H.E.T. (House of Experimental Therapy Centre) at University of Bonn in Germany. All animal study was approved by the Landesamt für Natur, Umwelt und Verbraucherschutz, NRW, Germany.

Table 1. Primer list of genotyping

Primer	Forward (5´- 3´)
Adiponectin-Cre(15381)	ACG GAC AGA AGC ATT TTC CA
Adiponectin-Cre(18564)	GGA TGT GCC ATG TGA GTC TG
Adiponectin-Cre(oIMR 7388)	CTA GGC CAC AGA ATT GAA AGA TCT
Adiponectin-Cre(oIMR 7339)	GTA GGT GGA AAT TCT AGC ATC ATC C
YAP_forward	AGG ACA GCC AGG ACT ACA CAG
YAP_reverse	CAC CAG CCT TTA AAT TGA GAA C

2.2.2 High-fat diet experiments

For diet induced obesity experiments, YKO and littermate ctrl mice were fed a high-fat diet (HFD) (60% of calories from fat, D12492) or normal chow control diet (CD) (D12450B) for 12

weeks (Ssniff GmbH, Germany). Male mice were used for the experiments and the mice were weighed weekly.

2.2.3 Body composition

Body composition (lean mass, water and fat mass) was determined using a benchtop NMR device Minispec (Bruker Corporation). For HFD experiments, body composition was measured before sacrifice.

2.2.4 Indirect calorimetry (TSE measurement)

Oxygen consumption (VO_2) was measured using a Phenomaster device (TSE systems). At the last week of CD or HFD (12 weeks), the mice were housed at 23°C for 24-hours to measure oxygen consumption. During the study, the mice were maintained on a daily cycle of 12 h light (06:00–18:00 hours) and 12 h darkness (18:00–06:00 hours), and were allowed free access to indicated diet and water.

2.2.5 Glucose tolerance test (GTT)

GTT was performed in mice fed CD or HFD at 11 weeks old and they were fasted for 5 hours before the assay. The mice were *i.p.* injected with 8 µl of glucose solution (0.25 g/ml)/ body weight (g) and the blood glucose was measured from tail vein at 0, 30, 60, 90 and 120 minutes after injection.

2.3 Cells

Bovine Serum Albumin (BSA), Fatty acid free (Sigma-Aldrich)

Collagenase Type Ⅱ (Worthington, UK)

d-Biotin (Sigma-Aldrich)

Dexamethasone (Sigma-Aldrich)

Dimethylsulfoxide (DMSO) (Carl Roth)

Dulbecco's Modified Eagle Medium Glutamax I +4500mg/dl Glucose (DMEM) (Thermo Fisher Scientific)

HEPES (Sigma-Aldrich)

Insulin (Sigma-Aldrich)

Isobutylmethylxanthine (IBMX) (Sigma-Aldrich)

L-Ascorbate (Sigma-Aldrich)

Panthothenate (Sigma-Aldrich)

P/S (Biochrom)

Rosiglitazone (Sigma-Aldrich)

T3 (Sigma-Aldrich)

Trypan Blue Solution, 0.4% (Thermo Fisher Scientific)

Trypsin (+EDTA) (Thermo Fisher Scientific)

2.3.1 BAT-MSCs (mesenchymal stem cells) isolation

BAT-MSCs (hereafter, called as brown preadipocytes) were isolated from interscapular BAT pads of newborn C57Bl/6J mice as previously described (Haas et al. 2009). The isolated fat pads were immerged in isolation buffer and incubated in 37°C water bath for 30 minutes with hand shaking every 5 minutes. Thereafter, the tissue remnants were removed by filtration with a 100 µm nylon mesh (Millipore) and the suspension was placed on ice for 30 minutes. After the incubation, the middle phase containing MSCs fraction was filtered through a 30 µm nylon mesh (Millipore) and centrifuged at 700 g for 10 minutes. The cell pellets were resuspended in culture media and seeded on 6-well plates. Cells were incubated at 37°C and 5% CO_2. For loss of function study of YAP in adipocytes, primary BAT-MSCs (primary brown preadipocytes) were isolated from BAT pads of newborn littermatched *YAP*$^{loxP/loxP}$ (ctrl) or *YAP*$^{loxP/loxP}$*;Apn-Cre* (YKO) mice in a same way.

Isolation buffer (pH 7.4)

NaCl	123 mM
KCl	5 mM
$CaCl_2$	1.3 mM
Glucose	5 mM
HEPES	100 mM

Dissolved in H_2O, adjust pH, sterile filtered, and stored at 4°C

Before use, following substances were added and sterile filtered again

BSA,Fatty acid free	1.5 %
Collagenase Type Ⅱ	0.2 %

Culture media

DMEM Glutamax I +4500mg/dl Glucose	
FBS	10 %
P/S	1 %
Insulin	4 nM

T3	4 nM
HEPES	10 nM
Sodium ascorbate	25 μg/ml

2.3.2 Immortalization of primary BAT-MSCs

BAT-MSCs (brown preadipocytes) were immortalized 24 hours after isolation by transduction with a lentivirus expressing SV 40 large T-antigen under control of the phosphoglycerate kinase (PGK) promoter (Haas et al. 2009). Immortalized cells were expanded in growth medium (GM) at 37°C and 5% CO_2. The cells were not used beyond passage 6.

Growth media (GM)

DMEM Glutamax I +4500mg/dl Glucose	
FBS	10 %
P/S	1 %

2.3.3 Cryopreservation

The cells were maintained in growth medium in 37°C and 5% CO_2 incubation till confluency. For detachment, the cells were washed with PBS and treated with Trypsin-EDTA for 5 minutes in the incubator. The detached cells were resuspended in GM and centrifuged at 1000 rpm for 10 minutes. Afterwards, the cells were counted with trypan blue (1:1) in a Neubauer counting chamber (Labomedic). One million cells per tube were cryopreserved in cryo-medium for 24 hours at -80°C and following stored at -150°C.

Cryo-medium

DMEM Glutamax I +4500mg/dl Glucose	
FBS	10 %
P/S	1 %
DMSO	10 %

2.3.4 Adipogenic differentiation of immortalized BAT-MSCs

BAT-MSCs (brown preadipocytes) were seed in GM on a 6-well plate in a density of 1.6 x 10^5 cells per well or a 12-well plate in a density of 0.8 x 10^5 cells per well (day -4). After 48 hours (day -2), the medium was replaced by differentiation medium (DM). On day 0, the cells were confluent and then treated with induction medium (IM) for 48 hours. After the induction, the medium was changed to DM for the next 5 days (day +7, mature brown adipocytes), which was replenished every second day (Haas et al. 2009) (Figure 5).

Differentiation medium (DM)

DMEM Glutamax I +4500mg/dl Glucose	
FBS	10 %

P/S	1 %
Insulin	4 nM
T3	4 nM

Induction medium (IM)

DM	
Dexamethasone	1 µM
IBMX	0.5 mM

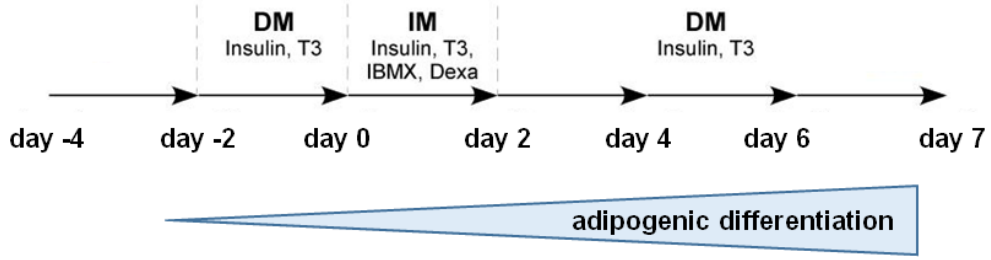

Fugure 5. **The scheme of differentiation protocol of immortalized BAT-MSCs (from brown preadipocytes to mature brown adipocytes).**

2.3.5 Isolation of WAT-MSCs

WAT-derived MSCs (hereafter, white preadipocytes) were isolated from inguinal white fat (WATi) pads of 6–14 weeks old WT C57Bl/J mice. The isolated tissues were coarsely chopped and transferred in digestion buffer for 30 minutes at 37°C with intermittent shaking. The digested tissues were placed at RT for 10 minutes and the floating adipocyte fraction was removed by taking off the upper phase. Afterwards, the cells were filtered through a 100 µm nylon mesh and centrifuged at 1000 rpm for 10 minutes. The collected cells were resuspended and seeded in white adipocytes growth medium (WA-GM) on T–75 plates and placed in incubator (at 37°C and 5% CO_2). After cell attachment, flasks were washed with PBS and replaced with fresh GM. For crypreservation, the confluent cells were detached from the flask by trypsin-EDTA and the collected cells were resuspended in cryo-medium as described above (2.3.3). For loss of function study of YAP in white adipocytes, WAT-MSCs (white adipocytes) were isolated from WATi of littermatched *YAP$^{loxP/loxP}$* (ctrl) or *YAP$^{loxP/loxP}$;Apn-Cre* (YKO) mice in a same way.

Digestion medium

DMEM Glutamax I +4500mg/dl Glucose	
BSA	0.5 %
Collagenase Type Ⅱ	1.5 mg/ml

White adipocytes Growth medium (WA-GM)

DMEM Glutamax I +4500mg/dl Glucose + Pyruvate	
FBS	10 %
P/S	1 %

Cryo-medium

FBS	
DMSO	10 %

2.3.6 Adipogenic differentiation of WAT-MSCs (white adipocytes)

For differentiation, the cells were seeded in WA-GM on a 6-well TPP plate in a density of 1.6 x 10^5 cells per well and placed at 37°C and 5% CO_2. On reaching confluency (day -2), the cells were kept in WA-GM for 2 additional days (day 0). On day 0, white adipocytes induction medium (WA-IM) were treated in the cells for 2 days (day +2) and differentiated in maintenance medium (MM) for the next 8 days, which was replenished every second day.

White adipocytes induction medium (WA-IM)

DMEM Glutamax I +4500mg/dl Glucose +Pyruvate	
FBS	5 %
P/S	1 %
Insulin	172 nM
Dexamethasone	0.25 µM
IBMX	0.5 mM
T3	1 nM
ABP	
L-Ascorbat	50 µg/ml
d-Biotin	1 µM
Panthothenat	17 mM
Rosiglitazone	1 µM

Maintenance medium (MM)

DMEM Glutamax I +4500mg/dl Glucose +Pyruvate	
FBS	5 %
P/S	1 %
Insulin	172 nM
T3	1 nM
ABP	

2.3.7 Isolation and differentiation of primary BAT-derived MSCs

Primary BAT-derived MSCs (hereafter, primary brown adipocytes) were isolated from BAT pads of 7-14 weeks old *YAP$^{loxP/loxP}$* (ctrl) or *YAP$^{loxP/loxP}$;Apn-Cre* (YKO) mice as described above (2.3.1) . For differentiation, the cells were seeded in on a Seahorse XF24 V7 PS Cell Culture Microplates and placed at 37°C and 5% CO_2. On reaching confluency (day -2), the cells were kept in GM for 2 additional days (day 0). On day 0, primary brown adipocytes induction medium (BA-IM) were in the cells for 2 days (day +2) (Trajkovski et al. 2012) and differentiated in DM for the next 7 days, which was replenished every second day.

Primary brown adipocytes induction medium (BA-IM)

DM	
Dexamethasone	1 µM
IBMX	0.5 mM
Rosiglitazone	1 µM
Indomethacin	125 nM

2.3.8 Lentiviral infection

pLenti6.3V5-HA-hM3D(Gq)-mCherry (Dq) lentiviral vectors were provided by Bryan Roth, University of North Carolina. The lentiviral vectors were generated at the viral platform of this laboratory (Institute of Pharmacology and Toxicology, University of Bonn, Bonn) (Haas et al. 2009; Jennissen et al. 2012). The CMV-Cre lentiviral vector and control lentiviral vector (CMV-rrl-156) were described previously (Pfeifer et al. 2001). For the viral infection, the cells were seeded on a 6-well in GM and incubated at 37°C and 5% CO_2 for 6-8 hours for adherent to the wells. Thereafter, the cells were treated with lentiviruses corresponding to 75 ng/well of Dq virus; 100 ng/well of CMV-Cre or CMV-rrl-156 in a fresh GM. Upon virus transduction, the cells were further differentiated as described above (2.3.4).

2.3.9 Substances

All cells were treated with following substances.

Clozapine-N-oxide (CNO) (Tocris, 1µM)

Y27632 (Tocris, 10µM)

CL-316,243 (Tocris, 1µM)

2.4 Western blotting and Phos-tag gel

Acrylamide,Rotiphorese ® Gel 30 (37.5:1) (Carl Roth)

Bovine Serum Albumin (BSA) (Carl Roth)

Coomassie dye, Coomassie brilliant blue (Merck Millipore)

Protease inhibitor cocktail, Complete® EDTA-free (Roche)

2.4.1 Protein extraction and quantification

Lysis buffer containing indicated protease below was freshly prepared for protein isolation from cells and tissues. Cells were collected using cell scraper and tissues were homogenized using hand-held tissue homogenizer. The extracted samples were ultrasonicated for 30-60 seconds, followed by centrifugation (13000rpm, 4°C) for 20 minutes. The supernatant was carefully collected in a new tube.

Lysis buffer

Tris, pH 7.5	50 mM
Sodium chloride (NaCl)	150 mM
NP-40	1%
Sodium deoxycholate	0.5%
Sodium-dodecyl sulphate (SDS)	0.1%
Ethylenediaminetetraacetic acid (EDTA)	0.1 mM
ethylene glycol-bis(β-aminoethyl ether)-N,N,N′,N′-tetraacetic acid (EGTA)	0.1 mM

Dissolved in H2O, sterile filtered and stored at 4°C

Before use the following substances were added

Complete protease inhibitor cocktail	1 mM
Na_3VO_4	1 mM
NaF	10 mM

Protein content was determined by the Bradford method. 2 µl of protein lysates were added into 98 µl of 0.15 nM NaCl for the protein samples and 100 µl of 0.15 nM NaCl was used for the blank. To measure colorimetric absorbance, 1 ml of coomassie solution was included in the mixture of protein lysate and 0.15 nM NaCl, followed by measuring at 595 nm to determine protein concentration (µg/ml).

Coomassie solution

Coomassie brilliant blue G-250	0.01 %
Methanol	5 %
H_3PO_4	17 %

Dissolved in H_2O and stored at 4°C

2.4.2 Sodium dodecyle-sulphate polyacrylamide gel electrophoresis (SDS-PAGE)

For discontinuous gel electrophoresis, polyacrylamide gels were prepared with the mini trans-blot® electrophoretic transfer cell system, whose components are shown below table.

Separation gel (10 ml)

	10%	15%
H_2O	4 ml	2.3 ml
30% Acrylamide	3.3 ml	5 ml
1.5 M Tris (pH 8.8)	2.5 ml	2.5 ml
20% ammonium persulfate	0.05 ml	0.05 ml
N,N,N′,N′-Tetramethylethylenediamine (TEMED)	4 µl	4 µl

Stacking gel

	5%
H_2O	3.4 ml
30% Acrylamide	0.83 ml
1.5 M Tris (pH 6.8)	0.63 ml
20% ammonium persulfate	0.02 ml
N,N,N′,N′-Tetramethylethylenediamine (TEMED)	8 µl

After adjusting equal amounts of protein concentration (30-50 µg), three times concentrated loading buffer (3x Laemmli) were added to the protein lysates and the samples were boiled at 95°C for 5 minutes. The samples were loaded into the wells of prepared gel cassette. SDS-PAGE was performed in 1x electrophoresis at 100V for 90-120 minutes at room temperature (RT).

3x Laemmli buffer

Tris-HCL, pH 6.8	125 mM
SDS	17 %
Bromphenol Blue	0.015 %

Dissloved in H_2O and stored at -20°C

Before use, β-Mercaptoethanol was added (final concentration 10%)

10x electrophoresis buffer

Tris	250 mM
Glycine	2 M
SDS	0.01 %

Dissolved in H_2O and stored at RT

Before use, 10x electrophoresis buffer was diluted to 1x concentration

2.4.3 Western blotting and immune-detection

After separating the proteins by SDS-PAGE, a transfer construction was assembled using mini trans-blot® electrophoretic transfer cell system. Proteins from the gel were electrically transferred onto the nitrocellulose membrane with transfer buffer under 300 mA for 90 minutes. After completing transfer process, the membranes were removed from the cassette and blocked in 5% BSA containing TBS-T for 1 hour at RT.

Transfer buffer

10x electrophoresis buffer	10 %
Methanol	20 %
H_2O	70 %

TBS-T (pH 8.8)

Tris	10 mM
NaCl	140 mM
Tween-20	0.01 %

Thereafter, membranes were incubated in primary antibody at 4°C overnight in blocking buffer. On the next day, the membranes were washed three times in TBS-T for 5 minutes, followed by incubation in appropriate HRP-conjugated secondary antibody at RT for 1 hour. After secondary antibody incubation, membranes were washed three times for 5 minutes in TBS-T and immerged in enhanced chemiluminescence (ECL) solution. ImageQuant LAS 4000 chemiluminescence reader was used for the chemiluminescence based detection. Upon the completion of detection, membranes were shortly washed in TBS-T and stripped with stripping buffer for 15 minutes. After 3x5 minutes washing with TBS-T, membranes were blocked and incubated with primary antibody in blocking buffer for the next protein of interest. The primary and secondary antibodies are listed in the table below (Table 2).

Stripping buffer (pH 2.0)

Glycine	2.5 M
SDS	1 %

Dissolved in H_2O and adjusting pH with HCl

2.4.4 Phos-tag SDS-PAGE

Phos-tag™ (Phos-tag™ AAL-107) is a synthesized chemical compound that binds phosphorylated ions and this molecule can be used for mobility shift detection of phosphorylated proteins using phosphate affinity SDS-PAGE. Phos-tag™ acrylamide and manganese chloride ($MnCl_2$) are incorporated into the SDS-PAGE separation gel to capture the phosphate groups of proteins in the sample. Phos-tag bound phosphorylated proteins decrease the migration speed enabling separation of phosphorylated and non-phosphorylated forms (Figure 6). The components of separation gel containing Phos-tag™ and $MnCl_2$ are described in below. The preparation of stacking gel and SDS-PAGE process are same as described above (2.4.2). Upon the completion of electrophoresis, the gel was soaked in a transfer buffer containing 1 mM EDTA to eliminate the manganese ion for 10 minutes, followed by incubation in a transfer buffer without 1 mM EDTA for 10 minutes. Further immunoblotting was performed according to the explanation above.

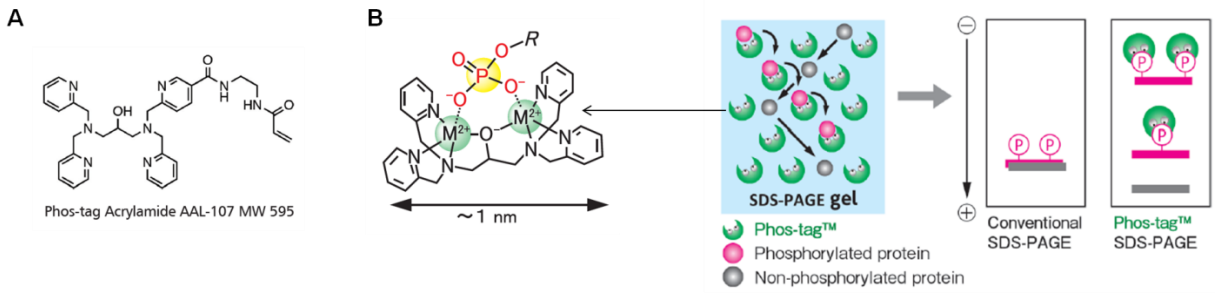

Figure 6. (A) Basic structure of Phos-tag™ AAL-107. (B) The structure of Phos-tag™ acrylamide and $MnCl_2$ in SDS-PAGE separation gel (left) and the principle of Phos-tag SDS-PAGE (right) (Modified from: Wako chemicals).

Phos-tag separation gel (7 ml)

	10%
H_2O	2.604 ml
30% Acrylamide	2.33 ml
1.5 M Tris (pH 8.8)	1.75 ml
10% ammonium persulfate	0.10 ml
5.0 mM Phos-tag™ AAL-107	98 µl
10 mM $MnCl_2$	98 µl
N,N,N′,N′-Tetramethylethylenediamine (TEMED)	20 µl

Table 2. Antibody list

Antibody	Company
Phospho-YAP (Ser127)	Cell signaling (13008)
YAP	Cell signaling (14074)
YAP/TAZ	Cell signaling (8418)

UCP1	Sigma-Aldrich (sc-6529)
PPARg	Cell signaling (2430)
aP2	Cell signaling (2120)
tubulin	Dianova (MS-719-P0)
GAPDH	Cell signaling (2118)
calnexin	Merck Millipore (208880)
Anti-rabbit-HRP	Cell signaling (7074)
Anti-mouse-HRP	Dianova (115-035-146)

2.5 mRNA expression

2.5.1 RNA isolation and reverse transcription

Diethyl pyrocarbonate (DEPC) (Carl Roth)

InnuSolv RNA reagent (Analytik Jena)

NanoDrop 2000 (Thermo Fisher Scientific)

First Strand cDNA Synthesis Kit (NEB)

In cells, 1 ml of InnuSolv reagent was added to the well and the solution was transferred to new tubes. Afterwards, 200 µl chloroform was added to the solution and thoroughly shaken. After 5 minutes incubation at RT, the samples were centrifuged (13000 rpm, 4°C) for 10 minutues and the clear middle phases were collected in new tubes. For tissue explants, 500 µl of InnuSolv reagent was added, follwed by homogenization. Afterwards, 1 ml of InnuSolv reagent was additionally added and vigorously shaken. After 5 minutes incubation at RT, the samples were centrifuged (13000 rpm, 4°C) for 10 minutes. The homogenized samples were collected to new tubes avoiding the fatty monolayer on the top. 300 µl of chloroform was added and thoroughly shaken. After incubation for 3 minutes at RT, the samples were centrifuged (13000 rpm, 4°C) for 30 minutes and the upper aqueous phase were transferred to new tubes. Afterwards, 200 µl of chloroform was additionally added and vigorously shaken. The samples were then incubated for 3 minutes at RT, and centrifuged (13000 rpm, 4°C) for 10 minutes. After centrifugation, the clear aqueous phase was collected in new tubes. Into the cell or tissue samples, 500 µl of isopropanol was added, and the tubes were shaken vigorously. The samples were then centrifuged (13000 rpm, 4°C) for 10-minutues and the supernatant was discarded. The pellet was washed with 75% ethanol two times and the tubes were left to dry. Afterwards, the dried pellet was resolved in DEPC-H_2O, followed by incubation at 55°C for 10 minutes. RNA content were measured using NanoDrop.

1 µg of RNA was used for reverse transcription into complementary DNA (cDNA) using First Strand cDNA Synthesis Kit (NEB) according to the manufacturer´s instructions.

2.5.2 Quantitative real-time polymerase chain reaction (qRT-PCR)

Power SYBR Green PCR Master Mix (Applied Biosystems)

Real-time PCR cycler: Applied Biosystems StepOnePlus System (Thermo Fisher Scientific)

Quantitative real-time PCR (qPCR) analysis was performed on the diluted cDNA (1:10 dilution in water) with SYBR green fluorescent dye to determine mRNA expression. Power SYBR Green PCR Master Mix (Applied Biosystems) was mixed with target-specific primers to perform qPCR analysis in a StepOnePlus Real time PCR instrument (Thermo Fisher Scientific). Relative expression was calculated using ΔCt method, with murine hypoxanthine guanine phosphor-ribosyltransferase (HPRT) as house-keeping gene (internal control). The primers used for qPCR analysis are listed below (Table 3).

Table 3. Primer list for qRT-PCR.

Primer	Forward (5´- 3´)	Reverse (5´- 3´)
YAP	CAGGAATTATTTCGGCAGGA	CATCCTGCTCCAGTGTAGGC
TAZ	GAAGGTGATGAATCAGCCTCTG	GTTCTGAGTCGGGTGGTTCTG
CYR61	CAGCTCACTGAAGAGGCTTCCT	GCGTGCAGAGGGTTGAAAA
UCP1	TAAGCCGGCTGAGATCTTGT	GGCCTCTACGACTCAGTCCA
PPARg	ACTGCAGCCCCCTATAGT	GGATCAGTTGGGTCAGTGGG
PGC1a	GCACACACCGCAATTCTCCCTTGTA	ACGCTGTCCCATGAGGTATTGACCA
Elovl3	ATGCAACCCTATGACTTCGAG	ACGATGAGCAACAGATAGACG
Dio2	GCGATGGCAAAGATAGGTGA	GAATGGAGCTGGGTGTAGCA
Cidea	GTCAAAGCCACGATGTACGAGAT	CGTCATCTGTGCAGCATAGGA
HPRT	GTCCCAGCGTCGTGATTAGC	TCATGACATCTCGAGCAAGTCTTT
Leptin	TGGCTGGTGTCAGATTGCTC	TAGTGCAAGGTTCTCTGAGCG
IL-6	CCAGAGATACAAAGAAATGATGG	ACTCCAGAAGACCAGAGGAAAT
IL-10	CCAAGGTGTCTACAAGGCCA	GCTCTGTCTAGGTCCTGGAGT
TNF-a	GTCCCCAAAGGGATGAGAAGT	TTTGCTACGACGTGGGCTAC
F4/80	CTTTGGCTATGGGCTTCCAGT	GCAAGGAGGACAGAGTTTATCGTG
CCL2	TGGAGCATCCACGTGTTG	GCTGGTGAATGAGTAGCAGCA

2.6 Immunofluorescence

4% PFA in PBS

0.1% Triton X-100 (Prolabo)

BSA free fatty acid free (Sigma-Aldrich)

anti-YAP primary antibody (Santa Cruz Biotechnology)

Alexa Fluor-labeled secondary antibodies (Thermo Fisher Scientific)

4′,6-diamidino-2-phenylindole (DAPI) (Molecular Probes)

Shandon Immu-Mount (Thermo Fisher Scientific)

Glass coverslips were placed in 24 well plates and brown preadipocytes were seeded at a density of 2,000 cells per well. Cells were then fixed with 4% PFA, followed by washing twice with PBS. The fixed cells were permeabilized with 0.1% Triton X-100 for 5 minutes at 4°C and then incubated in blocking solution (0.5% BSA in PBS) for 30 minutes at RT. After blocking, the cells were incubated in blocking solution containing an anti-YAP primary antibody overnight at 4°C. The next day, the cells were visualized with Alexa Fluor-labeled secondary antibodies and 4′,6-diamidino-2-phenylindole (DAPI) for nuclear staining. Afterwards, cells were mounted on glass slides with Shandon Immu-Mount for visualization.

2.7 Oxygen consumption

2.7.1 Seahorse XF Cell Mito Stress assays

Seahorse XFe24 Analyzer

Seahorse XFe24 FluxPak (#102340-100)

Seahorse XF24 V7 PS Cell Culture Microplates

Seahorse XF DMEM medium (pH 7.4)

Glucose

Glutamin

Sodiumpyruvate

Oligomycin (Sigma Aldrich)

FCCP (Tocris)

Antimycin A (Sigma Aldrich)

Rotenone (Sigma Aldrich)

Seahorse Medium

2.5 M Glucose	500 µl
200 mM Glutamin	500 µl
200 mM Sodiumpyruvate	500 µl
Seahorse XF DMEM medium (pH 7.4)	48.5 ml

Freshly prepared before the assay

Oxygen consumption was measured using Agilent Seahorse XF24 cellular respirometer in adipocytes. The primary brown adipocytes or white preadipocytes were seeded in Seahorse XF24 V7 PS Cell Culture Microplates in a density of 15,000 cells per well and differentiated as described above (2.3.6-2.3.7). The differentiated cells were treated with XF assay medium

supplemented with 2 mM pyruvate (Gibco), 2 mM glutamine (Gibco), and 25 mM glucose (Sigma) at pH 7.4 and sequential additions of CL-316,243 (CL) (only in white adipocytes) [1 µM final], Oligomycin [2 µM final], FCCP [1 µM final], and Antimycin A/Rotenone [0.5 µM final] during respirometry. For cell counting, the cells were then stained with Hoechst for primary brown (1:1000) and white adipocytes (1:2000), respectively, and counted using Cytation 5 Cell Imaging Multi-Mode Reader. The OCR value was normalized to the cell numbers and all calculations of cellular respiration were followed as manufacturer's instruction.

2.7.2 *ex vivo* oxygen consumption

The adipose tissues were extracted from ctrl and YKO mice aged 7-16 week old (BAT: 3-4 mg, WATi: 10-12 mg) for measuring oxygen consumption using Oxygraph-2k (O2k, Oroboros Instruments, Austria) (Pesta et Gnaiger 2012). The tissue samples were weighted, and transferred to oxygraph chambers in 2 ml of MiRO5 buffer (0.5 mM EGTA, 3 mM $MgCl_2 \cdot 6H_2O$, 60 mM Lactobionic acid, 20 mM taurine, 10 mM KH_2PO_4, 20 mM HEPES, 110 mM D-sucrose, and 1 g/l bovine serum albumin without fatty acid, pH 7.1) at 37°C. The basal or substrate-saturated respiration was measured when reaching a steady state with sequential additions of digitonin [25 µg/ml], Octanoylcarnitine [1 mM], Pyruvate [2 mM], Glutamate [2 mM], Malate [10 mM], Succucinate [10 mM], GDP [2 mM], FCCP [10 mM], and NoNa3 [50 mM]. The oxygen capacity was analyzed using Datlab software (Oroboros Instruments, Austria) (Shabalina et al. 2013) and the respiration rates were normalized to tissue weight.

2.8 RNA-seq gene profiling

The C57Bl/6J mice fed CD or HFD for 12 weeks were sacrificed and the fat depots were extracted. RNA was isolated from the isolated mature adipocytes (floating fraction) (Church, Berry et Rodeheffer 2014) in all fat depots as descried above (2.5.1), and RNA-seq gene profiling was performed by bioinformatics department of University of Bonn. The values were normalized to reads.

2.9 Statistical analysis

Data have been represented as mean +/- s.e.m. Single comparisons (between two data sets) were done using the two-tailed *t*-test. Multiple comparisons were analyzed using one-way ANOVA with Newman-Keuls post-hoc test. Values below 0.05 were considered significant. All statistical analyses were performed with GraphPad Prism 6.0.

3. Results

3.1 $G\alpha_q$ signaling is closely involved in YAP activity in brown adipocytes

3.1.1 Selectively enhanced $G\alpha_q$ signaling stimulates YAP activation in brown adipocytes

Although the link between $G\alpha_q$ signaling and YAP activity has been extensively studied in various cell types (Feng et al. 2014; Zhou et al. 2015; Yu et al. 2013; Yu et al. 2014; Annala et al. 2019), not much is known about its role in brown adipocytes. To investigate the impact of enhanced $G\alpha_q$ signaling on YAP activity in brown adipocytes, $G\alpha_q$-coupled Designer Receptor Exclusively Activated by Designer drugs ($G\alpha_q$-DREADD) was used. $G\alpha_q$-DREADD (Dq) represents a modified M3 muscarinic receptor and it selectively binds to $G\alpha_{q/11}$ proteins in response to the designer drug Clozapine-N-oxide (CNO) (Armbruster et al. 2007; Conklin et al. 2008). Brown preadipocytes were isolated from interscapular BAT of newborn mice and lentiviral vectors expressing Dq were transduced in the cells. After differentiation into mature brown adipocytes, YAP activity was measured in response to CNO. The read-out of YAP activation includes YAP dephosphorylation, YAP nuclear translocation, and enhanced YAP target gene expression (Ardestani, Lupse et Maedler 2018; Hansen, Moroishi et Guan 2015). First, the protein level of YAP phosphorylation (pYAP) was determined by western blot and phos-tag gel assay. Phos-tag is a functional molecule which binds to phosphorylated protein (Wako chemicals). The phosphorylated proteins can be captured and separated in phos-tag containing gels during SDS-PAGE, thereby showing the slower migration velocity (Figure 6). Analysis of protein level revealed a decreased expression of pYAP in Dq expressing cells treated with CNO (Figure 7A). The finding was further confirmed with phos-tag gel analysis. The selectively induced $G\alpha_q$ signaling resulted in the accumulation of dephosphorylated YAP which is reflected by faster migration of YAP in phos-tag containing gels (Figure 7A). Next, YAP nuclear localization was determined by immunofluorescence in brown preadipocytes expressing Dq. CNO treatment induced significant translocation of YAP into the nucleus (Figure 7B). As a third approach, YAP-dependent gene *CYR61* expression was analyzed, which was shown to play a role in 3T3L1 differentiation (Yang et al. 2018). *CYR61* mRNA level was significantly increased in $G\alpha_q$ activated cells indicating increased YAP dependent transcriptional activity (Figure 7C). These findings demonstrated that YAP transcriptional activity is enhanced by $G\alpha_q$ signaling in brown adipocytes.

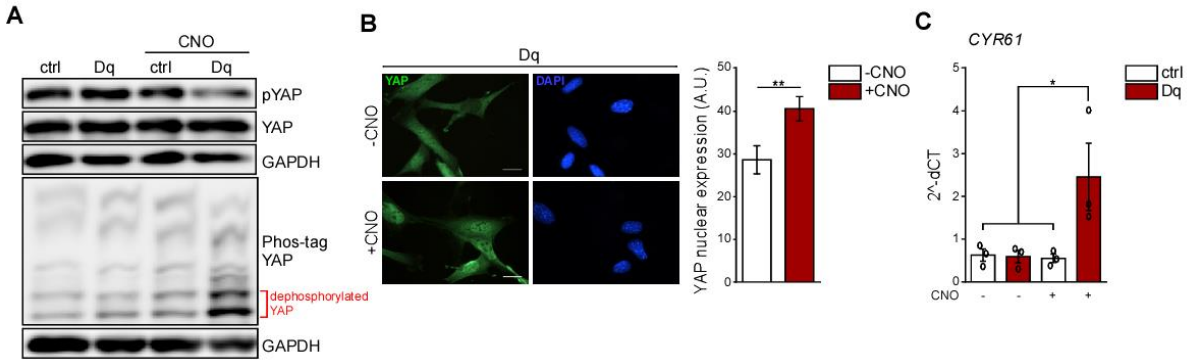

Figure 7. Increased YAP activation by selectively activated $G\alpha_q$ signaling by Gq-DREADD (Dq).

(A) Representative immunoblots and phos-tag SDS-PAGE of YAP phosphorylation (pYAP) in Dq expressing brown adipocytes with or without CNO (1 µM). GAPDH was used as a loading control. n=3. (B) (left) Immunofluorescence images of YAP (green) nuclear localization in brown preadipocytes transduced with Dq virus in presence or absence of CNO (1 µM). DAPI (blue) was used for nuclear staining. n=3 independent assays. (right) quantification of nuclear YAP represented as arbitrary units. n=30 cells. *t*-test. (C) YAP target gene *CYR61* mRNA expression in Dq expressing cells treated with or without CNO (1 µM). n=3. ANOVA. All data are shown as mean ± s.e.m. *P<0.05, **P<0.01.

3.1.2 Activation of YAP by Endothelin 1 (ET1)/Endothelin receptor type A (Ednra) signaling in brown adipocytes

Next, the effect of endogenous $G\alpha_q$ activation on YAP activity was analyzed in brown adipocytes. A previous study by our group showed that $G\alpha_q$-coupled receptor Endothelin receptor type A (Ednra) is highly expressed in brown adipocytes and the chronic treatment with Endothelin 1 (ET1) inhibits brown adipocyte differentiation through Ednra (Klepac et al., 2016). To stimulate ET1/Ednra signaling, brown adipocytes were treated with ET1 and YAP activity was assessed. The treatment with ET1 resulted in YAP dephosphorylation and accumulation of dephosphorylated YAP in phos-tag gel (Figure 8A). In addition, YAP immune detection showed significant nuclear translocation in response to ET1 (Figure 8B). YAP target gene *CYR61* expression was also significantly enhanced after ET1 stimulation (Figure 8C). Taken together, these results indicated that ET1-driven $G\alpha_q$ signaling promotes YAP dephosphorylation, nuclear localization, and target gene expression in brown adipocytes.

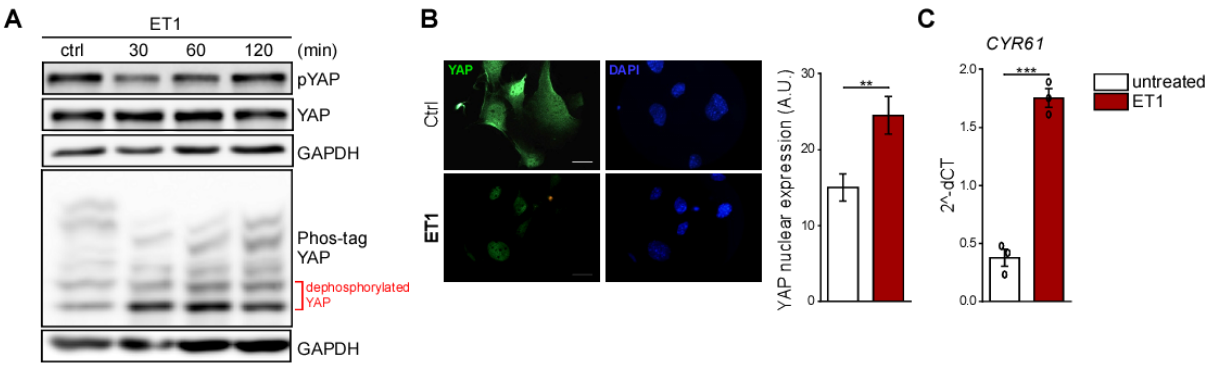

Figure 8. ET1 induced YAP activation in brown adipocytes.

(A) Representative immunoblots and phos-tag SDS-PAGE of YAP phosphorylation (pYAP) in response to ET1 (10 nM). GAPDH was used as a loading control. n=3. (B) (left) Immunofluorescence images of YAP (green) nuclear localization in brown preadipocytes treated with ET1 (10 nM). DAPI (blue) was used for nuclear staining. n=3 independent assays. (right) quantification of nuclear YAP represented as arbitrary units. n= 17 cells. *t*-test. (C) YAP target gene *CYR61* mRNA expression in presence of ET1 (10 nM). n=3. *t*-test. All data are shown as mean ± s.e.m. *P<0.05, **P<0.01, ***P<0.001.

3.1.3 RhoA/ROCK is involved in $G\alpha_q$-mediated YAP regulation

The $G\alpha_q$-driven YAP activation is mediated by RhoA/ROCK signaling circuitry (Yu et al. 2012; Feng et al. 2014; Sandbo et al. 2016), a pathway known as an important regulator of brown adipocyte differentiation (Haas et al. 2009; Klepac et al. 2016; Klepac et al. 2019). To determine whether RhoA/ROCK is involved YAP regulation by $G\alpha_q$, Dq expressing brown preadipocytes were treated with ROCK inhibitor Y27632 together with CNO. Immunostaining of YAP displayed that CNO treatment stimulated YAP nuclear localization, but its nuclear translocation was significantly (P<0.05) inhibited by Y27632 treatment (Figure 9A). *CYR61* expression was further analyzed by qRT-PCR, showing that CNO stimulated *CYR61* expression was significantly repressed by ROCK inhibitor (Figure 9B).

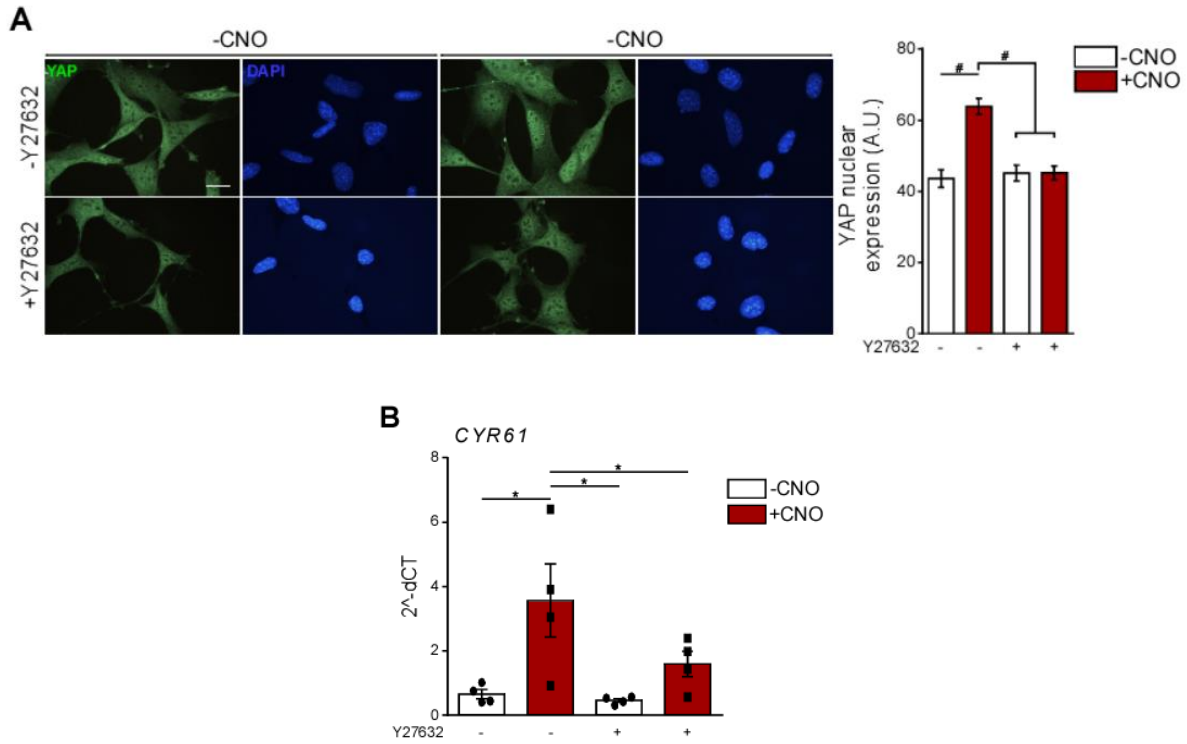

Figure 9. RhoA/ROCK inhibition in Gα$_q$-DREADD (Dq) expressing brown adipocytes.

(A) (left) Immunofluorescence images of YAP (green) nuclear localization in Dq expressing brown preadipocytes treated with CNO (1 µM), Y27632 (10µM) or both. n=3 independent assays. (right) quantification of nuclear YAP represented as arbitrary units. n= 37 cells. ANOVA. (B) YAP target gene *CYR61* mRNA expression in presence of CNO (1 µM), Y27632 (10µM) or both. n=4. ANOVA. All data are shown as mean ± s.e.m. *P<0.05, **P<0.01, ***P<0.001, #P<0.0001.

Similar results were observed with ET1 treatment. ET1 treatment induced YAP nuclear localization, however, ROCK inhibitor Y27632 significantly blocked ET1-induced YAP nuclear translocation (Figure 10A). In addition, ET1 stimulation inhibited YAP phosphorylation indicating YAP activation, however, Y27632 treatment suppressed ET1-induced YAP dephosphorylation (Figure 10B). These results suggested that activation of YAP by Dq- or ET1-driven Gα$_q$ signaling is regulated through RhoA/ROCK in brown adipocytes.

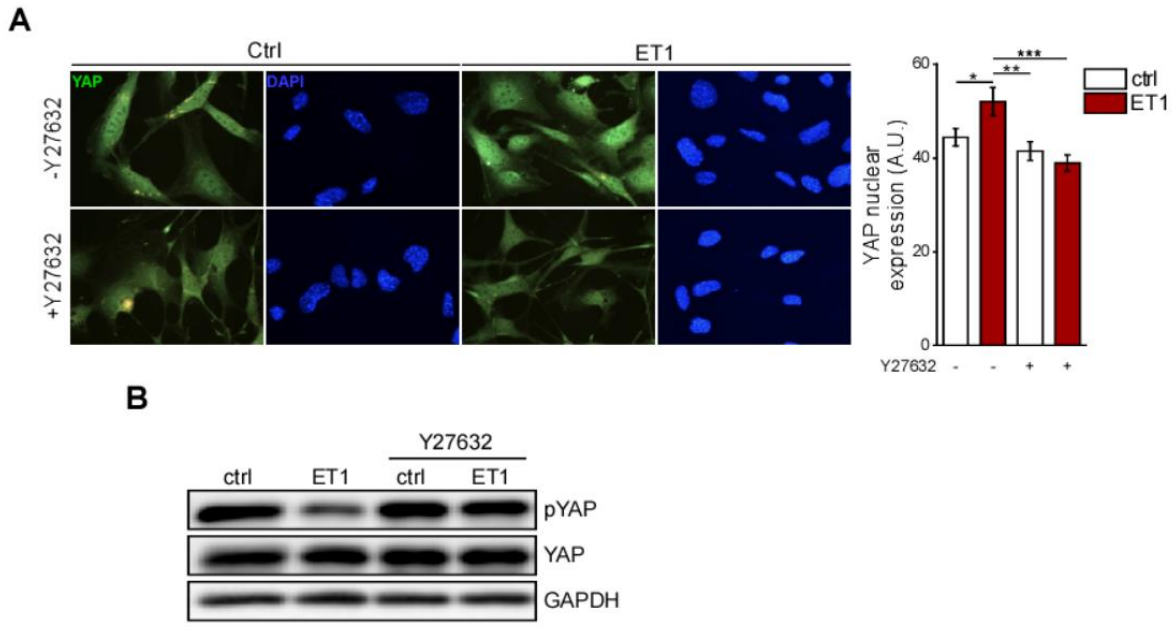

Figure 10. RhoA/ROCK inhibition in ET1-treated brown adipocytes.

(A) (left) Immunofluorescence images of YAP (green) nuclear localization in brown preadipocytes treated with ET1 (10 nM), Y27632 (10µM) or both. n=3 independent assays. DAPI (blue) was used for nuclear staining. (right) quantification of nuclear YAP represented as arbitrary units. n= 24 cells. ANOVA. (B) Representative immunoblots of pYAP in brown adipocytes treated with ET1 (10 nM), Y27632 (10µM) or both. n=3. All data are shown as mean ± s.e.m. *P<0.05, **P<0.01, ***P<0.001.

3.2 The importance of YAP in brown adipocytes

3.2.1 Gene expression of YAP in adipocytes and adipose tissues

YAP and TAZ have been identified as important regulators of adipocyte differentiation in 3T3-L1 cells (Yu et al. 2012). So far, only one study showed the role of YAP/TAZ in brown adipocytes, which promotes thermogenesis via UCP1 in differentiated brown/beige adipocytes (Tharp et al. 2018). Although YAP and TAZ are generally considered to be functionally similar because of highly conserved sequence homology (60%), differences of these two proteins in physiological role and structure suggest that they might have distinct, non-overlapping functions (Plouffe et al. 2018). In order to investigate a potential role of YAP and TAZ in brown and white adipocyte differentiation, first, the expression of *YAP* and *TAZ* was assessed by qRT-PCR. *YAP* was highly expressed in brown preadipocytes (d-2) and mature adipocytes (d+7), but the expression was significantly lower (58%) in mature brown adipocytes indicating the *YAP* expression is decreased during differentiation (Figure 11A). To further check the *YAP* expression in white adipocytes, WAT-derived MSCs (white preadipocytes) were isolated from inguinal WAT (WATi) of mice. During white adipocyte differentiation, *YAP* expression was significantly downregulated by 60%. YAP paralog, *TAZ* showed the highest expression in brown preadipocytes as compared to mature brown adipocytes and white adipocytes, however, *TAZ* expression in both brown and white adipocytes was not significantly changed during differentiation (Figure 11B). Given the alteration of gene expression during adipocyte differentiation, these data indicated that YAP, not TAZ, might have a regulatory role in adipogenesis in both brown and white adipocytes.

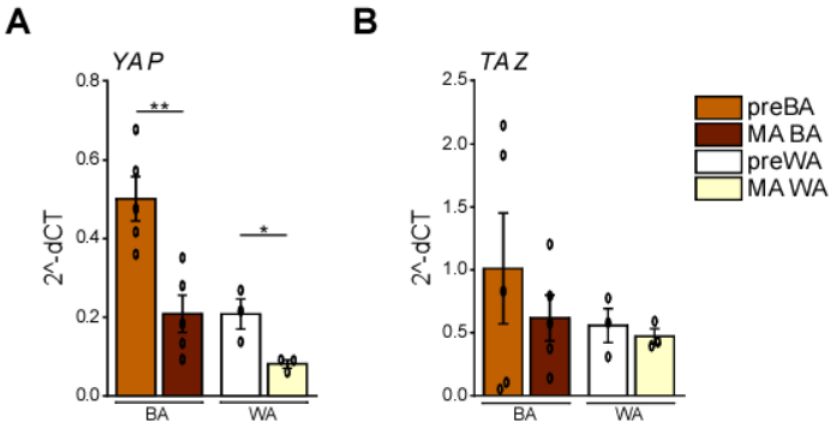

Figure 11. Gene expression of *YAP* and *TAZ* in brown and white adipocytes.

(A, B) qRT-PCR analysis of YAP (A) and TAZ (B) in brown preadipocytes (pre BA), mature brown adipocytes (MA BA), white preadipocytes (pre WA), and mature white adipocytes (MA WA). brown adipocytes; n=5, white adipocytes; n=3. *t*-test. All data are shown as mean ± s.e.m. *P<0.05, **P<0.01.

The expression of *YAP* and *TAZ* was further examined in adipose tissues. As YAP and TAZ are critical regulators of organ development (Varelas 2014), their expression was analyzed in BAT of new born mice and aged (20 weeks old) BAT, WATi, and WATg. Consistent with the known role of YAP and TAZ in processing tissue development (Varelas 2014), both *YAP* and *TAZ* showed the highest expression in BAT of new born mice, but their expression was decreased in BAT of aged mice (*YAP* and *TAZ* expression were reduced by 52% and 48%, respectively) (Figure 12A, B). In adult mice, *YAP* expression was 2.8-fold and 4.8-fold higher in BAT than in WATi and WATg, respectively, but the expression in WATi and WATg was comparable (Figure 12A). On the other hand, TAZ expression was comparable in all fat depots in aged mice (Figure 12B).

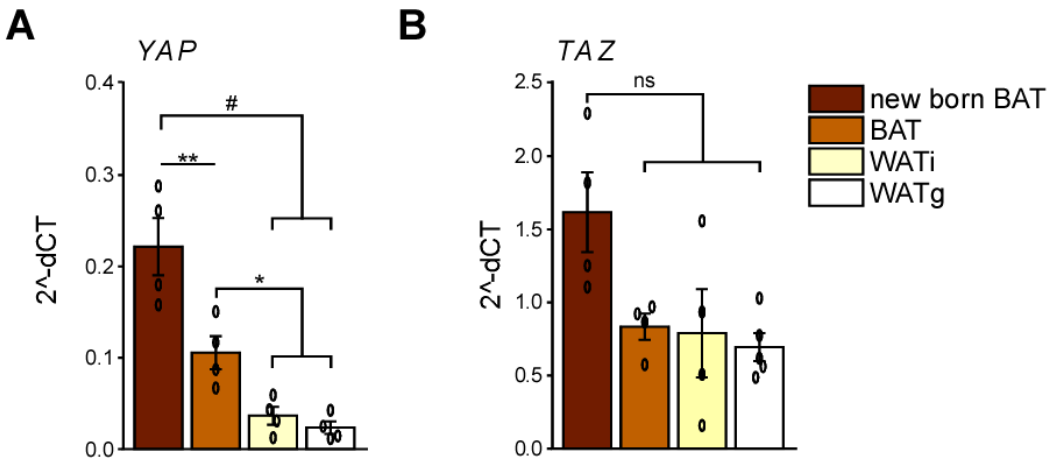

Figure 12. Gene expression of *YAP* and *TAZ* in adipose tissues.

(A, B) qRT-PCR analysis of *YAP* (A) and *TAZ* (B) in new born BAT and aged BAT, WATi, and WATg. n=4. ANOVA. All data are shown as mean ± s.e.m. *P<0.05, **P<0.01, ***P<0.001, #P<0.0001.

To further assess the expression of YAP and TAZ in fat depots of obese mice, a mouse model of diet-induced obesity was used. The mice were fed normal chow diet (CD) or high-fat diet (HFD, 60% of calories from fat) for 12 weeks and the RNA transcripts of *YAP* and *TAZ* in adipose tissues were analyzed by RNA-sequencing (RNA-seq) gene profiling. The mature adipocytes were isolated from the floating fraction of BAT, WATi, and WATg (Church, Berry et Rodeheffer 2014). Interestingly, *YAP* gene expression was 1.4-fold and 1.2-fold higher in BAT and WATi of HFD fed mice, respectively, as compared to normal chow-diet (CD) fed mice (Figure 13A). In WATg, *YAP* expression did not significantly change after HFD. The expression of *TAZ* was also validated by RNA-seq showing comparable expression in BAT and WATi of mice fed CD or HFD (Figure 13B). Given the alteration of *YAP* gene expression during adipocyte differentiation as well as in BAT and WATi of mice fed CD or HFD, I focused on the role of YAP for further study.

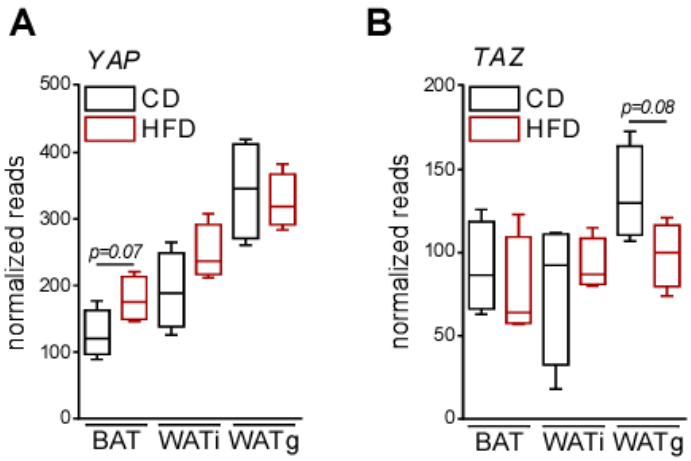

Figure 13. *YAP* and *TAZ* expression in adipose tissues of mice fed CD or HFD.

(A, B) RNA-seq gene profiling of *YAP* (A) and *TAZ* (B) in BAT, WATi, and WATg of mice fed CD or HFD for 12 weeks. The values were normalized to read. CD; n=4, HFD; n=4. *t*-test. All data are shown as mean ± s.e.m. *P<0.05.

3.2.2 YAP-dependent transcriptional regulation in adipocytes and adipose tissues

To study the functional relevance of YAP signaling, YAP target gene *CYR61* expression was further assessed. *CYR61* levels were validated with qRT-PCR in brown and white adipocytes during differentiation. In line with *YAP* expression, the expression of *CYR61* was significantly reduced in mature brown adipocytes and mature white adipocytes by 84% and 75%, respectively, as compared to their corresponding preadipocytes (Figure 14A). *CYR61* level was further analyzed in diet-induced obese mice *in vivo*. Interestingly, *CYR61* was significantly increased not only in BAT (6.5-fold) but also in WATi (3.0-fold) of mice fed HFD compared to the mice fed CD (Figure 14B). Also in WATg, *CYR61* was increased by 3.2-fold, albeit not significantly. While obesity results in impaired function of brown and beige fat, cold stress is the physiological stimulus for activation of thermogenic fat (Cannon et Nedergaard 2004; Kajimura, Seale et Spiegelman 2010). Surprisingly, levels of *CYR61* were significantly reduced in BAT, WATi and WATg by 37%, 55%, and 42%, respectively, after cold exposure indicating a decreased YAP signaling (Figure 14C). This observation proposed that YAP signaling is enhanced in diet-induced obesity, whereas it is diminished during cold stimulation. In summary, all these results indicated that YAP has a potential, regulatory role in adipogenesis and adipose function.

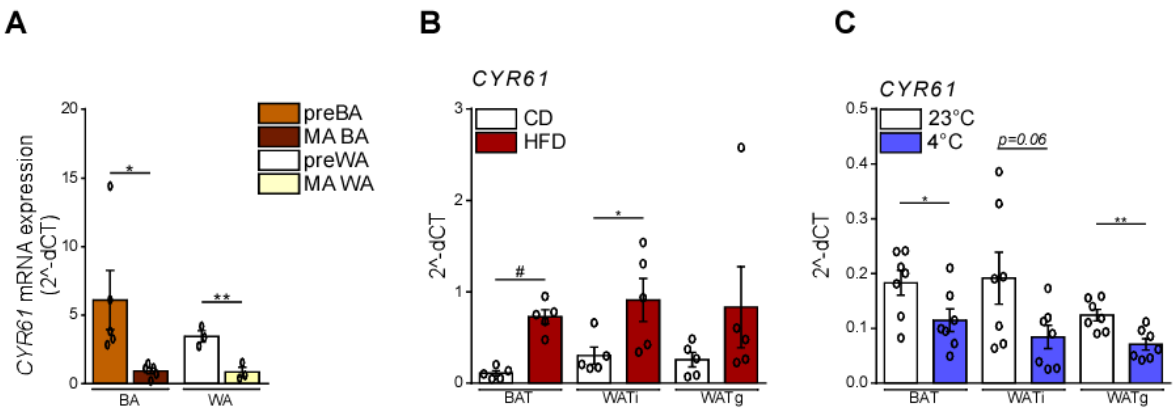

Figure 14. YAP target gene *CYR61* mRNA expression *in vitro* and *in vivo*.

(A) qRT-PCR analysis of *CYR61* in brown preadipocytes (pre BA), mature brown adipocytes (MA BA), white preadipocytes (pre WA), and mature white adipocytes (MA WA). brown adipocytes; n=5, white adipocytes; n=3. *t*-test. (B) qRT-PCR analysis of *CYR61* in BAT, WATi, and WATg of mice fed CD or HFD for 12 weeks. CD; n=5, HFD; n=5. *t*-test. (C) qRT-PCR analysis of *CYR61* in BAT, WATi, and WATg of mice maintained at 23°C or 4°C for 1 week. 23°C; n=7, 4°C; n=7. *t*-test. All data are shown as mean ± s.e.m. *P<0.05, **P<0.01, ***P<0.001, #P<0.0001.

3.3 Increased UCP1 expression in YAP deficient brown adipocytes

To investigate the functional role of YAP in brown adipocyte differentiation, a loss of function study was performed using Cre-loxP system. Brown preadipocytes were isolated from BAT of new born YAP-floxed ($YAP^{loxP/loxP}$) mice, and the cells were transduced with Cre virus ($YAP^{0/0}$) or control virus (ctVirus). Upon differentiation, Cre-induced recombination was verified by qRT-PCR and western blot. The YAP mRNA expression was significantly decreased by 55% as compared to ctVirus treated cells, which is further confirmed by western blot showing ablation of YAP protein expression (Figure 15A, B). TAZ expression did not significantly change in absence of YAP (Figure 15B, C).

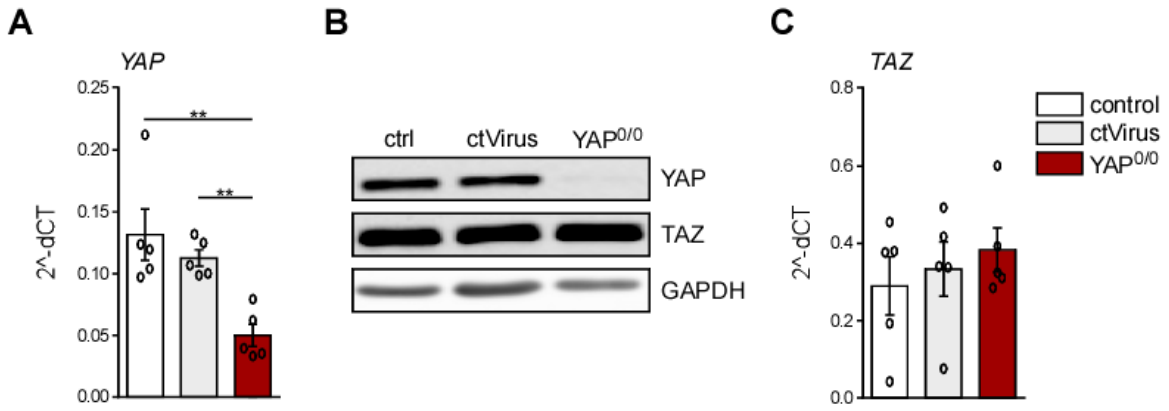

Figure 15. Cre-mediated YAP deletion in brown adipocytes.

(A, C) qRT-PCR analysis of YAP (A) and *TAZ* (C) in $YAP^{loxP/loxP}$ brown adipocytes transduced with control virus (ctVirus) or CMV-Cre virus ($YAP^{0/0}$). n=5. ANOVA. (B) Representative immunoblots of YAP and TAZ in $YAP^{loxP/loxP}$ brown adipocytes transduced with control virus (ctVirus) or CMV-Cre virus ($YAP^{0/0}$). n=5. All data are shown as mean ± s.e.m. *P<0.05, **P<0.01.

Next, the effect of loss of YAP on brown adipocyte differentiation was further determined. Interestingly, qRT-PCR analysis showed a significant increase of *UCP1* mRNA level by 1.9-fold in $YAP^{0/0}$ cells as compared to control virus treated cells (Figure 16A). However, the adipogenic markers *PPARg* and *aP2* expression did not significantly change in absence of YAP. Moreover, BAT-specific transcriptional co-factor *PGC1a* expression was also increased by 1.9-fold in $YAP^{0/0}$ adipocytes (Figure 16B).

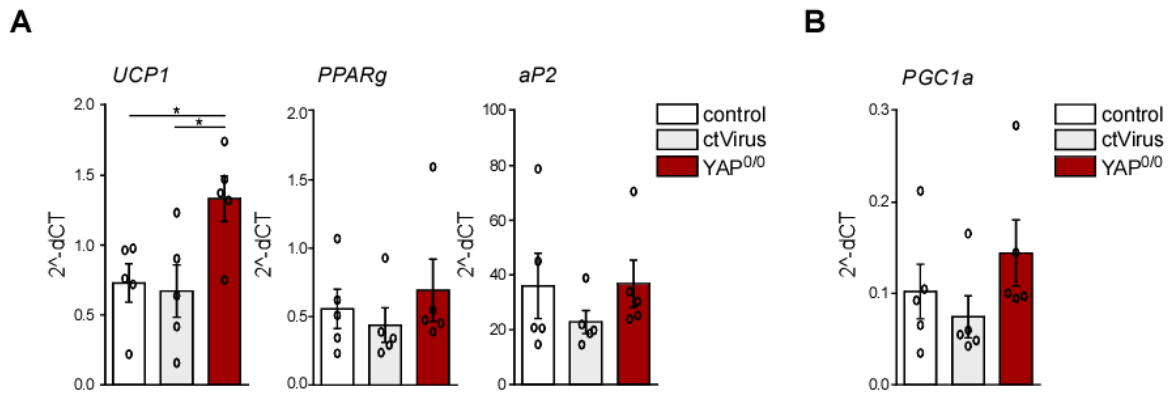

Figure 16. Effect of loss of YAP on thermogenic and adipogenic mRNA expression.

(A, B) qRT-PCR analysis of *UCP1, PPARg, aP2* (A) and *PGC1a* (B) in $YAP^{loxP/loxP}$ brown adipocytes transduced with control virus (ctVirus) or CMV-Cre virus ($YAP^{0/0}$). n=5. ANOVA. All data are shown as mean ± s.e.m. *P<0.05.

Similar results were observed by western blot analysis. $YAP^{0/0}$ cells showed 4.5-fold increase of thermogenic protein UCP1 expression compared to control virus treated cells (Figure 17). The adipogenic markers PPARg and aP2 were also enhanced in the cells without YAP by 1.4-fold and 2.5-fold, respectively, albeit not significantly. Collectively, the deletion of YAP increased UCP1 level during brown adipocyte differentiation, indicating an enhanced thermogenic program.

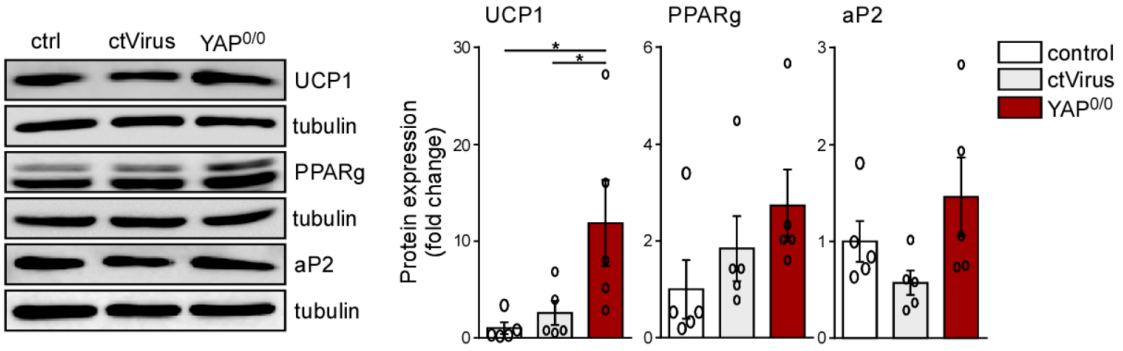

Figure 17. Effect of YAP deletion on thermogenic and adipogenic markers.

(left) Representative immunoblots of UCP1, PPARg, aP2 and tubulin in $YAP^{loxP/loxP}$ brown adipocytes transduced with control virus (ctVirus) or CMV-Cre virus ($YAP^{0/0}$). (right) quantification of UCP1, PPARg, aP2 protein expression. Relative protein expression of UCP1, PPARg, and aP2 was normalized to tubulin. n=5. ANOVA. All data are shown as mean ± s.e.m. *P<0.05.

3.4 The effect of loss of YAP on diet-induced obesity

3.4.1 Generation of adipocyte-specific YAP knockout mice

In order to investigate the role of YAP *in vivo*, tissue-specific YAP knockout model was used, because global YAP knockout mice are embryonic lethal (Morin-Kensicki et al. 2006). Adipocyte-specific YAP knockout (YKO) mice were generated by crossing YAP-floxed ($YAP^{loxP/loxP}$) mice with adiponectin-Cre (*Apn-Cre*) transgenic mice (Figure 18A). In YKO mice, YAP protein expression was reduced in BAT (77%), WATi (75%), and WATg (71%), identifying Cre-mediated YAP knockout under adiponectin promotor (Figure 18B, C). The expression of TAZ was not significantly changed when YAP expression was decreased.

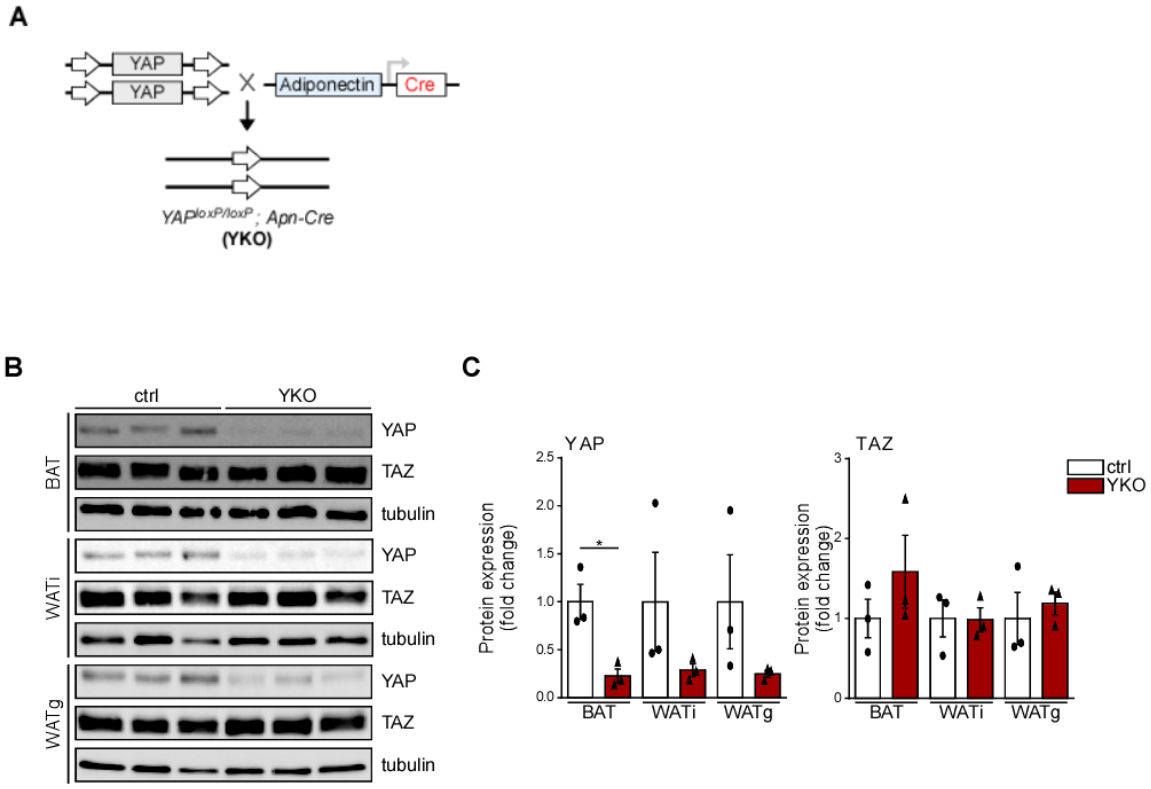

Figure 18. Generation of adipocyte-specific YAP knockout mice.

(A) Scheme of generation of adipocyte-specific YAP knock-out (YKO) mice. (B) Representative immunoblots and (C) quantification of YAP and TAZ in BAT, WATi, and WATg of litter-matched ctrl and YKO mice. Relative protein expression of YAP and TAZ was normalized to tubulin. ctrl; n=3, YKO; n=3. *t*-test. All data are shown as mean ± s.e.m. *P<0.05.

3.4.2 Effect of adipocyte-specific YAP knockout on body weight

To investigate the effect of YAP knockout on obesity, both ctrl and YKO mice were fed CD or HFD for 12 weeks. During the indicated diet period, the body weight of ctrl and YKO mice had gradually increased in either age- or diet- dependent manner, however, no significant differences in body weight were found between genotypes (Figure 19). The mice on HFD revealed a modest (4.6%), but not significant reduction in body weight in YKO mice.

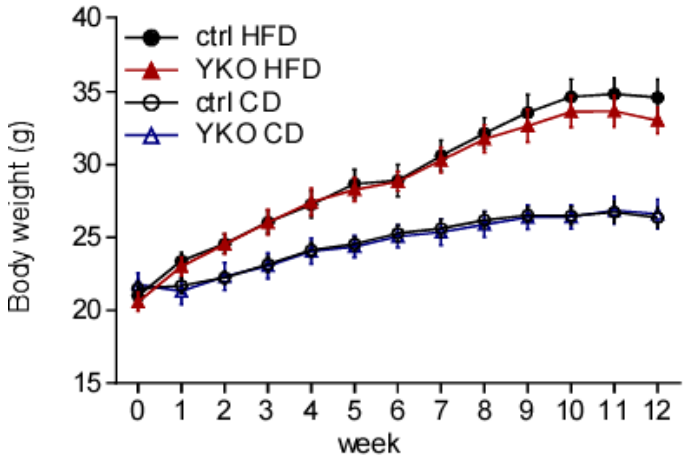

Figure 19. Body weight of ctrl and YKO mice fed CD or HFD.

(A) Body weight in litter-matched ctrl and YKO mice fed CD or HFD for 12 weeks. ctrl CD; n= 10, YKO CD; n=8, ctrl HFD; n=10, YKO HFD; n=9. All data are shown as mean ± s.e.m. *P<0.05.

The body composition was further measured showing a reduction of fat mass by 11%, albeit not significantly (Figure 20 A, B). The lean mass was comparable in ctrl and YKO mice after feeding either CD or HFD (Figure 20B).

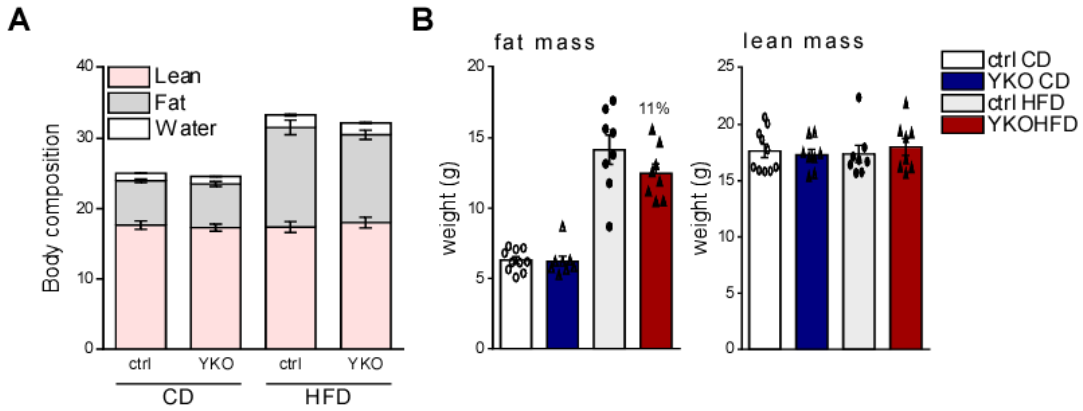

Figure 20. Body composition in ctrl and YKO mice fed CD or HFD.

(A, B) Body composition (A), fat mass, and lean mass (B) of ctrl and YKO mice fed CD or HFD for 12 weeks. ctrl CD; n=10, YKO CD; n=8, ctrl HFD; n=8, YKO HFD; n=8. *t*-test. All data are shown as mean ± s.e.m. *P<0.05.

After CD or HFD feeding, the mice were sacrificed for further analysis. First, the tissue weights were measured. The weight of BAT in ctrl and YKO under CD or HFD was comparable (Figure 21). Interestingly, the fat depots of WATi and WATg in YKO mice fed HFD were significantly reduced both by 30% (Figure 21). The mice on CD also revealed a modest (7%), but not significant reduction in fat mass of WATi and WATg in YKO mice.

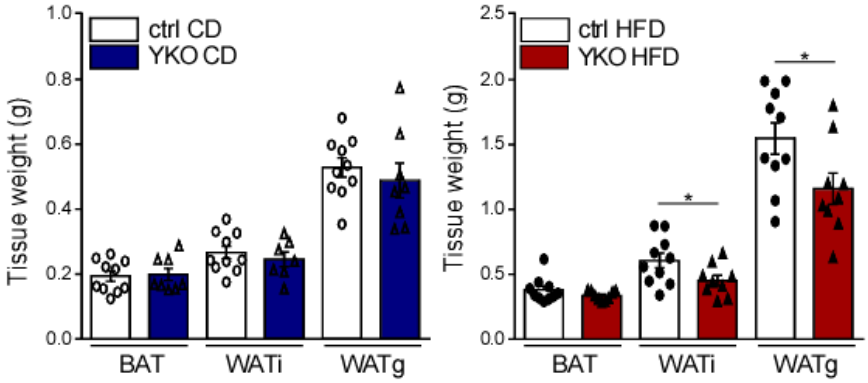

Figure 21. Adipose tissue weight in ctrl and YKO mice fed CD or HFD.

Tissue weights of BAT, WATi, and WATg in litter-matched ctrl and YKO mice fed CD or HFD. ctrl CD; n=10, YKO CD; n=7-8, ctrl HFD; n=10, YKO HFD; n=9. *t*-test. All data are shown as mean ± s.e.m. *P<0.05.

3.4.3 Whole body metabolism in YKO mice under HFD

To investigate the effect of YAP knockout on whole body metabolism, oxygen consumption was measured in ctrl or YKO mice fed CD or HFD using indirect calorimetry method. The oxygen consumption did not show a significant difference in ctrl or YKO mice either fed CD or HFD (Figure 22A, B).

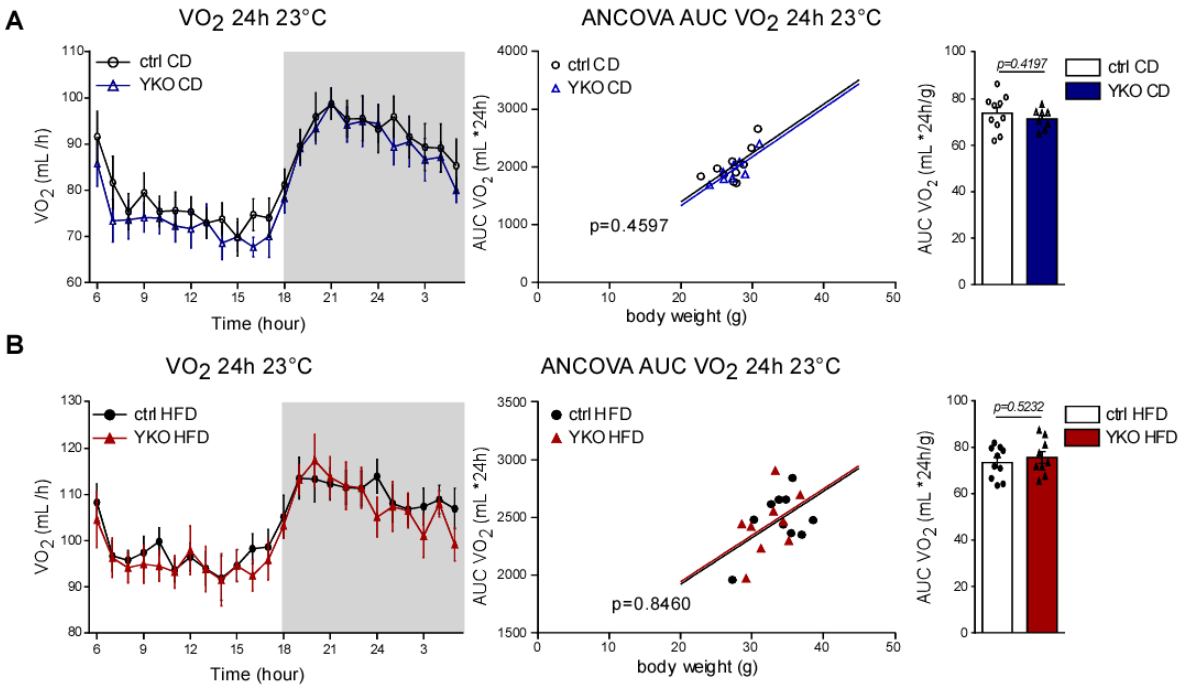

Figure 22. Whole body oxygen consumption (VO_2) of ctrl and YKO fed CD or HFD.

(A, B) (left) 24-hour oxygen consumption (VO_2) in litter-matched ctrl and YKO mice during light (white background) and dark (grey background) cycle after feeding CD or HFD for 12 weeks. (middle, right) area under the curve (AUC) of VO_2 per each mouse was further normalized to the corresponding body weight of each mouse. ctrl CD; n= 10, YKO CD; n=8, ctrl HFD; n=10, YKO HFD; n=9. *t*-test. All data are shown as mean ± s.e.m. *P<0.05.

In addition, glucose tolerance test (GTT) was performed to investigate the glucose metabolism in adipocyte-specific YAP knockout mice. No significant changes in GTT were observed in ctrl or YKO mice fed either CD or HFD. (Figure 23). Collectively, the loss of YAP in adipocytes might not induce changes in whole body metabolism including VO_2, and glucose tolerance.

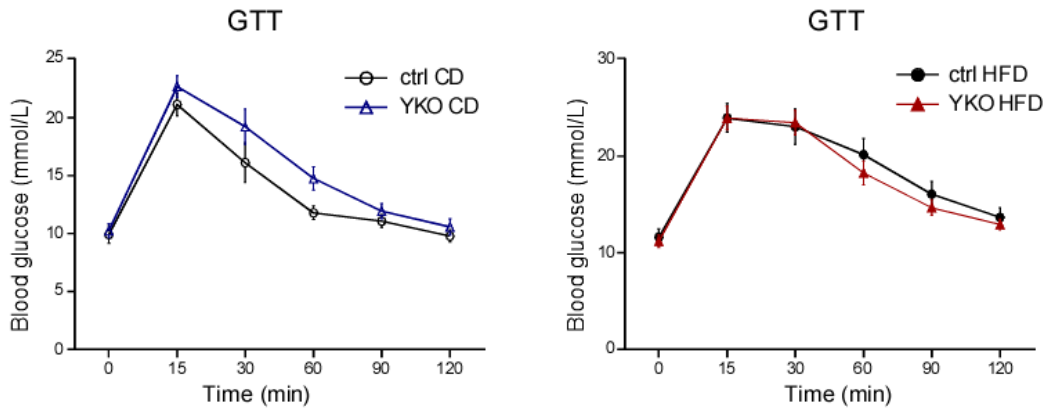

Figure 23. Glucose tolerance test (GTT) of ctrl and YKO fed CD or HFD.

Blood glucose level of litter-matched ctrl and YKO mice on CD or HFD. ctrl CD; n= 10, YKO CD; n=8, ctrl HFD; n=10, YKO HFD; n=9. *t*-test. All data are shown as mean ± s.e.m. *P<0.05.

3.4.4 Loss of YAP ameliorated whitening of BAT against HFD

Next, isolated BAT of ctrl and YKO mice fed CD or HFD was analyzed by assessing the expression of thermogenic and adipogenic markers by qRT-PCR. mRNA transcript of *UCP1* was significantly elevated in BAT of YKO mice fed HFD compared to that of ctrl littermates (Figure 24A). However, the adipogenic marker *PPARg* level was not altered. Moreover, UCP1 protein level was also increased by 2.2-fold in BAT of YKO mice fed HFD compared to the litter-matched ctrl (Figure 24B). In the mice fed CD, BAT showed comparable mRNA or protein expression of UCP1 in ctrl or YKO mice.

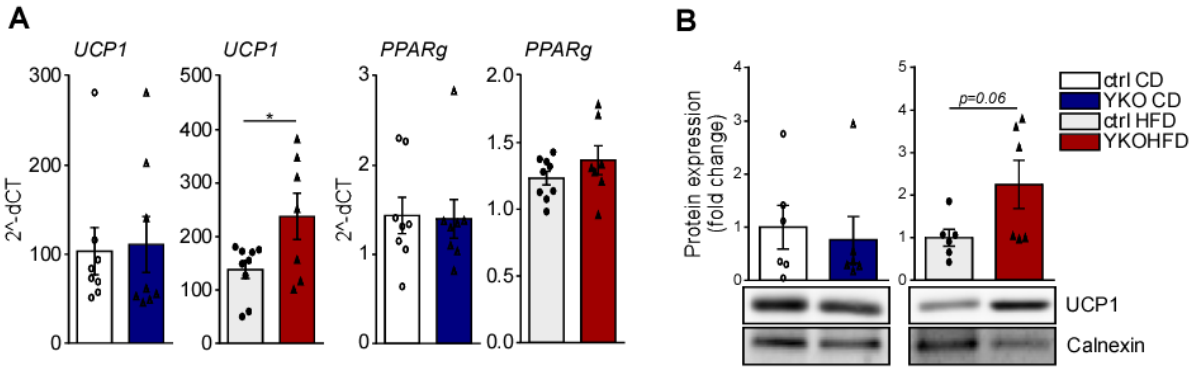

Figure 24. Thermogenic and adipogenic marker expression in BAT of ctrl and YKO mice fed CD or HFD.

(A) qRT-PCR analysis of *UCP1* and *PPARg* in BAT of litter-matched ctrl and YKO mice fed CD or HFD. ctrl CD; n=8, YKO CD; n=8, ctrl HFD; n=9, YKO HFD; n=7. *t*-test. (B) Representative immunoblots of UCP1 in BAT of litter-matched ctrl and YKO fed CD or HFD. Relative protein expression of UCP1 was normalized to calnexin. ctrl CD; n=6, YKO CD; n=6, ctrl HFD; n=6, YKO HFD; n=6. *t*-test. All data are shown as mean ± s.e.m. *P<0.05.

Obesity impairs the function of BAT and produces white-like brown adipocytes with enlarged lipid droplets, which is referred to as whitening of BAT (Roh et al. 2018; Kotzbeck et al. 2018; Shimizu et al. 2014). To check the whitening phenotype of BAT resulted from diet-induced obesity, immunohistochemistry was performed in BAT of ctrl and YKO mice fed CD or HFD. In control groups, HFD resulted in white-like enlarged, unilocular lipid droplets in BAT, which is compatible with a whitening of BAT (Figure 25). In contrast, BAT of YKO mice fed HFD exhibited small lipid droplets, a phenotype more like CD fed mice (Figure 25).

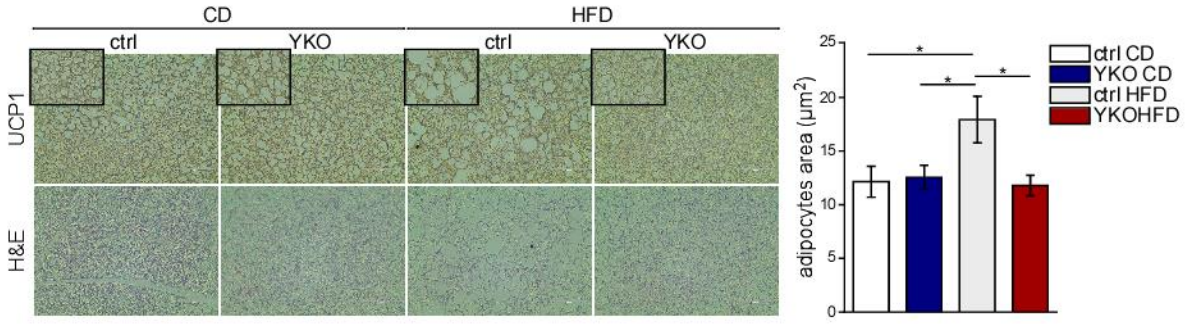

Figure 25. Histological analysis of BAT in ctrl and YKO mice fed CD or HFD.

(left) Representative UCP1 and hematoxylin and eosin (H&E) staining of BAT of ctrl and YKO mice fed CD or HFD. (right) quantification of adipocyte area (μm^2) in H&E staining of BAT in ctrl and YKO mice fed CD or HFD. n=~500 adipocytes per mouse were randomly selected for a quantification using Image J software. ctrl CD; n=5, YKO CD; n=5, ctrl HFD; n=5, YKO HFD; n=5. ANOVA. All data are shown as mean ± s.e.m. *P<0.05.

Furthermore, white-fat marker leptin expression was analyzed. Leptin is usually expressed in white adipocytes, but white-like brown adipocytes also show an increased leptin expression (Cinti et al. 1997; Cancello et al. 1998). The qRT-PCR analysis revealed a significant decrease of *leptin* by 27% in BAT of YKO mice fed HFD as compared to their corresponding controls (figure 26A). *leptin* mRNA level was also lower in BAT of YKO mice fed CD by 43%, albeit not significantly (figure 26A).

Obesity leads to an accumulation of adipose tissue macrophages and induces adipose tissue inflammation. Previous studies have suggested that whitening of BAT is accompanied with tissue inflammation (Kotzbeck et al. 2018; Xu et al. 2003; Weisberg et al. 2003). Interestingly, the expression of macrophage marker *F4/80* was significantly decreased by 38% in BAT of YKO mice fed HFD (Figure 26B). The expression of pro-inflammation markers *TNFa*, *CCL2*, *IL-6*, and *IL-10* were diminished in YKO BAT of HFD fed mice compared to their respective controls, albeit only significant for *IL-10* (decrease in *TNFa*; 55%, *CCL2*; 70%, *IL-6*; 50%, *IL-10*; 67%, respectively) (Figure 26B). In CD fed mice, YKO BAT revealed a reduction of *F4/80* (35%), *CCL2* (21%), *IL-6* (26%), *IL-10* (28%), albeit not significantly (P<0.05). Taken together, YKO mice fed HFD revealed a decrease of adipocyte area, *leptin* expression, and immune response against HFD, suggesting that brown phenotype remains intact against diet-induced obesity.

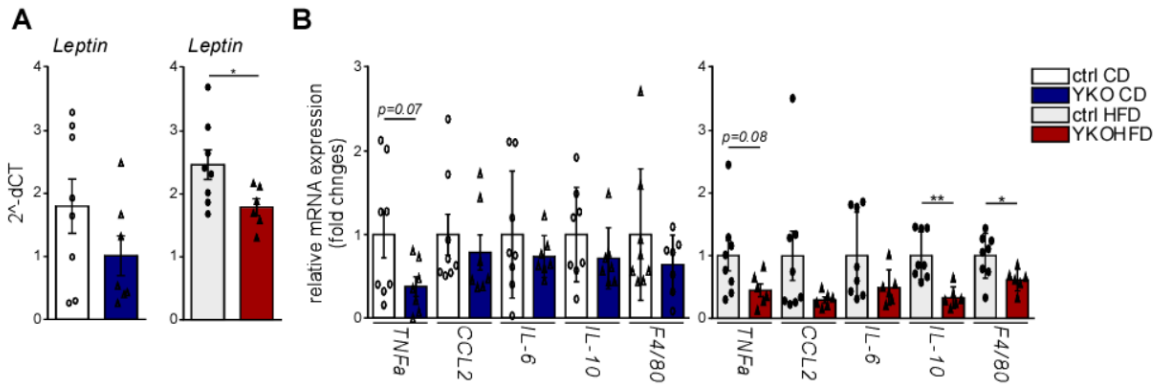

Figure 26. mRNA expression of *leptin* and immune markers in BAT of ctrl and YKO mice fed CD or HFD.

(A, B) qRT-PCR analysis of *leptin* (A), macrophage marker *F4/80* and pro-inflammation markers (*TNFa, CCL2, IL-6, IL-10*) (B) in BAT of litter-matched ctrl and YKO mice fed CD or HFD. ctrl CD; n=8, YKO CD; n=7, ctrl HFD; n=8, YKO HFD; n=6. *t*-test. All data are shown as mean ± s.e.m. *P<0.05, **P<0.01.

3.4.5 Enhanced browning of WATi in adipocyte-specific YAP knockout mice

Next, WATi isolated from ctrl and YKO mice fed CD or HFD was analyzed. WATi is the depot with the highest capacity of browning and the beige adipocytes possess the characteristics of brown adipocytes such as higher BAT-specific gene expression including UCP1 and small lipid droplets (Cannon et Nedergaard 2004; Harms et Seale 2013). Loss of YAP in WATi showed a significant ($P<0.05$) increase of *UCP1* mRNA in CD fed mice (Figure 27A). YKO mice fed HFD also revealed a higher UCP1 mRNA in WATi as compared to control HFD mice, albeit not significantly. Interestingly, all BAT-selective markers (*Elovl3*, *Cidea*, *Pgc1a*, and *Dio2*) assessed were significantly enhanced in WATi of YKO mice fed HFD, as compared to the littermate control mice fed HFD (Figure 27B), but adipogenic marker *PPARg* expression was not significantly altered. Moreover, histological staining of UCP1 and hematoxylin and eosin (H&E) revealed small, multilocular adipocytes within WATi of YKO mice fed CD, as compared to their control littermates (Figure 27C). In mice fed a HFD, both ctrl and YKO WATi showed larger adipocytes compared to CD fed mice, however, the size of adipocytes in YKO WATi was 31% smaller than in the corresponding depot of control mice. All these data indicated that WATi of YKO mice shows enhanced browning in either CD or HFD condition.

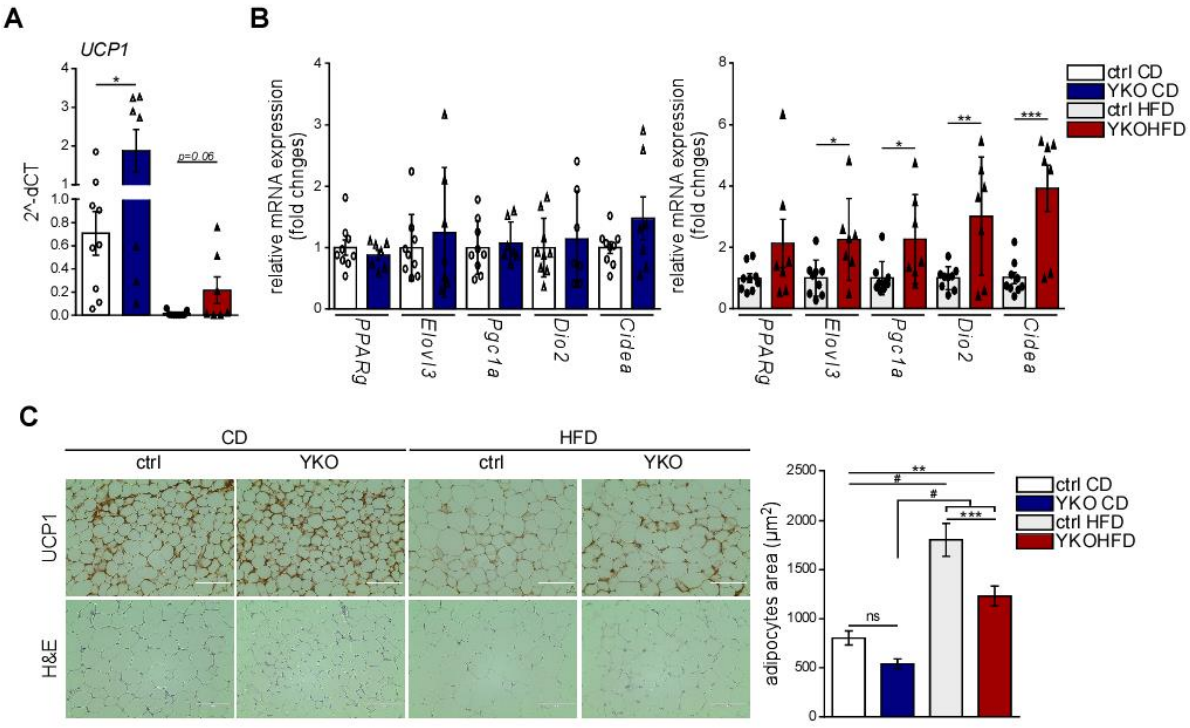

Figure 27. Browning effect in WATi of ctrl and YKO mice fed CD or HFD.

(A, B) qRT-PCR analysis of *UCP1* (A)*, PPARg* and BAT-specific markers (*Elovl3, Pgc1a, Dio2,* and *Cidea*) (B) in WATi of litter-matched ctrl and YKO mice fed CD or HFD. ctrl CD; n=9, YKO CD; n=7, ctrl HFD; n=9, YKO HFD; n=7. *t*-test. (B) (left) Representative UCP1 and hematoxylin and eosin (H&E) staining of WATi of ctrl and YKO mice fed CD or HFD. (right) quantification of adipocyte area (µm^2) in H&E staining of WATi in ctrl and YKO mice fed CD or HFD. n=~20 adipocytes per mouse were randomly selected for a quantification using Image J software. ctrl CD; n=5, YKO CD; n=5, ctrl HFD; n=5, YKO HFD; n=5. ANOVA. All data are shown as mean ± s.e.m. *P<0.05, **P<0.01, ***P<0.001, #P<0.0001.

3.5 Cell autonomous effect of YAP knockout on browning in white adipocytes *in vitro*

As the browning phenotype was observed in WATi of YKO mice *in vivo*, it was further investigated whether the effect of loss of YAP on browning is a cell autonomous. White preadipocytes were isolated from ctrl and YKO mice, and the cells were differentiated into mature adipocytes. *YAP* expression was determined by qRT-PCR showing significantly decreased expression of *YAP* in YKO white adipocytes (Figure 28A). In absence of YAP, qRT-PCR analysis revealed a significant (P<0.05) increase of *UCP1* mRNA expression in white adipocytes (Figure 28B). Besides, UCP1 protein was also enhanced by 13.6-fold in YKO white adipocytes, as compared to ctrl white adipocytes (Figure 28C). Together, these results demonstrated that loss of YAP results in the increased browning in white adipocytes.

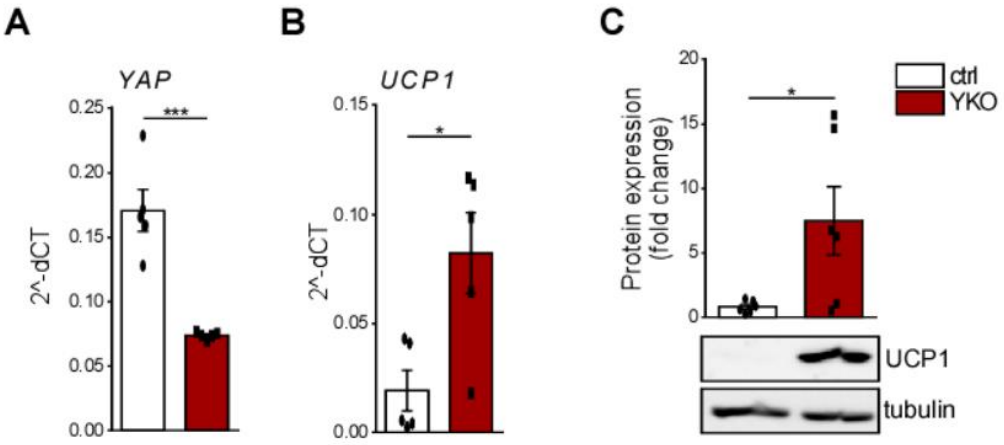

Figure 28. Enhanced UCP1 expression in YAP deficient white adipocytes.

(A, B) qRT-PCR analysis of *YAP* (A) and *UCP1* (B) in differentiated white adipocytes isolated from ctrl and YKO mice. n=4. *t*-test. (C) Representative immunoblots and quantification of UCP1 in differentiated white adipocytes isolated from ctrl and YKO mice. Relative protein expression of UCP1 was normalized to tubulin. n=6. *t*-test. All data are shown as mean ± s.e.m. *P<0.05, **P<0.01, ***P<0.001.

Conversion of white adipocytes to brown-like cells is induced by a selective β3-agonist, CL-316,243 (CL) (Cannon et Nedergaard 2004). To further induce browning in white adipocytes, both ctrl and YKO white adipocytes were treated with CL. CL treatment resulted in a significant ($P<0.05$) increase of *UCP1* mRNA expression in both ctrl or YKO white adipocytes, by far the highest expression was observed in YKO cells in response to CL (Figure 29A). UCP1 protein expression was also enhanced in response to CL in both ctrl and YKO white adipocytes by 1.5-fold and 2.2-fold, respectively (Figure 29B). Notably, CL-treated YKO white adipocytes revealed the highest expression of UCP1. All these results indicate that loss of YAP in white adipocytes enhances either basal- or CL- induced browning, showing YAP as a cell autonomous regulator for browning.

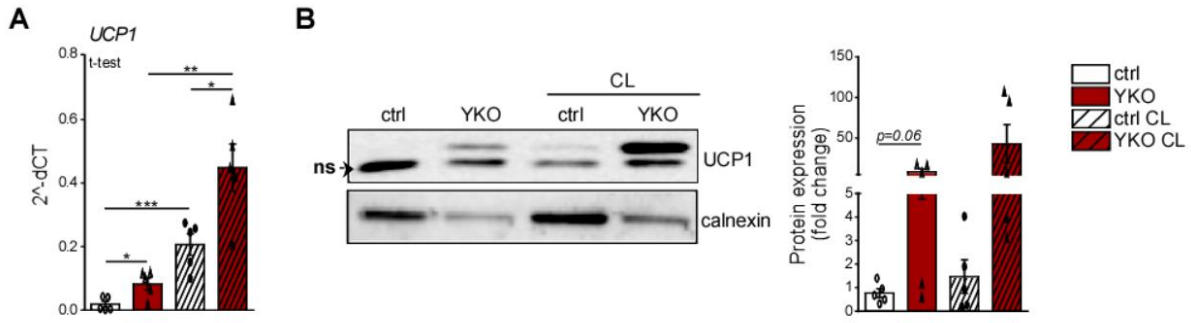

Figure 29. CL-316,243 (CL) induced browning in ctrl and YKO white adipocytes.

(A) qRT-PCR analysis of *UCP1* in differentiated white adipocytes isolated from ctrl and YKO mice treated with or without CL. n=5. *t*-test. (B) Representative immunoblots and quantification of UCP1 in differentiated white adipocytes isolated from ctrl and YKO mice with or without CL. Relative protein expression of UCP1 was normalized to calnexin. n=5. *t*-test. All data are shown as mean ± s.e.m. *P<0.05, **P<0.01, ***P<0.001.

3.6 The effect of YAP deficiency on oxygen consumption

3.6.1 Increased oxygen consumption in brown fat of adipocyte-specific YAP knockout mice

Since absence of YAP in BAT showed higher UCP1 expression and small lipid size under HFD condition (3.4.4), thermogenic capacity was further explored in BAT of ctrl and YKO mice by measuring oxygen consumption *ex vivo*. The basal respiration was comparable in BAT of ctrl and YKO mice (Figure 30A). Interestingly, UCP1-dependent respiration was significantly enhanced by 2.6-fold in BAT of YKO mice (Figure 30A). To complement *ex vivo* data, the cellular oxygen rate in primary brown adipocytes was measured using Seahorse Mitostress assay. The SVF fraction of interscapular BAT (primary brown preadipocytes) were isolated from ctrl or YKO mice, and the cells were differentiated to functional mature adipocytes (Church, Berry et Rodeheffer 2014). Notably, the overall oxygen consumption was also significantly enhanced in YKO brown adipocytes with enhanced basal- and maximum-respiration (Figure 30B). H^+ leak is one of the primary indicator of uncoupling reaction, whose increase is catalyzed by uncoupling protein such as UCP1 (Cheng et al. 2017). Loss of YAP in primary brown adipocytes revealed 1.3-fold increase of H^+ leak indicating increased uncoupling reaction. Moreover, coupling efficiency was calculated, which is links to ATP synthesis. ATP synthesis is inhibited by uncoupling reaction through UCP1, therefore, decreased coupling efficiency indicates conversely increased uncoupling efficiency. In line with H^+ leak data, coupling efficiency was significantly lower, which conversely indicates uncoupling efficiency is enhanced (Figure 30C). Thus, these data suggested that ablation of YAP promotes cellular respiration that is involved in regulating thermogenic function in brown adipocytes.

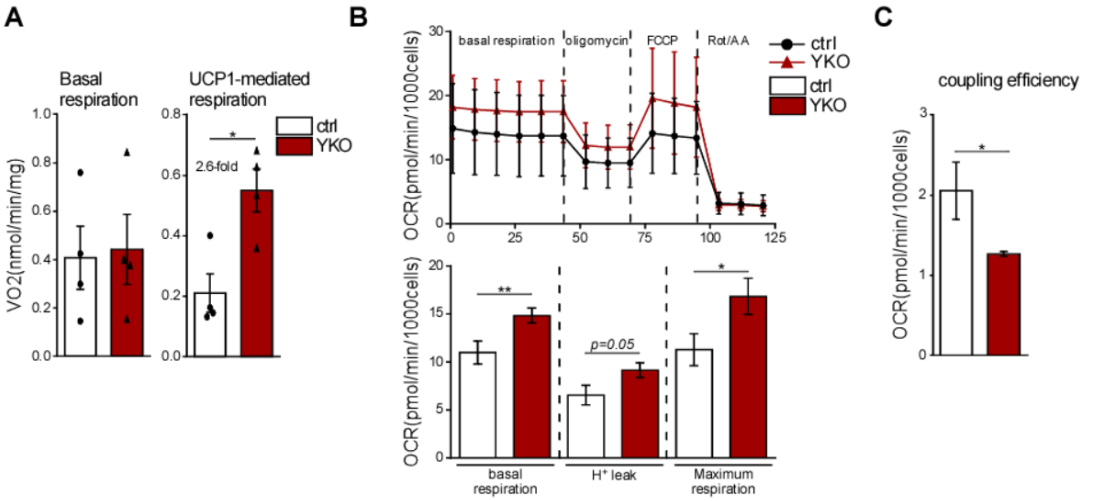

Figure 30. Oxygen consumption in absence of YAP in brown fat and brown adipocytes.

(A) *ex vivo* oxygen consumption measured by Oxygraph-2k in BAT of litter-matched ctrl and YKO mice. n=4. *t*-test. (B) Cellular respiration measured by Seahorse XF24 Cell Mito Stress Test in primary brown adipocytes isolated from ctrl or YKO mice. (C) Coupling efficiency was calculated from oxygen consumption based in (B). n=3 independent assay (3-5 replicates/n). *t*-test. All data are shown as mean ± s.e.m. *P<0.05, **P<0.01.

3.6.2 Increased oxygen consumption in white fat of adipocyte-specific YAP knockout mice

Given the observation of browning in YKO WATi (3.4.5) and white adipocytes (3.5), thermogenic capacity was further measured in WATi of ctrl of YKO mice. The rate of basal or UCP1-mediated oxygen consumption in WATi of YKO mice was 1.9-fold and 1.6-fold higher, respectively, compared to the litter-matched controls (Figure 31A). Furthermore, cellular oxygen consumption was measured in white adipocytes using a Seahorse XF-24 Extra cellular analyzer. The white preadipocytes isolated from WATi of ctrl and YKO mice were differentiated to mature adipocytes. In absence of YAP in white adipocytes, both basal respiration and H^+ leak revealed a significant increase in cellular respiration, indicating enhanced uncoupling reaction (Figure 31B). In addition, CL treatment significantly promoted oxygen consumption in both ctrl and YKO cells, by far the highest oxygen consumption was observed YKO cells in response to CL. The coupling efficiency in YKO white adipocytes was significantly lower by 52% than in control cells even without CL treatment, which conversely suggests that YKO cells have enhanced uncoupling reaction (Figure 31C). With the results of increased UCP1 in YKO white adipocytes (3.5), the higher cellular oxygen consumption in YKO white adipocytes may probably mediated via upregulation of UCP1.

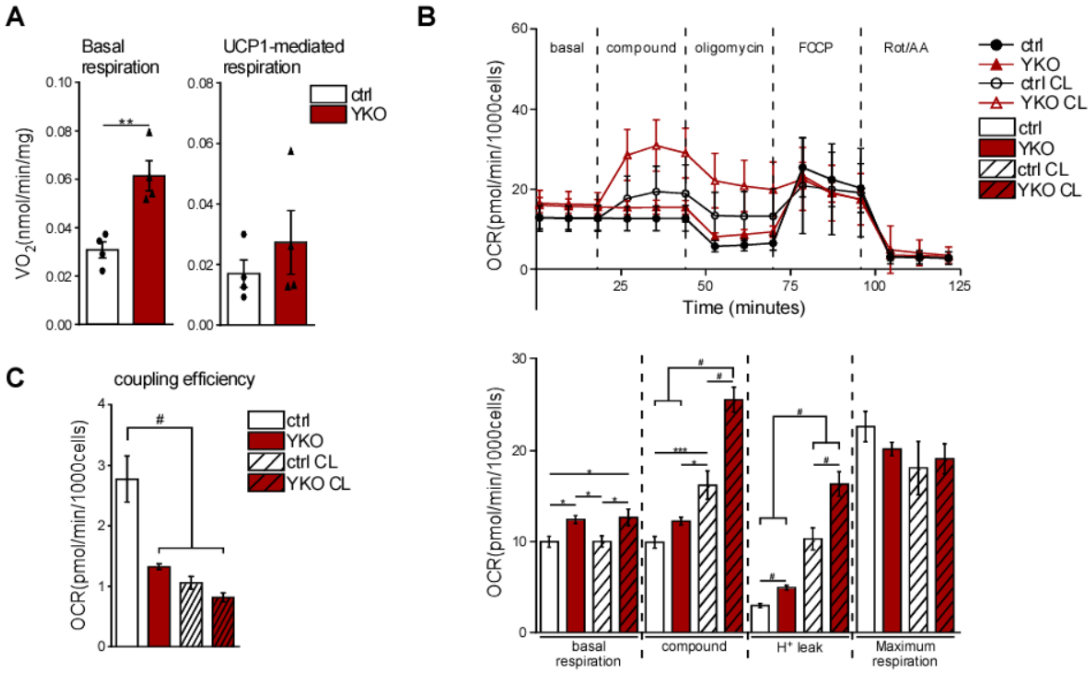

Figure 31. Oxygen consumption in absence of YAP in white fat and white adipocytes.

(A) *ex vivo* oxygen consumption measured by Oxygraph-2k in WATi of litter-matched ctrl and YKO mice. n=4. *t*-test. (B) Cellular respiration measured by Seahorse XF24 Cell Mito Stress Test in in differentiated white adipocytes isolated from ctrl or YKO mice. (C) Coupling efficiency was calculated from oxygen consumption based in (B). n=4 independent assay (3-5 replicates/n). *t*-test. All data are shown as mean ± s.e.m. *P<0.05, **P<0.01, ***P<0.001, #P<0.0001.

3.7 cGMP signaling inhibits YAP activity in brown adipocytes

To date, very little is known which signaling components are related to YAP activation/ deactivation in brown adipocytes. In order to further investigate a potential regulator of YAP in brown adipocytes, I focused on the second messenger cyclic guanosine 3′,5′-monophosphate (cGMP) as an important regulator of brown adipocytes. cGMP activates PKGI-mediated inhibition of the RhoA/ROCK signaling cascade thereby promoting brown adipogenesis (Haas et al. 2009). So far, since there is no previous study about the role of cGMP on YAP regulation, it was investigated the effect of cGMP on YAP activity. Brown adipocytes were treated with 8-pCPT-cGMP (cGMP) and YAP activity was measured. Interestingly, cGMP treatment inhibited YAP activity, as shown by increased YAP phosphorylation by immune blotting (Figure 32A). The phos-tag gel also exhibited reduced accumulation of dephosphorylated YAP. Besides, YAP cytoplasmic retention in response to cGMP was observed by immunofluorescence staining (Figure 32B) and *CYR61* expression was also significantly reduced by cGMP treatment (Figure 32C). These results revealed that cGMP stimulation inhibits YAP activity in brown adipocytes. While $G\alpha_q$-coupled signaling induces activation of RhoA/ROCK pathway leading to inhibition of brown adipogenesis (Klepac et al. 2016), cGMP induces inhibition of RhoA/ROCK promoting brown adipogenesis, which indicates the importance of RhoA/ROCK (Haas et al. 2009). The data presented in this thesis (3.1.3) show that the $G\alpha_q$-driven YAP activation is controlled via RhoA/ROCK. Thus, all these findings postulate a possibility of interplay between $G\alpha_q$ signaling and cGMP pathway on YAP regulation via RhoA/ROCK in brown adipocytes.

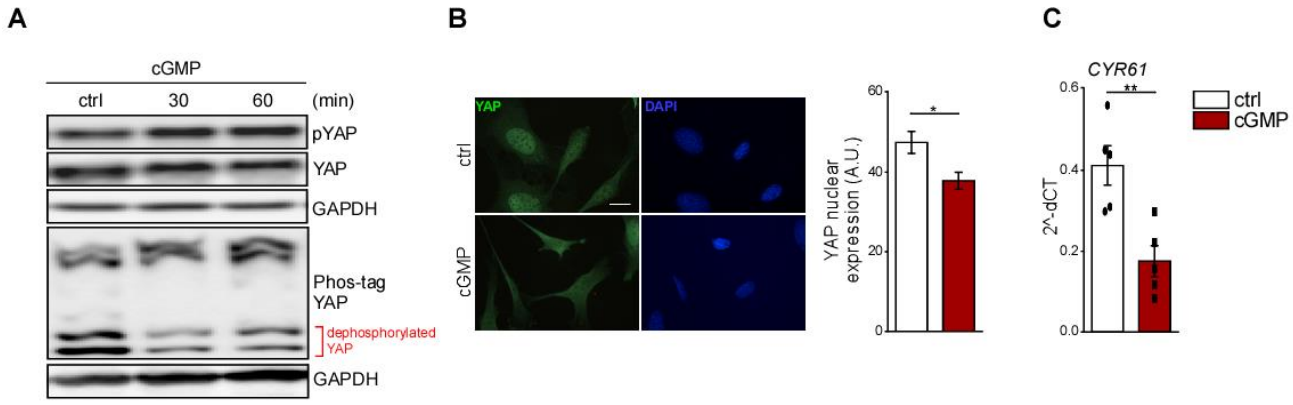

Figure 32. Decreased YAP activity in response to cGMP.

(A) Representative immunoblots and phos-tag SDS-PAGE of pYAP in brown adipocytes treated with cGMP (200µM). GAPDH was used as a loading control. n=3. (B) (left) Immunofluorescence images of YAP (green) nuclear localization in brown preadipocytes in presence of cGMP. DAPI (blue) was used for nuclear staining. n=3 independent assays. (right) quantification of nuclear YAP represented as arbitrary units. n=13 cells. *t*-test. (C) *CYR61* mRNA expression in cGMP treated brown adipocytes. *t*-test. n=5. All data are shown as mean ± s.e.m. *P<0.05, **P<0.01.

4. Discussion

Thermogenic adipose tissues including BAT and beige adipose tissue are specialized in depleting energy through heat production called non-shivering thermogenesis (Cannon et Nedergaard 2004; Kajimura, Seale et Spiegelman 2010; Pfeifer et Hoffmann 2015). In past decades, many research groups have made an effort to elucidate the underlying mechanisms in thermogenic adipose tissues. G-protein coupled receptors (GPCRs) are extensively studied regulator of BAT and beige fat. Even though the role of $G\alpha_s$-GPCR signaling to activate the thermogenic capacity in brown/beige adipocytes is well established (Cannon et Nedergaard 2004; Gnad et al. 2014), very little is known about other G protein signaling pathways involved. Recently, the role of $G\alpha_q$-GPCRs in brown adipocytes has been investigated, however, the exact function is still not clear. Previous work from our group showed that increased $G\alpha_q$-GPCR signaling disrupts brown adipocyte differentiation through RhoA/ROCK activation (Klepac et al. 2016). Another study revealed that antagonizing serotonin receptor type 2A (HTR2A), which initiates $G\alpha_q$ signaling, induces browning of white adipocytes with increased UCP1 expression and higher oxygen consumption (Kristóf et al. 2016). Most recently, regulators of G protein signaling 2 (RGS2) that preferentially inactivates $G\alpha_q$ signaling was described to increase brown adipogenesis by relieving the inhibitory effect of $G\alpha_q$/RhoA/ROCK on brown adipocytes differentiation (Klepac et al. 2019). All these results imply a negative effect of $G\alpha_q$ signaling on thermogenic adipocytes. In contrast, a positive effect of $G\alpha_q$-GPCRs on thermogenic adipocytes has been also described. GPR120, a $G\alpha_q$-coupled GPCR, was highly expressed in BAT and its expression was enhanced by cold exposure (Quesada-López et al. 2016). While GPR120 null mice revealed impaired thermogenesis and browning (Quesada-López et al. 2016; Quesada-López et al. 2019), agonism of GPR120 by TUG-891 promoted mitochondrial respiration in BAT (Schilperoort et al. 2018). Given this conflicting data, more studies on $G\alpha_q$-GPCRs and relevant mechanisms behind are needed.

In this thesis, the role of the transcriptional co-activator YAP in thermogenic adipose tissues was firstly determined. The activity of YAP is closely regulated by $G\alpha_q$-coupled receptor signaling. The data presented here showed that YAP acts as a downstream effector of $G\alpha_q$-coupled receptor signaling in brown adipocytes. Moreover, using a genetic approach, the loss-of-function of YAP in thermogenic adipose tissues was further investigated. Therefore, this thesis demonstrates a new role of YAP in relation to $G\alpha_q$-GPCR signaling in thermogenic adipocytes.

4.1 Enhanced YAP activity by $G\alpha_q$ signaling in brown adipocytes

In the past decades, Hippo pathway has been identified as important regulator for organ development and tissue homeostasis by contributing to cellular proliferation, differentiation, and apoptosis etc. (Zhao, Li et Guan 2010; Sudol et Harvey 2010). As a signaling nexus, multiple prominent pathways are involved in Hippo network including GPCRs (Hansen, Moroishi et Guan 2015). $G\alpha_s$-coupled GPCRs are known to activate the Hippo pathway. The second messenger cAMP activates PKA to stimulate LATS1/2, thereby suppressing YAP activity. In 3T3-L1 adipocytes, the inactivation of YAP is essential for PKA-induced adipocyte differentiation (Yu et al. 2013). In contrast to YAP inactivation by $G\alpha_s$ signaling, the phospholipids lysophosphatidic acid (LPA)- and sphingosine-1-phosphate (S1P)-induced $G\alpha_{12/13}$ signaling stimulates actin cytoskeleton assemble to activate YAP/TAZ through Rho

GTPases (Yu et al. 2012). Similarly, $G\alpha_q$-coupled receptor signaling also induces YAP/TAZ activation. A gain of function mutation of *GNAQ* and *GNA11* in uveal melanoma (UM) cells activates YAP, resulting in UM cell proliferation. The activation of YAP by $G\alpha_q$ signaling is independent from PLCβ, a canonical $G\alpha_q$ downstream effector, but acts through $G\alpha_q$-specific RhoGEF Trio-associated RhoA and Rac1 signaling network (Feng et al. 2014). The knock down of $G\alpha_q$ in UM cells results in YAP cytoplasmic retention and decreased target gene expression (Feng et al. 2014; Yu et al. 2014), in line with this, a pharmacological inhibition of $G\alpha_q$ by FR900359 treatment in $G\alpha_q$-activated UM cells also reveals a reduction of YAP activity by YAP phosphorylation and cytoplasmic retention (Annala et al. 2019).

The results presented in this thesis also showed that selectively activated $G\alpha_q$ signaling by $G\alpha_q$-DREADD (Dq) stimulates YAP activity through YAP dephosphorylation, nuclear localization, and target gene *CYR61* expression in brown adipocytes. The finding was further confirmed with ET1 treatment that signals through $G\alpha_q$-coupled Ednra, which is an endogenous $G\alpha_q$-GPCR in brown adipocytes. Mechanistically, YAP activation by $G\alpha_q$ signaling is controlled by RhoA/ROCK. ROCK inhibitor Y27632 inhibited Dq- or ET1-induced YAP nuclear translocation as well as ET1-induced YAP dephosphorylation. In line with this, a previous study showed that activated ET1/Ednra signaling stimulates the activation of Rho GTPase RhoA and ROCK kinase, thereby leading to YAP/TAZ dephosphorylation promoting cell proliferation in colon cancer cells (Wang et al. 2017). Taken together, these results suggest that $G\alpha_q$ signaling promotes YAP transcriptional activity in brown adipocytes via RhoA/ROCK cascade.

4.2 Importance of YAP in adipocytes and adipose tissues

As YAP plays a role as a downstream effector of $G\alpha_q$ signaling, understanding the role of YAP may give a new insight into the functional relevance of $G\alpha_q$-mediated YAP signaling pathway. Besides, the role of YAP in brown/beige adipocytes is poorly understood. Therefore, this thesis further analyzed the role of YAP in adipogenesis and adipocyte function. The expression data presented in this study showed that YAP is highly expressed in both brown and white adipocytes *in vitro*, by far the highest expression in brown preadipocytes. Interestingly, YAP expression was significantly reduced in both mature brown and white adipocytes as compared to their corresponding preadipocytes, suggesting a regulatory role of YAP during adipocyte differentiation. The expression of TAZ was also the highest in brown preadipocytes, but the expression did not change during adipocyte differentiation in brown and white adipocytes. The expression data in adipose tissues revealed the highest expression of YAP and TAZ in BAT of new born mice, the expression was significantly reduced in BAT of 20-week-old mice. As the function of YAP/TAZ is organizing tissue development (Varelas 2014), the highest expression of YAP/TAZ in newborn BAT is in line with their intrinsic function. In 20-week-old mice, YAP expression was higher in BAT compared to WATi and WATg by 2.8-fold and 4.8-fold, respectively, whereas the TAZ expression was comparable in all these three depots. Even though YAP and TAZ share the functional similarity, the function of YAP and TAZ is not absolutely identical and the distinct role of YAP and TAZ is not fully understood. One explanation for the differences between the two genes is that YAP global knockout mice are embryonic lethal (Morin-Kensicki et al. 2006), whereas TAZ knockout mice are partially lethal (Makita et al. 2008). This indicates an independent role of YAP and TAZ during development, however, it is not clear whether this is due to the expression distribution in tissues or actual

regulatory function (Makita et al. 2008). Since the data presented here showed the only alteration of YAP expression during adipocyte differentiation, it is speculated that YAP is a more prominent regulator for adipogenesis rather than TAZ in murine.

Next, it was further analyzed whether YAP-driven transcriptional activity is also altered during adipocyte differentiation by assessing YAP target gene CYR61 expression. Here, it was found that CYR61 expression was significantly reduced during differentiation in brown and white adipocytes *in vitro*. This observation is compatible with a previous, which shows the reduced CYR61 expression during adipocyte differentiation in primary marrow stromal cells and C3H10T1/2 (Yang et al. 2018). Next, CYR61 expression was further analyzed in adipose tissues. Interestingly, CYR61 expression was enhanced in BAT, WATi, and WATg of HFD-induced obese mice, whereas the expression was significantly reduced in all fat depots of cold exposed mice. This indicates that YAP signaling is enhanced in adipose tissues of diet-induced obese mice, whereas it is reduced by thermogenic activation induced by cold stimulation. Taken together, all these expression data suggest a functional contribution of YAP signaling in adipogenesis and adipocyte function.

4.3 An inhibitory role of YAP in thermogenic adipocytes

Next, the effect of loss of YAP on brown adipocyte differentiation was assessed *in vitro*. The mRNA and protein levels of the thermogenic gene UCP1 were significantly enhanced in YAP deleted brown adipocytes ($YAP^{0/0}$) during differentiation. The brown-selective marker PGC1a expression was also increased by 1.9-fold in $YAP^{0/0}$ cells. However, the adipogenic markers PPARg and aP2 did not significantly change, which imply that YAP is a key regulator of thermogenic program.

Moreover, the role of YAP in obesity was further explored. During obesity or thermoneutral condition (28°C-30°C), the function of BAT is impaired and the morphology of BAT is transformed into white-like adipocytes called “whitening” (Shimizu et al. 2014; Roh et al. 2018). The whitened BAT shows accumulation of large lipid droplets, decreased UCP1 levels, and mitochondrial dysfunction. The data presented here showed that adipocyte-specific YAP knockout mice (YKO) are protected from HFD-induced whitening of BAT showing higher UCP1 levels and small lipid droplet size as compared to litter-matched ctrl mice fed HFD. In order to further investigate the whitening phenotype of BAT induced by HFD, white-fat marker leptin expression was analyzed. Leptin is expressed in white fat, exclusively in mature white adipocytes, whereas its expression is considerably lower in brown fat (Cinti et al. 1997; Cancello et al. 1998). However, genetically obese (*db/db*) mice or the mice maintained 28°C show whitening of BAT with unilocular lipid droplets and high leptin expression. The leptin expression observed here revealed a significant reduction in BAT of YKO mice fed HFD compared to corresponding ctrl HFD mice. In addition, the macrophage marker *F4/80* and pro-inflammatory genes were highly reduced in BAT of YKO mice fed HFD. Since adipose tissue inflammation and infiltration of adipose tissue macrophages (ATM) are hallmarks of obesity (Kotzbeck et al. 2018; Weisberg et al. 2003), these data explain that decreased whitening phenotype in BAT of YKO mice under HFD might result from reduced inflammatory response.

With the findings of a positive effect on BAT in absence of YAP against HFD, the browning phenotype was also analyzed in WATi of YKO mice. Both CD and HFD fed YKO mice

developed beige adipocytes in WATi depots showing enhanced UCP1 mRNA expression and multilocular/small lipid droplets, albeit brown-specific markers are only significantly enhanced in YKO WATi under HFD. Notably, the fat mass of WATi in YKO mice fed CD (7%) or HFD (30%) were reduced as compared to corresponding control mice, which is because of the small lipid size of WATi of YKO mice. Along with this data, YAP deficient white adipocytes also showed enhanced browning effect in both basal or CL stimulated condition, indicating that YAP is a cell autonomous regulator for browning *per se*.

Functionally, BAT of YKO mice showed higher UCP1-mediated oxygen consumption *ex vivo*. In line with this result, primary brown adipocytes isolated from YKO mice also revealed an increase in overall respiration as well as in uncoupling reaction compared to the cells isolated from control mice. In WATi, the basal and UCP1-mediated oxygen consumption was 1.9-fold and 1.6-fold enhanced, respectively, in absence of YAP. Indeed, cellular oxygen consumption was also raised in YKO white adipocytes, by far the highest cellular respiration was observed in YKO white adipocytes in response to CL. Together, the knockout of YAP in brown and beige adipocytes increases UCP1 expression and oxygen consumption, which suggests YAP has an inhibitory role in thermogenic activity.

Despite the noticeable phenotype of YAP deficiency in cells and adipose tissues, whole body metabolism did not show distinct changes including body weight, EE, and glucose tolerance between ctrl and YKO mice. It is perhaps because that YAP protein is more important for progenitor cells of adipose tissues than mature cells. Since adiponectin promoter is specified only in mature adipocytes (Wang et al. 2010), the late stage of knockout of YAP in mice might be not enough to induce whole body metabolism changes. In a previous study, a global YAP overexpression in mice promoted the expansion of white adipose tissues and obesity, but the mice with YAP overexpression under adiponectin promotor did not show significant changes in body weight and fat mass (Kamura et al. 2018). Thus, this indicates that YAP overexpression in only mature adipocytes does not influence on whole body metabolism. In this theses, higher YAP expression in brown preadipocytes and BAT of new born mice was observed indicating an important role of YAP in preadipocytes rather than in mature cells. Actually, Cre-mediated YAP deletion in brown preadipocytes strongly promotes UCP1 expression during differentiation *in vitro*, hence, more obvious effects on whole body metabolism might be observed in YAP knockout of progenitor cell population. Another possible explanation about unchanged phenotype in whole body metabolism in YKO mice would be the presence of TAZ in YKO mice, which might have a compensatory effect to maintain a stable state of whole body. Previous studies have described the role of TAZ in adipocytes: (1) TAZ, but not YAP, inhibits PPARg-dependent transcription leading to decreased 3T3-L1 differentiation (Hong et al. 2005), and (2) adipocyte-specific TAZ knockout mice are protected against diet-induced obesity showing reduced adipocyte hypertrophy and inflammation (El Ouarrat et al. 2020). With these provided findings, TAZ might have a role in adipocytes *per se*, especially in relation to PPARg, giving a compensatory effect by TAZ in whole body metabolism in YKO mice. Actually, the results presented here showed unchanged expression of PPARg in fat depots of YKO mice under CD or HFD. In addition, TAZ expression was unchanged when YAP is depleted in YKO mice, which might contribute to remain the whole body metabolism, because overactive TAZ would be able to induce adipose tissue dysfunction. Regarding the role of TAZ in metabolism, the recent previous work showed that TAZ deletion in adipocytes improves glucose tolerance against diet-induced obesity (El Ouarrat et al. 2020), but the data presented here did not show a significant difference in glucose tolerance in YKO

mice. This may indicate that TAZ is key regulator of glucose metabolism rather than YAP. Therefore, it seems that YAP and TAZ have independent roles in adipose tissue metabolism; (1) YAP regulates the thermogenic program in brown and beige tissues, (2) TAZ is involved in glucose metabolism. In addition, YAP is ubiquitously expressed and plays a role in overall organs including skeletal muscle (Watt et al. 2018) and liver (Miyamura et Nishina 2018). Indirect effects on whole body metabolism by other organs that have a crosstalk with adipose tissues cannot be excluded.

For future studies, the effect of YAP overexpression in brown adipocytes should be further investigated. In addition, since the results in this thesis showed a specific effect of YAP deletion on induction of UCP1, a potential transcriptional target of YAP for regulation of UCP1 promotor activity should be discovered. Since YAP has no DNA binding motifs itself, the intermediator (e.g. TEAD transcription factor) is needed for YAP-mediated transcriptional regulation. One of the possible targets would be PGC1a, which initiates the thermogenic program of brown or beige adipocytes (Kajimura, Seale et Spiegelman 2010). In hepatocytes, YAP inhibits PGC1a activity, thereby PGC1a cannot bind transcription mediators from the promotors of its gluconeogenic targets (Hu et al. 2017). As PGC1a is one of the major drivers of UCP1 transcription, YAP might be possibly associated to control PGC1a for thermogenic activity. With supporting this idea, the expression of PGC1a assessed in $YAP^{0/0}$ brown adipocytes showed 1.9-fold increase and its expression in WATi of YKO mice fed HFD was also significantly upregulated. What is not clear, however, is how YAP controls PGC1a, therefore, more in depth study is further needed to prove this hypothesis.

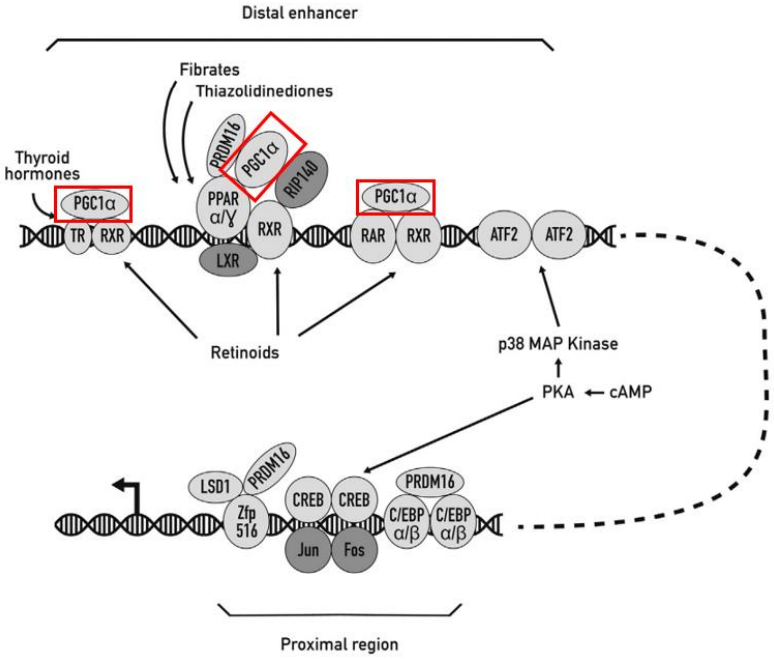

Figure 33. Scheme of the UCP1 promotor region and the main transcriptional mediators for UCP1 regulation. PGC1a (red rectangular) and its putative binding partners for UCP1 regulation (Modified from (Villarroya, Peyrou et Giralt 2017)).

Aside from my hypothesis, the previous finding by another group suggests that YAP/TAZ interacts with UCP1 proximal region (-1.8 kb upstream of UCP1), where is a putative TEAD binding motif, in mature brown adipocytes (Tharp et al. 2018). This study suggests that YAP/TAZ is involved in regulation of UCP1 promotor with TEAD, promoting UCP1 expression in mature brown adipocytes. Given the different observation regarding the UCP1 regulation by YAP, it is speculated that YAP has a different transcriptional regulation of UCP1 depending on the stage of adipogenesis (brown preadipocytes vs. mature adipocytes): (1) my thesis claims that a loss of YAP in brown preadipocytes induces UCP1 expression upon differentiation into mature adipocytes, on the other hand, (2) the previous study suggests that a loss of YAP in mature brown adipocytes decreases UCP1 expression (Tharp et al. 2018). The potential dual function of YAP in regulation of UCP1 might be mediated by different transcriptional mediators at a different stage of adipogenesis. In future studies, it would be interesting to focus on the different transcriptional regulation of YAP in UCP1 regulation at different stages of adipogenesis.

Up to now, only one study revealed a regulatory role of YAP/TAZ in thermogenic activity in brown/beige adipocytes (Tharp et al. 2018). This study suggests a favorable aspect of YAP/TAZ in metabolic health, by showing decreased UCP1 level and EE in heterogeneous $YAP^{fl/+}TAZ^{fl/+}UCP1\text{-}Cre^{+}$ mice. The differences observed might due to single allele deletion of YAP and TAZ in UCP1-positive brown adipocytes, meaning that heterozygous YAP/TAZ-floxed allele still express functional protein. Indeed, the partially reduced YAP/TAZ expression in BAT might give an unpredictable effect on thermogenic capacity for balancing energy homeostasis. Overall, the role of YAP in metabolism seems complex, therefore, further studies should be performed in the future. Nevertheless, both previous study by Tharp et al. and this thesis point to the crucial role of YAP for regulating thermogenic capacity.

4.4 Interplay between $G\alpha_q$ and cGMP pathway on YAP regulation

As the impact of $G\alpha_q$-RhoA/ROCK signaling on YAP activation was shown in this thesis, it was prompted here to investigate an additional pathway on YAP regulation in brown adipocytes. One of highlighted activator of brown adipocytes includes cGMP signaling (Haas et al. 2009). cGMP administration induces PKG1 activation, followed by inhibition of RhoA/ROCK, thereby promotes brown adipogenesis. YAP activity was further analyzed in presence of cGMP. Surprisingly, YAP phosphorylation was greatly increased indicating YAP inactivation, which is accompanied by YAP cytoplasmic retention and decreased CYR61 expression. Many of previous studies have proved the role of GPCRs-RhoA axis as an upstream effector of YAP (Feng et al. 2014; Sandbo et al. 2016; Zhou et al. 2015; Yu, Miyamoto et Brown 2016), thus, the inhibition of YAP activity by cGMP might act through RhoA/ROCK. In contrast to inhibition of RhoA/ROCK by cGMP, $G\alpha_q$ signaling increases RhoA/ROCK inhibiting brown adipocyte differentiation (Klepac et al. 2016). In addition, the crosstalk between $G\alpha_q$/RGS2 and cGMP pathway was recently described in brown adipocytes (Klepac et al. 2019). Thus, it could govern an additional mechanism of YAP regulation by $G\alpha_q$ signaling or cGMP signaling probably via RhoA/ROCK for regulating brown adipocyte physiology.

5. Summary

Brown and beige adipocytes play a role in dissipating energy via non-shivering thermogenesis, making them important metabolic target structures for energy homeostasis. During obesity, the thermogenic function of both brown and beige adipocytes is impaired and these adipocytes take on the appearance of white fat ("whitening"). Extensively studied activators of brown/beige fat are $G\alpha_s$-coupled receptors, whose activation promotes thermogenesis and lipolysis via cAMP-PKA signaling cascade. However, the function of other GPCRs coupling to other subclasses of G proteins is relatively unknown. Only a few studies have recently identified the role of $G\alpha_q$-coupled GPCRs in brown adipose tissue (BAT). One of them suggests that $G\alpha_q$-coupled GPR120 signaling enhances UCP1 expression and oxygen consumption in BAT. In contrast, a study by our group suggests a negative role of $G\alpha_q$ signaling in brown adipocytes and browning of white adipocytes via activation of RhoA/ROCK.

The focus of this thesis was to find a downstream effector of $G\alpha_q$-signaling and to investigate its role in brown/beige adipocytes. For this, I focused on the transcriptional co-factor YAP (yes-associated protein), one of the major components of Hippo signaling pathway. The Hippo pathway is crucial in organ development and the terminal downstream effector YAP and its paralogue TAZ are indispensable for cell proliferation, migration, differentiation and survival. As a signaling hub, Hippo signaling and its components are closely involved in diverse prominent signaling pathway including GPCRs. Indeed, YAP and TAZ can be activated or inactivated by GPCRs depending on the coupled G proteins. Results in this thesis revealed that activation of $G\alpha_q$ signaling by designer $G\alpha_q$-coupled GPCR ($G\alpha_q$-DREADD) in brown adipocytes promotes YAP transcriptional activity, which is further confirmed by ET1 treatment that signals through $G\alpha_q$-coupled Endothelin receptor type A (Ednra). Mechanistically, $G\alpha_q$-induced YAP activation in brown adipocytes was mediated by RhoA/ROCK signaling axis, which is an important regulator of adipocyte differentiation. Additionally, this study showed reduced YAP activity after cGMP treatment. While cGMP treatment inhibits RhoA/ROCK leading to brown adipogenesis, $G\alpha_q$ signaling hinders brown adipocyte differentiation via activation of RhoA/ROCK. Thus, this could represent a possibility of interplay between $G\alpha_q$ signaling and cGMP pathway on YAP regulation via RhoA/ROCK for brown adipogenesis.

Furthermore, since very little is known about YAP in thermogenic adipocytes, the role of YAP was further investigated in brown/beige adipocytes *in vitro* and *in vivo*. During adipocyte differentiation, YAP expression was altered indicating a regulatory role of YAP in adipogenesis *in vitro*. In line with this, the expression data presented here revealed the highest expression of YAP in BAT of new born mice as compared to that of 20-week-old mice. The functional relevance of YAP signaling was further verified by confirming YAP target gene CYR61 expression. Impressively, CYR61 expression was enhanced in BAT and inguinal white adipose tissue (WATi) of obese mice suggesting an increase of YAP signaling, whereas CYR61 expression was reduced in BAT and WATi of mice maintained in cold environment indicating decreased YAP signaling. A loss of function study was performed to elucidate the functional effect of YAP in thermogenic adipocytes. In absence of YAP *in vitro*, brown adipocytes showed a significant increase of thermogenic gene UCP1 expression and oxygen consumption. In addition, the browning effect was observed in YAP knock out white adipocytes with increased UCP1 expression and cellular oxygen consumption. The similar results were found in adipocytes-specific YAP knockout mice (YKO) *in vivo*. YAP knockout in BAT counteracted the whitening of BAT in diet-induced obesity, sustaining intrinsic BAT

characteristics with multilocular/small lipid size and higher UCP1 expression as compared to litter-matched control mice fed high-fat diet (HFD). Besides, mice lacking YAP in WATi developed beige adipocytes by promoting the expression of UCP1 and accumulating multilocular lipid droplets.

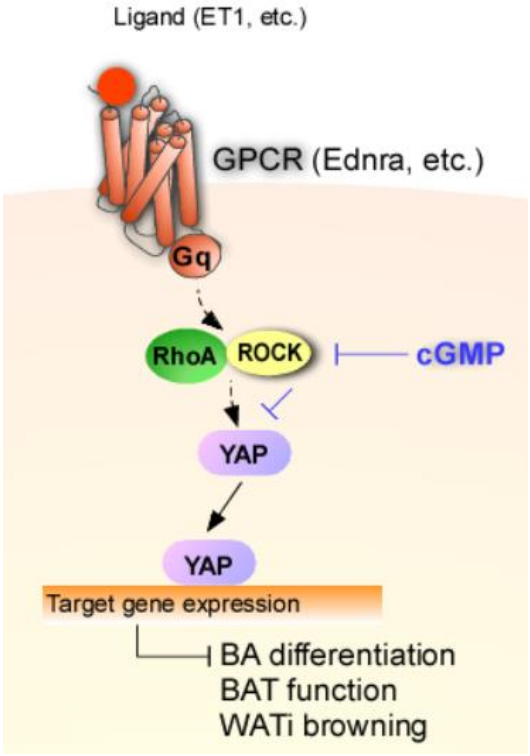

Figure 34. Scheme illustrating the $G\alpha_q$-driven YAP activation and the inhibitory role of YAP in BAT and browning of WATi

Taken together, all these data demonstrated that YAP is an important regulator of the thermogenic program in brown/beige adipocytes, and its activity is regulated by $G\alpha_q$/RhoA/ROCK signaling axis. In previous studies, the role of YAP in adipocytes has been only described in Mesenchymal stem cells (MSCs) fate decision to osteoblasts or adipocytes. In addition, most studies focus on mechanical stimuli such as cell density or cytoskeleton as an upstream influencer of YAP activity. This thesis revealed the underlying mechanism of $G\alpha_q$-mediated YAP signaling and its functional role in thermogenic adipocytes. GPCRs are important for adipose tissue function and drug targets; thus, identification of downstream effectors might provide a future therapeutic strategies. Inhibition of YAP might serve as a potential target to develop novel strategies for obesity therapies.

6. References

Amitani, Marie; Asakawa, Akihiro; Amitani, Haruka; Inui, Akio (2013) The role of leptin in the control of insulin-glucose axis. In : Frontiers in neuroscience, vol. 7, p. 51. DOI: 10.3389/fnins.2013.00051.

An, Yang; Kang, Qianqian; Zhao, Yaofeng; Hu, Xiaoxiang; Li, Ning (2013) Lats2 modulates adipocyte proliferation and differentiation via hippo signaling. In : PloS one, vol. 8, n° 8, e72042. DOI: 10.1371/journal.pone.0072042.

Annala, Suvi; Feng, Xiaodong; Shridhar, Naveen; Eryilmaz, Funda; Patt, Julian; Yang, JuHee et al. (2019) Direct targeting of Gαq and Gα11 oncoproteins in cancer cells. In : Science signaling, vol. 12, n° 573. DOI: 10.1126/scisignal.aau5948.

Ardestani, Amin; Lupse, Blaz; Maedler, Kathrin (2018) Hippo Signaling: Key Emerging Pathway in Cellular and Whole-Body Metabolism. In : Trends in endocrinology and metabolism: TEM, vol. 29, n° 7, p. 492–509. DOI: 10.1016/j.tem.2018.04.006.

Armbruster, Blaine N.; Li, Xiang; Pausch, Mark H.; Herlitze, Stefan; Roth, Bryan L. (2007) Evolving the lock to fit the key to create a family of G protein-coupled receptors potently activated by an inert ligand. In : Proceedings of the National Academy of Sciences of the United States of America, vol. 104, n° 12, p. 5163–5168. DOI: 10.1073/pnas.0700293104.

Bartelt, Alexander; Heeren, Joerg (2014) Adipose tissue browning and metabolic health. In : Nature reviews. Endocrinology, vol. 10, n° 1, p. 24–36. DOI: 10.1038/nrendo.2013.204.

Berry, Daniel C.; Stenesen, Drew; Zeve, Daniel; Graff, Jonathan M. (2013) The developmental origins of adipose tissue. In : Development (Cambridge, England), vol. 140, n° 19, p. 3939–3949. DOI: 10.1242/dev.080549.

Cancello, R.; Zingaretti, M. C.; Sarzani, R.; Ricquier, D.; Cinti, S. (1998) Leptin and UCP1 genes are reciprocally regulated in brown adipose tissue. In : Endocrinology, vol. 139, n° 11, p. 4747–4750. DOI: 10.1210/endo.139.11.6434.

Cannon, Barbara; Nedergaard, Jan (2004) Brown adipose tissue: function and physiological significance. In : Physiological reviews, vol. 84, n° 1, p. 277–359. DOI: 10.1152/physrev.00015.2003.

Chen, Q.; Shou, P.; Zheng, C.; Jiang, M.; Cao, G.; Yang, Q. et al. (2016) Fate decision of mesenchymal stem cells: adipocytes or osteoblasts? In : Cell death and differentiation, vol. 23, n° 7, p. 1128–1139. DOI: 10.1038/cdd.2015.168.

Cheng, Jiali; Nanayakkara, Gayani; Shao, Ying; Cueto, Ramon; Wang, Luqiao; Yang, William Y. et al. (2017) Mitochondrial Proton Leak Plays a Critical Role in Pathogenesis of Cardiovascular Diseases. In : Advances in experimental medicine and biology, vol. 982, p. 359–370. DOI: 10.1007/978-3-319-55330-6_20.

Church, Christopher D.; Berry, Ryan; Rodeheffer, Matthew S. (2014) Isolation and study of adipocyte precursors. In : Methods in enzymology, vol. 537, p. 31–46. DOI: 10.1016/B978-0-12-411619-1.00003-3.

Cinti, S.; Frederich, R. C.; Zingaretti, M. C.; Matteis, R. de; Flier, J. S.; Lowell, B. B. (1997) Immunohistochemical localization of leptin and uncoupling protein in white and brown adipose tissue. In : Endocrinology, vol. 138, n° 2, p. 797–804. DOI: 10.1210/endo.138.2.4908.

Coelho, Marisa; Oliveira, Teresa; Fernandes, Ruben (2013) Biochemistry of adipose tissue: an endocrine organ. In : Archives of medical science : AMS, vol. 9, n° 2, p. 191–200. DOI: 10.5114/aoms.2013.33181.

Conklin, Bruce R.; Hsiao, Edward C.; Claeysen, Sylvie; Dumuis, Aline; Srinivasan, Supriya; Forsayeth, John R. et al. (2008) Engineering GPCR signaling pathways with RASSLs. In : Nature methods, vol. 5, n° 8, p. 673–678. DOI: 10.1038/nmeth.1232.

Cooke, Dunstan; Bloom, Steve (2006) The obesity pipeline: current strategies in the development of anti-obesity drugs. In : Nature reviews. Drug discovery, vol. 5, n° 11, p. 919–931. DOI: 10.1038/nrd2136.

Cypess, Aaron M.; Kahn, C. Ronald (2010) Brown fat as a therapy for obesity and diabetes. In : Current opinion in endocrinology, diabetes, and obesity, vol. 17, n° 2, p. 143–149. DOI: 10.1097/MED.0b013e328337a81f.

El Ouarrat, Dalila; Isaac, Roi; Lee, Yun Sok; Oh, Da Young; Wollam, Joshua; Lackey, Denise et al. (2020) TAZ Is a Negative Regulator of PPARγ Activity in Adipocytes and TAZ Deletion Improves Insulin Sensitivity and Glucose Tolerance. In : Cell metabolism, vol. 31, n° 1, 162-173.e5. DOI: 10.1016/j.cmet.2019.10.003.

Etienne-Manneville, Sandrine; Hall, Alan (2002) Rho GTPases in cell biology. In : Nature, vol. 420, n° 6916, p. 629–635. DOI: 10.1038/nature01148.

Feng, Xiaodong; Degese, Maria Sol; Iglesias-Bartolome, Ramiro; Vaque, Jose P.; Molinolo, Alfredo A.; Rodrigues, Murilo et al. (2014) Hippo-independent activation of YAP by the GNAQ uveal melanoma oncogene through a trio-regulated rho GTPase signaling circuitry. In : Cancer cell, vol. 25, n° 6, p. 831–845. DOI: 10.1016/j.ccr.2014.04.016.

Gesta, Stephane; Tseng, Yu-Hua; Kahn, C. Ronald (2007) Developmental origin of fat: tracking obesity to its source. In : Cell, vol. 131, n° 2, p. 242–256. DOI: 10.1016/j.cell.2007.10.004.

Gnad, Thorsten; Scheibler, Saskia; Kügelgen, Ivar von; Scheele, Camilla; Kilić, Ana; Glöde, Anja et al. (2014) Adenosine activates brown adipose tissue and recruits beige adipocytes via A2A receptors. In : Nature, vol. 516, n° 7531, p. 395–399. DOI: 10.1038/nature13816.

Gumbiner, Barry M.; Kim, Nam-Gyun (2014) The Hippo-YAP signaling pathway and contact inhibition of growth. In : Journal of cell science, vol. 127, n° Pt 4, p. 709–717. DOI: 10.1242/jcs.140103.

Haas, Bodo; Mayer, Peter; Jennissen, Katja; Scholz, Daniela; Berriel Diaz, Mauricio; Bloch, Wilhelm et al. (2009) Protein kinase G controls brown fat cell differentiation and mitochondrial biogenesis. In : Science signaling, vol. 2, n° 99, ra78. DOI: 10.1126/scisignal.2000511.

Hansen, Carsten Gram; Moroishi, Toshiro; Guan, Kun-Liang (2015) YAP and TAZ: a nexus for Hippo signaling and beyond. In : Trends in cell biology, vol. 25, n° 9, p. 499–513. DOI: 10.1016/j.tcb.2015.05.002.

Harms, Matthew; Seale, Patrick (2013) Brown and beige fat: development, function and therapeutic potential. In : Nature medicine, vol. 19, n° 10, p. 1252–1263. DOI: 10.1038/nm.3361.

Hong, Jeong-Ho; Hwang, Eun Sook; McManus, Michael T.; Amsterdam, Adam; Tian, Yu; Kalmukova, Ralitsa et al. (2005) TAZ, a transcriptional modulator of mesenchymal stem cell differentiation. In : Science (New York, N.Y.), vol. 309, n° 5737, p. 1074–1078. DOI: 10.1126/science.1110955.

Hu, Yue; Shin, Dong-Ju; Pan, Hui; Lin, Zhiqiang; Dreyfuss, Jonathan M.; Camargo, Fernando D. et al. (2017) YAP suppresses gluconeogenic gene expression through PGC1α. In : Hepatology (Baltimore, Md.), vol. 66, n° 6, p. 2029–2041. DOI: 10.1002/hep.29373.

Iglesias-Bartolome, Ramiro; Torres, Daniela; Marone, Romina; Feng, Xiaodong; Martin, Daniel; Simaan, May et al. (2015) Inactivation of a Gα(s)-PKA tumour suppressor pathway in skin stem cells initiates basal-cell carcinogenesis. In : Nature cell biology, vol. 17, n° 6, p. 793–803. DOI: 10.1038/ncb3164.

Jennissen, Katja; Siegel, Franziska; Liebig-Gonglach, Michaela; Hermann, Michaela-Rosemarie; Kipschull, Stefanie; van Dooren, Sander et al. (2012) A VASP-Rac-soluble guanylyl cyclase pathway controls cGMP production in adipocytes. In : Science signaling, vol. 5, n° 239, ra62. DOI: 10.1126/scisignal.2002867.

Johnston, Christopher A.; Siderovski, David P. (2007) Receptor-mediated activation of heterotrimeric G-proteins: current structural insights. In : Molecular pharmacology, vol. 72, n° 2, p. 219–230. DOI: 10.1124/mol.107.034348.

Juan, Wen Chun; Hong, Wanjin (2016) Targeting the Hippo Signaling Pathway for Tissue Regeneration and Cancer Therapy. In : Genes, vol. 7, n° 9. DOI: 10.3390/genes7090055.

Kajimura, Shingo; Saito, Masayuki (2014) A new era in brown adipose tissue biology: molecular control of brown fat development and energy homeostasis. In : Annual review of physiology, vol. 76, p. 225–249. DOI: 10.1146/annurev-physiol-021113-170252.

Kajimura, Shingo; Seale, Patrick; Spiegelman, Bruce M. (2010) Transcriptional control of brown fat development. In : Cell metabolism, vol. 11, n° 4, p. 257–262. DOI: 10.1016/j.cmet.2010.03.005.

Kamura, Keiichiro; Shin, Jihoon; Kiyonari, Hiroshi; Abe, Takaya; Shioi, Go; Fukuhara, Atsunori; Sasaki, Hiroshi (2018) Obesity in Yap transgenic mice is associated with TAZ downregulation. In : Biochemical and biophysical research communications, vol. 505, n° 3, p. 951–957. DOI: 10.1016/j.bbrc.2018.10.037.

Kang, Jun Goo; Park, Cheol-Young (2012) Anti-Obesity Drugs: A Review about Their Effects and Safety. In : Diabetes & metabolism journal, vol. 36, n° 1, p. 13–25. DOI: 10.4093/dmj.2012.36.1.13.

Klepac, Katarina; Kilić, Ana; Gnad, Thorsten; Brown, Loren M.; Herrmann, Beate; Wilderman, Andrea et al. (2016) The Gq signalling pathway inhibits brown and beige adipose tissue. In : Nature communications, vol. 7, p. 10895. DOI: 10.1038/ncomms10895.

Klepac, Katarina; Yang, JuHee; Hildebrand, Staffan; Pfeifer, Alexander (2019) RGS2: A multifunctional signaling hub that balances brown adipose tissue function and differentiation. In : Molecular metabolism, vol. 30, p. 173–183. DOI: 10.1016/j.molmet.2019.09.015.

Kotzbeck, Petra; Giordano, Antonio; Mondini, Eleonora; Murano, Incoronata; Severi, Ilenia; Venema, Wiebe et al. (2018) Brown adipose tissue whitening leads to brown adipocyte death and adipose tissue inflammation. In : Journal of lipid research, vol. 59, n° 5, p. 784–794. DOI: 10.1194/jlr.M079665.

Kral, John G.; Näslund, Erik (2007) Surgical treatment of obesity. In : Nature clinical practice. Endocrinology & metabolism, vol. 3, n° 8, p. 574–583. DOI: 10.1038/ncpendmet0563.

Kristóf, E.; Doan-Xuan, Q-M; Sárvári, A. K.; Klusóczki, Á.; Fischer-Posovszky, P.; Wabitsch, M. et al. (2016) Clozapine modifies the differentiation program of human adipocytes inducing browning. In : Translational psychiatry, vol. 6, n° 11, e963. DOI: 10.1038/tp.2016.230.

Lefkowitz, R. J. (2007) Seven transmembrane receptors: something old, something new. In : Acta physiologica (Oxford, England), vol. 190, n° 1, p. 9–19. DOI: 10.1111/j.1365-201X.2007.01693.x.

Makita, Ryosuke; Uchijima, Yasunobu; Nishiyama, Koichi; Amano, Tomokazu; Chen, Qin; Takeuchi, Takumi et al. (2008) Multiple renal cysts, urinary concentration defects, and pulmonary emphysematous changes in mice lacking TAZ. In : American journal of physiology. Renal physiology, vol. 294, n° 3, F542-53. DOI: 10.1152/ajprenal.00201.2007.

Milligan, Graeme; Kostenis, Evi (2006) Heterotrimeric G-proteins: a short history. In : British journal of pharmacology, 147 Suppl 1, S46-55. DOI: 10.1038/sj.bjp.0706405.

Miyamura, Norio; Nishina, Hiroshi (2018) YAP regulates liver size and function. In : Cell cycle (Georgetown, Tex.), vol. 17, n° 3, p. 267–268. DOI: 10.1080/15384101.2017.1407390.

Morin-Kensicki, Elizabeth M.; Boone, Brian N.; Howell, Michael; Stonebraker, Jaclyn R.; Teed, Jeremy; Alb, James G. et al. (2006) Defects in yolk sac vasculogenesis, chorioallantoic fusion, and embryonic axis elongation in mice with targeted disruption of Yap65. In : Molecular and cellular biology, vol. 26, n° 1, p. 77–87. DOI: 10.1128/MCB.26.1.77-87.2006.

Nedergaard, Jan; Bengtsson, Tore; Cannon, Barbara (2007) Unexpected evidence for active brown adipose tissue in adult humans. In : American journal of physiology. Endocrinology and metabolism, vol. 293, n° 2, E444-52. DOI: 10.1152/ajpendo.00691.2006.

Neves, Susana R.; Ram, Prahlad T.; Iyengar, Ravi (2002) G protein pathways. In : Science (New York, N.Y.), vol. 296, n° 5573, p. 1636–1639. DOI: 10.1126/science.1071550.

Overington, John P.; Al-Lazikani, Bissan; Hopkins, Andrew L. (2006) How many drug targets are there? In : Nature reviews. Drug discovery, vol. 5, n° 12, p. 993–996. DOI: 10.1038/nrd2199.

Pan, Houhua; Xie, Youtao; Zhang, Zequan; Li, Kai; Hu, Dandan; Zheng, Xuebin et al. (2017) YAP-mediated mechanotransduction regulates osteogenic and adipogenic differentiation of BMSCs on hierarchical structure. In : Colloids and surfaces. B, Biointerfaces, vol. 152, p. 344–353. DOI: 10.1016/j.colsurfb.2017.01.039.

Pan, Jin-Xiu; Xiong, Lei; Zhao, Kai; Zeng, Peng; Wang, Bo; Tang, Fu-Lei et al. (2018) YAP promotes osteogenesis and suppresses adipogenic differentiation by regulating β-catenin signaling. In : Bone research, vol. 6, p. 18. DOI: 10.1038/s41413-018-0018-7.

Panciera, Tito; Azzolin, Luca; Cordenonsi, Michelangelo; Piccolo, Stefano (2017) Mechanobiology of YAP and TAZ in physiology and disease. In : Nature reviews. Molecular cell biology, vol. 18, n° 12, p. 758–770. DOI: 10.1038/nrm.2017.87.

Pesta, Dominik; Gnaiger, Erich (2012) High-resolution respirometry: OXPHOS protocols for human cells and permeabilized fibers from small biopsies of human muscle. In : Methods in molecular biology (Clifton, N.J.), vol. 810, p. 25–58. DOI: 10.1007/978-1-61779-382-0_3.

Pfeifer, A.; Brandon, E. P.; Kootstra, N.; Gage, F. H.; Verma, I. M. (2001) Delivery of the Cre recombinase by a self-deleting lentiviral vector: efficient gene targeting in vivo. In : Proceedings of the National Academy of Sciences of the United States of America, vol. 98, n° 20, p. 11450–11455. DOI: 10.1073/pnas.201415498.

Pfeifer, Alexander; Hoffmann, Linda S. (2015) Brown, beige, and white: the new color code of fat and its pharmacological implications. In : Annual review of pharmacology and toxicology, vol. 55, p. 207–227. DOI: 10.1146/annurev-pharmtox-010814-124346.

Pierce, Kristen L.; Premont, Richard T.; Lefkowitz, Robert J. (2002) Seven-transmembrane receptors. In : Nature reviews. Molecular cell biology, vol. 3, n° 9, p. 639–650. DOI: 10.1038/nrm908.

Plouffe, Steven W.; Lin, Kimberly C.; Moore, Jerrell L.; Tan, Frederick E.; Ma, Shenghong; Ye, Zhen et al. (2018) The Hippo pathway effector proteins YAP and TAZ have both distinct and overlapping functions in the cell. In : The Journal of biological chemistry, vol. 293, n° 28, p. 11230–11240. DOI: 10.1074/jbc.RA118.002715.

Quesada-López, Tania; Cereijo, Rubén; Turatsinze, Jean-Valery; Planavila, Anna; Cairó, Montserrat; Gavaldà-Navarro, Aleix et al. (2016) The lipid sensor GPR120 promotes brown fat activation and FGF21 release from adipocytes. In : Nature communications, vol. 7, p. 13479. DOI: 10.1038/ncomms13479.

Quesada-López, Tania; Gavaldà-Navarro, Aleix; Morón-Ros, Samantha; Campderrós, Laura; Iglesias, Roser; Giralt, Marta; Villarroya, Francesc (2019) GPR120 controls neonatal brown adipose tissue thermogenic induction. In : American journal of physiology. Endocrinology and metabolism, vol. 317, n° 5, E742-E750. DOI: 10.1152/ajpendo.00081.2019.

Rath, Nicola; Olson, Michael F. (2012) Rho-associated kinases in tumorigenesis: re-considering ROCK inhibition for cancer therapy. In : EMBO reports, vol. 13, n° 10, p. 900–908. DOI: 10.1038/embor.2012.127.

Rodgers, R. John; Tschöp, Matthias H.; Wilding, John P. H. (2012) Anti-obesity drugs: past, present and future. In : Disease models & mechanisms, vol. 5, n° 5, p. 621–626. DOI: 10.1242/dmm.009621.

Roh, Hyun Cheol; Tsai, Linus T. Y.; Shao, Mengle; Tenen, Danielle; Shen, Yachen; Kumari, Manju et al. (2018) Warming Induces Significant Reprogramming of Beige, but Not Brown, Adipocyte Cellular Identity. In : Cell metabolism, vol. 27, n° 5, 1121-1137.e5. DOI: 10.1016/j.cmet.2018.03.005.

Saito, Masayuki; Okamatsu-Ogura, Yuko; Matsushita, Mami; Watanabe, Kumiko; Yoneshiro, Takeshi; Nio-Kobayashi, Junko et al. (2009) High incidence of metabolically active brown adipose tissue in healthy adult humans: effects of cold exposure and adiposity. In : Diabetes, vol. 58, n° 7, p. 1526–1531. DOI: 10.2337/db09-0530.

Sánchez-Fernández, Guzmán; Cabezudo, Sofía; García-Hoz, Carlota; Benincá, Cristiane; Aragay, Anna M.; Mayor, Federico; Ribas, Catalina (2014) Gαq signalling: the new and the old. In : Cellular signalling, vol. 26, n° 5, p. 833–848. DOI: 10.1016/j.cellsig.2014.01.010.

Sanchez-Gurmaches, Joan; Hung, Chien-Min; Sparks, Cynthia A.; Tang, Yuefeng; Li, Huawei; Guertin, David A. (2012) PTEN loss in the Myf5 lineage redistributes body fat and

reveals subsets of white adipocytes that arise from Myf5 precursors. In : Cell metabolism, vol. 16, n° 3, p. 348–362. DOI: 10.1016/j.cmet.2012.08.003.

Sandbo, N.; Smolyaninova, L. V.; Orlov, S. N.; Dulin, N. O. (2016) Control of Myofibroblast Differentiation and Function by Cytoskeletal Signaling. In : Biochemistry. Biokhimiia, vol. 81, n° 13, p. 1698–1708. DOI: 10.1134/S0006297916130071.

Sargent, Bruce J.; Moore, Nicholas A. (2009) New central targets for the treatment of obesity. In : British journal of clinical pharmacology, vol. 68, n° 6, p. 852–860. DOI: 10.1111/j.1365-2125.2009.03550.x.

Schilperoort, Maaike; van Dam, Andrea D.; Hoeke, Geerte; Shabalina, Irina G.; Okolo, Anthony; Hanyaloglu, Aylin C. et al. (2018) The GPR120 agonist TUG-891 promotes metabolic health by stimulating mitochondrial respiration in brown fat. In : EMBO molecular medicine, vol. 10, n° 3. DOI: 10.15252/emmm.201708047.

Seale, Patrick; Bjork, Bryan; Yang, Wenli; Kajimura, Shingo; Chin, Sherry; Kuang, Shihuan et al. (2008) PRDM16 controls a brown fat/skeletal muscle switch. In : Nature, vol. 454, n° 7207, p. 961–967. DOI: 10.1038/nature07182.

Seale, Patrick; Kajimura, Shingo; Yang, Wenli; Chin, Sherry; Rohas, Lindsay M.; Uldry, Marc et al. (2007) Transcriptional control of brown fat determination by PRDM16. In : Cell metabolism, vol. 6, n° 1, p. 38–54. DOI: 10.1016/j.cmet.2007.06.001.

Seo, Jimyung; Kim, Joon (2018) Regulation of Hippo signaling by actin remodeling. In : BMB reports, vol. 51, n° 3, p. 151–156. DOI: 10.5483/bmbrep.2018.51.3.012.

Shabalina, Irina G.; Petrovic, Natasa; Jong, Jasper M. A. de; Kalinovich, Anastasia V.; Cannon, Barbara; Nedergaard, Jan (2013) UCP1 in brite/beige adipose tissue mitochondria is functionally thermogenic. In : Cell reports, vol. 5, n° 5, p. 1196–1203. DOI: 10.1016/j.celrep.2013.10.044.

Shimizu, Ippei; Aprahamian, Tamar; Kikuchi, Ryosuke; Shimizu, Ayako; Papanicolaou, Kyriakos N.; MacLauchlan, Susan et al. (2014) Vascular rarefaction mediates whitening of brown fat in obesity. In : The Journal of clinical investigation, vol. 124, n° 5, p. 2099–2112. DOI: 10.1172/JCI71643.

Sudol, Marius; Harvey, Kieran F. (2010) Modularity in the Hippo signaling pathway. In : Trends in biochemical sciences, vol. 35, n° 11, p. 627–633. DOI: 10.1016/j.tibs.2010.05.010.

Tharp, Kevin M.; Kang, Michael S.; Timblin, Greg A.; Dempersmier, Jon; Dempsey, Garret E.; Zushin, Peter-James H. et al. (2018) Actomyosin-Mediated Tension Orchestrates Uncoupled Respiration in Adipose Tissues. In : Cell metabolism, vol. 27, n° 3, 602-615.e4. DOI: 10.1016/j.cmet.2018.02.005.

Trajkovski, Mirko; Ahmed, Kashan; Esau, Christine C.; Stoffel, Markus (2012) MyomiR-133 regulates brown fat differentiation through Prdm16. In : Nature cell biology, vol. 14, n° 12, p. 1330–1335. DOI: 10.1038/ncb2612.

Trayhurn, P.; Beattie, J. H. (2001) Physiological role of adipose tissue: white adipose tissue as an endocrine and secretory organ. In : The Proceedings of the Nutrition Society, vol. 60, n° 3, p. 329–339. DOI: 10.1079/pns200194.

van Marken Lichtenbelt Wouter D.; Vanhommerig Joost W.; Smulders Nanda M.; Drossaerts Jamie M.A.F.L.; Kemerink Gerrit J.; Bouvy Nicole D. et al. Cold-Activated Brown Adipose Tissue in Healthy Men.

Varelas, Xaralabos (2014) The Hippo pathway effectors TAZ and YAP in development, homeostasis and disease. In : Development (Cambridge, England), vol. 141, n° 8, p. 1614–1626. DOI: 10.1242/dev.102376.

Vassilatis, Demetrios K.; Hohmann, John G.; Zeng, Hongkui; Li, Fusheng; Ranchalis, Jane E.; Mortrud, Marty T. et al. (2003) The G protein-coupled receptor repertoires of human and mouse. In : Proceedings of the National Academy of Sciences of the United States of America, vol. 100, n° 8, p. 4903–4908. DOI: 10.1073/pnas.0230374100.

Villarroya, Francesc; Peyrou, Marion; Giralt, Marta (2017) Transcriptional regulation of the uncoupling protein-1 gene. In : Biochimie, vol. 134, p. 86–92. DOI: 10.1016/j.biochi.2016.09.017.

Virtanen Kirsi A.; Lidell Martin E.; Orava Janne; Heglind Mikael; Westergren Rickard; Niemi Tarja et al. Functional Brown Adipose Tissue in Healthy Adults.

Wang, Jialu; Gareri, Clarice; Rockman, Howard A. (2018) G-Protein-Coupled Receptors in Heart Disease. In : Circulation research, vol. 123, n° 6, p. 716–735. DOI: 10.1161/CIRCRESAHA.118.311403.

Wang, Kepeng; Wong, Yung H. (2009) G protein signaling controls the differentiation of multiple cell lineages. In : BioFactors (Oxford, England), vol. 35, n° 3, p. 232–238. DOI: 10.1002/biof.39.

Wang, Zhao V.; Deng, Yingfeng; Wang, Qiong A.; Sun, Kai; Scherer, Philipp E. (2010) Identification and characterization of a promoter cassette conferring adipocyte-specific gene expression. In : Endocrinology, vol. 151, n° 6, p. 2933–2939. DOI: 10.1210/en.2010-0136.

Wang, Zhen; Liu, Peng; Zhou, Xin; Wang, Tianxiang; Feng, Xu; Sun, Yi-Ping et al. (2017) Endothelin Promotes Colorectal Tumorigenesis by Activating YAP/TAZ. In : Cancer research, vol. 77, n° 9, p. 2413–2423. DOI: 10.1158/0008-5472.CAN-16-3229.

Watt, Kevin I.; Goodman, Craig A.; Hornberger, Troy A.; Gregorevic, Paul (2018) The Hippo Signaling Pathway in the Regulation of Skeletal Muscle Mass and Function. In : Exercise and sport sciences reviews, vol. 46, n° 2, p. 92–96. DOI: 10.1249/JES.0000000000000142.

Weisberg, Stuart P.; McCann, Daniel; Desai, Manisha; Rosenbaum, Michael; Leibel, Rudolph L.; Ferrante, Anthony W. (2003) Obesity is associated with macrophage accumulation in adipose tissue. In : Journal of Clinical Investigation, vol. 112, n° 12, p. 1796–1808. DOI: 10.1172/JCI200319246.

Wettschureck, Nina; Offermanns, Stefan (2005) Mammalian G proteins and their cell type specific functions. In : Physiological reviews, vol. 85, n° 4, p. 1159–1204. DOI: 10.1152/physrev.00003.2005.

Worzfeld, Thomas; Wettschureck, Nina; Offermanns, Stefan (2008) G(12)/G(13)-mediated signalling in mammalian physiology and disease. In : Trends in pharmacological sciences, vol. 29, n° 11, p. 582–589. DOI: 10.1016/j.tips.2008.08.002.

Xu, Haiyan; Barnes, Glenn T.; Yang, Qing; Tan, Guo; Yang, Daseng; Chou, Chieh J. et al. (2003) Chronic inflammation in fat plays a crucial role in the development of obesity-related

insulin resistance. In : The Journal of clinical investigation, vol. 112, n° 12, p. 1821–1830. DOI: 10.1172/JCI19451.

Yang, Yongxu; Qi, Qi; Wang, Yi; Shi, Yaru; Yang, Weili; Cen, Yunzhu et al. (2018) Cysteine-rich protein 61 regulates adipocyte differentiation from mesenchymal stem cells through mammalian target of rapamycin complex 1 and canonical Wnt signaling. In : FASEB journal : official publication of the Federation of American Societies for Experimental Biology, vol. 32, n° 6, p. 3096–3107. DOI: 10.1096/fj.201700830RR.

Yu, Fa-Xing; Luo, Jing; Mo, Jung-Soon; Liu, Guangbo; Kim, Young Chul; Meng, Zhipeng et al. (2014) Mutant Gq/11 promote uveal melanoma tumorigenesis by activating YAP. In : Cancer cell, vol. 25, n° 6, p. 822–830. DOI: 10.1016/j.ccr.2014.04.017.

Yu, Fa-Xing; Zhang, Yifan; Park, Hyun Woo; Jewell, Jenna L.; Chen, Qian; Deng, Yaoting et al. (2013) Protein kinase A activates the Hippo pathway to modulate cell proliferation and differentiation. In : Genes & development, vol. 27, n° 11, p. 1223–1232. DOI: 10.1101/gad.219402.113.

Yu, Fa-Xing; Zhao, Bin; Panupinthu, Nattapon; Jewell, Jenna L.; Lian, Ian; Wang, Lloyd H. et al. (2012) Regulation of the Hippo-YAP pathway by G-protein-coupled receptor signaling. In : Cell, vol. 150, n° 4, p. 780–791. DOI: 10.1016/j.cell.2012.06.037.

Yu, Olivia M.; Miyamoto, Shigeki; Brown, Joan Heller (2016) Myocardin-Related Transcription Factor A and Yes-Associated Protein Exert Dual Control in G Protein-Coupled Receptor- and RhoA-Mediated Transcriptional Regulation and Cell Proliferation. In : Molecular and cellular biology, vol. 36, n° 1, p. 39–49. DOI: 10.1128/MCB.00772-15.

Zhao, Bin; Li, Li; Guan, Kun-Liang (2010) Hippo signaling at a glance. In : Journal of cell science, vol. 123, n° Pt 23, p. 4001–4006. DOI: 10.1242/jcs.069070.

Zhao, Bin; Li, Li; Wang, Lloyd; Wang, Cun-Yu; Yu, Jindan; Guan, Kun-Liang (2012) Cell detachment activates the Hippo pathway via cytoskeleton reorganization to induce anoikis. In : Genes & development, vol. 26, n° 1, p. 54–68. DOI: 10.1101/gad.173435.111.

Zhao, Bin; Wei, Xiaomu; Li, Weiquan; Udan, Ryan S.; Yang, Qian; Kim, Joungmok et al. (2007) Inactivation of YAP oncoprotein by the Hippo pathway is involved in cell contact inhibition and tissue growth control. In : Genes & development, vol. 21, n° 21, p. 2747–2761. DOI: 10.1101/gad.1602907.

Zhou, Xin; Wang, Zhen; Huang, Wei; Lei, Qun-Ying (2015) G protein-coupled receptors: bridging the gap from the extracellular signals to the Hippo pathway. In : Acta biochimica et biophysica Sinica, vol. 47, n° 1, p. 10–15. DOI: 10.1093/abbs/gmu108.